U.PORTO
FACULDADE DE CIÊNCIAS
UNIVERSIDADE DO PORTO

Development of New Peptide-Drug Conjugates for Cancer Therapy

Abigail Filipe Ferreira

Biochemistry Master's Dissertation presented to
Faculty of Sciences, University of Porto

2015

UCIBIO
@ REQUIMTE

U.PORTO
INSTITUTO DE CIÊNCIAS BIOMÉDICAS ABEL SALAZAR
UNIVERSIDADE DO PORTO

U.PORTO
FACULDADE DE CIÊNCIAS
UNIVERSIDADE DO PORTO

Development of New Peptide-Drug Conjugates for Cancer Therapy

Abigail Filipe Ferreira
Master Degree in Biochemistry
Department of Chemistry and Biochemistry
2015

Supervisor
Dr. Nuno Filipe de Sousa Vale,
FCT Researcher, UCIBIO/REQUIMTE – Faculty of Sciences of the University of Porto

Co-Supervisor
Dr. Paula Alexandra de Carvalho Gomes,
Associated Professor, Faculty of Sciences of the University of Porto

Todas as correções determinadas pelo júri, e só essas, foram efetuadas.
O Presidente do Júri,

Porto, _____/_____/_____

AGRADECIMENTOS (ACKNOWLEDGEMENTS)

Em primeiro lugar, tenho que agradecer ao Dr. Nuno Vale, por ser um verdadeiro orientador, em todos os sentidos da palavra, e também um professor. Obrigada pelo incansável acompanhamento diário, pelo esforço que dedicou a este projeto, pela enorme capacidade de trabalho, pela paciência, ajuda, otimismo e palavras de incentivo nas alturas que mais precisei. Não há palavras suficientes para agradecer tudo o que fez por mim durante este projeto.

À Professora Paula Gomes, por ter coorientado este projeto, mostrando sempre preocupação em acompanhar o trabalho que estava a ser desenvolvido e por toda a força e confiança que sempre me transmitiu.

À Iva Fernandes, agradeço a oportunidade de realizar os ensaios biológicos. Obrigada por tudo o que me ensinaste, pela tua paciência e por estares sempre disponível para me ajudar.

Agradeço também à Sílvia Maia, por realizar as análises de espetrometria de massa e pela ajuda na sua interpretação.

A todos os que passaram pelo laboratório 2.28 durante a realização deste trabalho tenho que agradecer por me proporcionarem o melhor ambiente de trabalho que podia pedir. Obrigada ao Stephane Azevedo, que na sua curta passagem por este laboratório, teve sempre a capacidade de me pôr um sorriso na cara. Ao Lorenzo Cianni, por proporcionar uns jantares inesquecíveis. E ao Rafael Almeida pela simpatia e boa disposição.

Mas tenho que deixar um agradecimento (muito) especial às meninas “da casa”, Ana, Joana, Luísa, Mariana e Rita. Obrigada Ana por seres a melhor química (e não só!) de sempre e pela tua ajuda e disponibilidade absolutamente incansável. Obrigada Luísa e Mariana por todas as gargalhadas que demos em conjunto (algumas das quais não irei esquecer). Joana, obrigada por seres única e não teres medo de o mostrar. E Rita, porque entendes uma outra faceta de mim melhor que ninguém, obrigada por tudo!

Aos meus amigos bioquímicos que de alguma forma também me apoiaram nesta difícil jornada (Margarida, Ricardo, Mariana, …), obrigada.

À minha família e especialmente aos meus pais, obrigada por acreditarem em mim e me puxarem para cima, sempre. Vocês sabem o quanto vos amo.

ABSTRACT

In developed countries, cancer is one of the major causes of death, along with cardiovascular diseases. One of the main reasons that can be attributed to this high mortality is the failure of current treatment options. The hard distinction of normal and cancer cells, but also the phenomenon of resistance and the inefficacy to treat metastases, are the main obstacles when treating cancer patients.

Gemcitabine (2′,2′-difluorodeoxycytidine), commercially available as Gemzar® by Eli Lilly and Company, is a nucleoside analogue which has been proven efficient against a wide range of solid tumors. The use of gemcitabine hydrochloride was approved in 1996 by the Food and Drug Administration (FDA) as first-line treatment for patients with locally advanced (non-resectable Stage II or Stage III) or metastatic (Stage IV) pancreatic adenocarcinoma previously treated with fluorouracil (5-FU). Gemcitabine is activated *in vivo* via phosphorylation of its 5'-hydroxyl group to gemcitabine monophosphate by deoxycytidine kinase, and is subsequently phosphorylated by intracellular kinases to the triphosphate form. However, gemcitabine may be deaminated to its inactive uridine metabolite, 2',2'-difluorodeoxyuridine, by cytidine deaminase (CDA), which is present at high levels in both human plasma and liver.

This project aims at the chemical modification of gemcitabine and subsequent conjugation to Cell-Penetrating Peptides (CPPs), in an effort to both prevent (or retard) deamination of that drug and facilitate its delivery into cancer cells, taking advantage of the fact that all CPPs are able to efficiently pass through cell membranes while being non-cytotoxic and carrying a wide variety of cargos inside cells.

Two CPP-drug conjugates have been successfully synthesized, purified and characterized by HPLC and LC-MS. The time-dependent kinetics of gemcitabine release from hydrolysis of these new conjugates was studied in phosphate-buffered saline (PBS) at physiological pH and temperature. Furthermore, the biological activity of these two new conjugates was evaluated against three different human tumoral cell lines: MKN-28 (human gastric cancer), Caco-2 (heterogeneous human epithelial colorectal adenocarcinoma) and HT-29 (human colon adenocarcinoma).

RESUMO

Nos países desenvolvidos, o cancro é uma das principais causas de morte, juntamente com as doenças cardiovasculares. Uma das razões fundamentais que pode ser atribuída à elevada mortalidade desta doença é a baixa taxa de sucesso das opções terapêuticas atualmente disponíveis. O tratamento de doenças oncológicas enfrenta alguns obstáculos, como a difícil distinção entre células saudáveis e células tumorais (que conduz a sérios efeitos secundários associados à terapia), mas também o aparecimento de fenómenos de resistência a quimioterapêuticos e a ineficácia do tratamento de metástases.

A Gemcitabina (2′,2′- difluorodesoxicitidina) é um análogo de nucleósido comercializado pela farmacêutica Eli Lilly and Company como Gemzar® cuja atividade contra uma grande variedade de tumores sólidos foi já extensivamente comprovada. O uso de cloridrato de gencitabina foi aprovado em 1996 pelo órgão governamental dos Estados Unidos da América responsável pelo controlo dos alimentos e medicamentos (*Food and Drug Administration*, USA) como opção terapêutica de primeira linha para doentes com adenocarcinoma pancreático localmente avançado (inoperável, fase II ou II) ou metastático (fase IV) previamente tratados com 5-fluorouracilo (5-FU, um outro análogo de nucleósido). A gencitabina é ativada *in vivo* por fosforilação na posição 5'- a monofosfato de gencitabina pela enzima desoxicitidina cinase, e é subsequentemente fosforilada por outras cinases intracelulares à forma trifosfatada, que tem capacidade de inibir a síntese de ADN. No entanto, a gencitabina também pode ser inativada, sendo convertida no metabolito uridínico pela enzima citidina desaminase, presente em elevados níveis no plasma e fígado humano.

Com este projeto pretendeu-se modificar quimicamente a gencitabina e subsequentemente conjugar o seu derivado a Péptidos Penetradores Celulares (CPPs), esperando que estes novos pro-fármacos consigam aumentar a entrada deste agente nas células cancerígenas, tirando partido da propriedade intrínseca dos CPPs, péptidos capazes de atravessar eficazmente membranas celulares, podendo transportar para o interior de diferentes tipos de células inúmeras moléculas, sem comprometer a integridade da membrana.

Foram sintetizados dois conjugados Fármaco–Péptido, que foram purificados e caracterizados por Cromatografia Líquida de Alta Pressão e por Espetrometria de Massa acoplada a Cromatografia Líquida de Baixa Pressão. A cinética de libertação de gencitabina na sua forma livre foi estudada em condições fisiológicas e foi ainda avaliada a atividade biológica destes novos conjugados contra três linhas tumorais humanas: MKN-28 (cancro gástrico), Caco-2 e HT-29 (provenientes do cólon).

INDEX

LIST OF FIGURES

LIST OF TABLES

LIST OF ABBREVIATIONS

5'-NT: 5'-nucleotidase

AA: amino acid

ACN: acetonitrile

AMP: Antimicrobial Peptide

Boc: *tert*-butoxycarbonyl

Bzl: benzyl

CARPA: complement activation-related pseudoallergy

CDA: cytidine deaminase

CMP: cytidine monophosphate

CPP: Cell-Penetrating Peptide

C_t: C-terminus

Da: Dalton (unified atomic mass unit)

dCK: deoxycytidine kinase

DCM: dichloromethane

DCTD: deoxycytidylate deaminase

dFdC: 2′,2′-difluorodeoxycytidine (gemcitabine)

dFdCMP / dFdCDP / dFdCTP: gemcitabine monophosphate / diphosphate / triphosphate

dFdU: 2',2'-difluorodeoxyuridine

dFdUMP / dFdUDP / dFdUTP: 2',2'-difluorodeoxyuridine monophosphate / diphosphate / triphosphate

DMSO: dimethylsulfoxide

DIPEA: *N*-ethyl-*N,N*-diisopropylamine

DMF: *N,N*-dimethylformamide

DNA: deoxyribonucleic acid

EE: encapsulation efficiency

ESI-IT MS: Electrospray Ionization – Ion Trap Mass Spectrometry

FBS: fetal bovine serum

FDA: Food and Drug Administration (USA)

Fmoc: 9-fluorenylmethoxycarbonyl

Fmoc-AA-OH: amino acid residue N^{α}-protected with an Fmoc group

GAGs: glycosaminoglycans

HBTU: *O*-(benzotriazol-1-yl)-*N,N,N′,N′*-tetramethyluronium hexafluorophosphate

hCNT: human concentrative nucleoside transporter

hENT: human equilibrative nucleoside transporter

HOBt·H_2O: 1-hydroxybenzotriazole (mono hydrated)

HPLC-DAD: High-Performance Liquid Chromatography with Diode-Array Detection

HSR: hypersensitivity reactions

LC-MS: Liquid Chromatography hyphenated to Mass Spectrometry

m/z: mass-to-charge ratio

MAP: Membrane Active Peptide

MAPS: Microwave-Assisted Peptide Synthesis

MBHA: 4-methylbenzhydrylamine-functionalized resin

MS: Mass Spectrometry

MW: microwave radiation

MW-SPPS: Microwave-Assisted Solid-Phase Peptide Synthesis

NMP: *N*-methyl-2-pyrrolidone

N_t: *N*-terminus

Pbf: pentamethyl-2,3-dihydrobenzofuran-5-sulfonyl

PBS: phosphate-buffered saline

PEG: polyethylene glycol

Rink: (*R*,*S*)-2-{4-[amino(2,4-dimethoxyphenyl)methyl]phenoxy}acetic acid

RP-MPLC: Reversed Phase Medium-Pressure Liquid Chromatography

r_t: retention time

SEM: Standard Error of the Mean

SPPS: Solid Phase Peptide Synthesis

TBTU: *O*-(Benzotriazol-1-yl)-*N,N,N',N'*-tetramethyluronium tetrafluoro borate

^{t}Bu: *tert*-butyl

TCA: trichloroacetic acid

TFA: trifluoroacetic acid

TIS: triisopropylsilane

Trt: trityl

UMP: uridine monophosphate

OBJECTIVES

The main goal of the work developed in this thesis was the development of new gemcitabine prodrugs, obtained through chemical modification of that anticancer agent, followed by conjugation of the modified derivative with Cell-Penetrating Peptides Penetratin and pVEC, activated with an *N*-terminal cystein residue.

Cys-Penetratin: C-RQIKIWFQNRRMKWKK

Cys-pVEC: C-LLIILRRRIRKQAHAHSK

Furthermore, the work also aimed at the study of the time-dependent kinetics of gemcitabine release from hydrolysis of the new conjugates under physiological conditions.

Gemcitabine – Linker – Penetratin

Gemcitabine – Linker – pVEC

1. INTRODUCTION

1.1. Cancer Management

In developed countries, cancer is one of the major causes of death, along with cardiovascular diseases. This condition involves the abnormal growth of any type of cell with the potential to invade or spread to other parts of the body. One of the main reasons that can be attributed to the high mortality of this group of diseases is the failure of current treatment options. The hard distinction between normal and cancer cells and difficulty in targeting only the altered cells, the phenomenon of resistance, and the inefficacy to treat metastases are the main obstacles when treating cancer patients.

Cancer management and treatment plans depend on several factors, such as the type, location, and grade of the cancer as well as the patient's health and personal choices. Treatments may be curative or aimed at improving life quality. There are many treatment options for cancer, including surgery, chemotherapy, radiotherapy, hormonal therapy and palliative care.

Although surgery is the primary method used in most isolated solid cancers and is often an important part of determining the definitive diagnosis, chemotherapy is a major treatment choice. This type of therapy is recurrently used in combination with hormonal therapy (pharmacotherapy) and with other cancer treatments, such as radiotherapy, surgery, and/or hyperthermia therapy. Chemotherapy consists on the administration of chemical substances, especially one or more anti-cancer drugs (chemotherapeutic agents), which are traditionally cytotoxic agents, killing cells that divide rapidly, one of the main properties of most cancer cells. However, these substances will also reach other cells in our body that divide rapidly under normal circumstances, as cells in the bone marrow, digestive tract, and hair follicles. This can lead to various severe side effects, frequently associated with chemotherapy. These adverse reactions in addition to the limited effectiveness of oncologic treatments make the development of new therapeutic options that are able to be more selective and effective an imperative need.

Alternative targeted therapies have been put forward, aiming at efficiently treating specific types of cancer while decreasing the severe side effects associated with these treatments. According to the National Cancer Institute of the United States of America (NCI, USA), targeted therapies are deliberately chosen or designed to interact with and act on specific molecular targets that are associated with cancer, whereas most standard chemotherapies act on all rapidly dividing normal and cancerous cells (many standard chemotherapies were identified because they kill cells) [1]. These targeted therapies are often cytostatic (that is, they block tumor cell proliferation), whereas standard chemotherapy agents are cytotoxic (that is, they kill tumor cells).

Still, there are some limitations to targeted therapeutic approaches: cancer cells can become resistant to them and, for this reason, targeted therapies may work best in combination; another current limitation of targeted therapies is that drugs for some identified targets are difficult to develop because of the target's structure and/or the way its function is regulated in the cell. Moreover, although targeted therapies are designed to reduce side effects, some patients receiving this type of therapy suffer from substantial adverse effects, the most common including diarrhea and liver problems, such as hepatitis and elevated liver enzymes. Nevertheless, several experimental targeted therapies for specific types of cancer are currently being studied in clinical trials and some have already been approved by the Food and Drug Administration (FDA).

1.2. Gemcitabine

The current treatment of cancer using chemotherapy is largely based on the use of nucleoside analogues and gemcitabine, or 2′,2′-difluorodeoxycytidine (**1**, Figure 1), is one of such analogues. Despite the similarities with other nucleoside analogues, gemcitabine has many distinctive properties, including its spectrum of activity.

Gemcitabine is commercially available as Gemzar® and was developed by the pharmaceutical Eli Lilly and Company in the 1980s. Although gemcitabine was originally investigated for its antiviral effects [2], this drug has been proven efficient against a wide range of solid tumors and has since been developed as an active agent for cancer therapy. The FDA has also approved the use of gemcitabine (a) in combination with carboplatin for the treatment of advanced ovarian cancer that has relapsed at least 6 months after completion of platinum-based therapy [3]; (b) in combination with paclitaxel, for first-line treatment of metastatic breast cancer after failure of prior anthracycline-containing adjuvant chemotherapy, unless anthracyclines were clinically contraindicated [4]; (c) in combination with cisplatin for the treatment of non-small cell lung cancer (NSCLC) [5] and (d) as a single agent for the treatment of pancreatic cancer [6]. Gemcitabine is particularly effective against pancreatic cancer, and the use of its hydrochloride salt was approved by the FDA in 1996 as first-line treatment for patients with locally advanced (non-resectable Stage II or Stage III) or metastatic (Stage IV) pancreatic adenocarcinoma previously treated with fluorouracil (5-FU) [7].

However, treatment with gemcitabine leads to some severe adverse reactions, which are dependent on dosage and duration of the treatment, clinical indication and cancer stage, gender, age and patients' clinical history. The most common include myelosuppression, hepatic and renal toxicity, cardiovascular alterations (such as hypotension, capillary leak syndrome,…) nausea/vomiting, fever, thrombocytopenia and dyspnea [8].

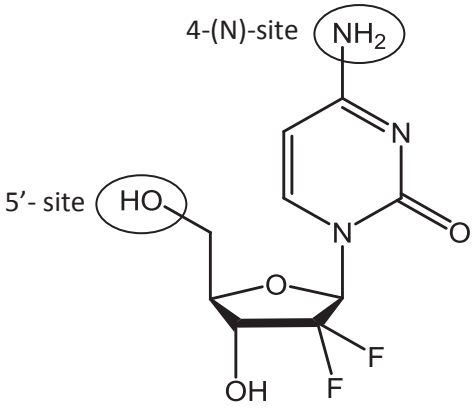

(1)

Figure 1: Chemical structure of Gemcitabine (2′,2′-difluorodeoxycytidine), where 4-(N)- and 5'- sites are highlighted.

1.2.1. Biodistribution and Mechanism of Action

Gemcitabine is a polar drug with low membrane permeability, and is primarily administered by intravenous infusions. It has a very short plasma circulation time and the elimination half-life depends upon the infusion time, age and gender of the patient, ranging from 42 to 94 min for short infusions and from 4 to 10 h for infusions of 70 min [9]. An increased toxicity is associated with longer infusions and, at higher doses, major toxicity can be observed, such as neutropenia, reversible hepatic transaminase increase and high levels of hepatoxicity, renal toxicity, myelosuppression, thrombocytopaenia, anemia, proteinuria, nausea and vomiting, mild flulike syndrome, and mild skin rash. Also, gemcitabine is rapidly cleared from the body upon its enzymatic conversion in the blood, liver, kidney, and various tumor tissues [10, 11].

Upon administration, gemcitabine is transported in the plasma and crosses the plasma membrane into cells via nucleoside transporters. These transporters can be sodium-dependent (human concentrative nucleoside transporter, hCNTs) or sodium-independent (human equilibrative nucleoside transporter, hENTs) [12]. There are two equilibrative nucleoside transporters (hENT1 and hENT2) and three concentrative nucleoside transporters (hCNT1, hCNT2, and hCNT3). Kinetic studies have shown that gemcitabine intracellular uptake is preferentially directed by hENT1 and, to a lesser extent, by hCNT1 and hCNT3 [13, 14]. Also, several studies have shown the importance of the presence of the hENT1 transporter for an optimal response to gemcitabine [15].

Once inside the cells, gemcitabine needs to be activated, and undergoes a series of phosphorylation steps catalyzed by intracellular enzymes (Figure 2). First, deoxycytidine kinase (dCK) phosphorylates gemcitabine to a monophosphate derivative, dFdCMP. Then, nucleoside monophosphate kinase (UMP/CMP) phosphorylates dFdCMP to gemcitabine diphosphate (dFdCDP) and finally diphosphate kinase yields gemcitabine triphosphate (dFdCTP), the active form of this drug [16].

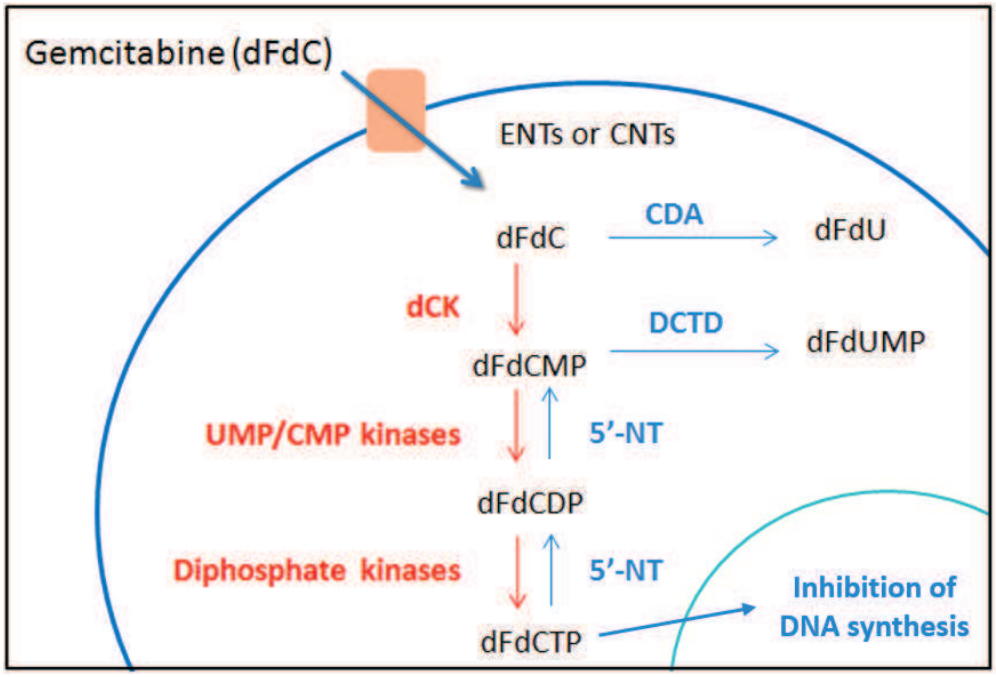

Figure 2: Mechanism of intracellular activation of gemcitabine. Adapted from [17].

However, gemcitabine can also be inactivated inside cells. This inactivation is due to the conversion of gemcitabine into its inactive uridine metabolite, 2',2'-difluorodeoxyuridine (dFdU), catalyzed by cytidine deaminase (CDA), as well as to the deamination of gemcitabine monophosphate into dFdUMP, which is catalyzed by deoxycytidylate deaminase (DCTD). Furthermore, the phosphorylated metabolites of gemcitabine are inactivated via reduction by cellular 5'-nucleotidase (5'-NT). CDA is present at high levels in both human plasma and liver, and the enzymatic conversion of gemcitabine rapidly clears it from the body [16].

In its triphosphate form, dFdCTP, gemcitabine acts as an antimetabolic drug, being a competitive substrate of deoxycytidine triphosphate to DNA polymerases, and causes cell death by apoptosis. This action is possible because of the analogy between dFdCTP and deoxycytidine triphosphate: gemcitabine triphosphate is incorporated into DNA during replication (making it an S-phase-specific drug) thus inhibiting chain elongation of DNA because DNA polymerases are unable to proceed after one deoxynucleotide is added [18]. This action is called "masked chain termination", and it appears to lock the drug into DNA because proof-reading exonucleases are unable to remove gemcitabine nucleotide from this penultimate position [19]. The inhibitory action of gemcitabine is further improved by its nondetection in the DNA chain.

Additionally, because the diphosphate form of gemcitabine (dFdCDP) inhibits ribonucleoside diphosphate reductase (RNR), an enzyme of DNA synthesis which permits the formation of nucleoside triphosphates, there is a significant decrease in the concentration of cellular deoxycytidine triphosphate (dCTP) and a change in the ratio of dCTP/dFdCTP in favor of dFdCTP.

The accumulation of gemcitabine triphosphate and the intracellular reduction of dCTP results in the inhibition of dFdCMP inactivation by DCTD, which requires sufficient concentrations of dCTP to be active [20]. Active metabolites of gemcitabine can also inhibit ribonucleotide reductase (RR), dCMP deaminase, and CTP synthetase, thus enhancing gemcitabine activation, due to a unique property called self-potentiation.

1.2.2. Resistance to Gemcitabine

The rise of drug resistance is a major obstacle in the treatment of many forms of cancer, and this phenomenon usually appears very rapidly after the beginning of the treatment, when cells are typically sensitive to the drug. It is critical to have a better understating oh this phenomenon so that drugs can be replaced by more efficient substituents, combination therapies can be developed or the targeting of the drugs can be improved.

There are many factors contributing to the development of resistance to gemcitabine, from transporters expression to abnormal levels of the enzymes involved in the activation, metabolism and mechanism of action of gemcitabine. One of the major causes of resistance to gemcitabine can be attributed to alterations in transporters. hENT1 is a preferential transporter and studies have found a strong correlation between gemcitabine resistance and a deficiency of hENT1 expression in human breast and pancreatic cancer cells [21, 22]. Additionally, studies have shown that the determination of hENT1 but also hCNT3 expression can be used as a prognostic marker for patients treated with gemcitabine [23, 24].

There are many enzymes involved in the metabolism of gemcitabine, and alterations on the expression levels of any of these enzymes can make cells resistant to this drug or, on the other hand, make it more cytotoxic. One of the key enzymes is deoxycytidine kinase (dCK), responsible for the first phosphorylation of gemcitabine. This is the rate-limiting enzyme involved in the metabolism of gemcitabine and its expression has been postulated to correlate with gemcitabine resistance [25]. This can be caused by mutations of the *dCK* gene [26] or by low levels of dCK enzyme activity [27]. Also, high levels of the catabolic enzymes cytidine deaminase (CDA), dCMP deaminase and 5′-nucleotidase (5′-NT) are associated with resistance to gemcitabine [28].

Another factor in gemcitabine resistance is the overexpression of ribonucleotide reductase (RR) [29]. This enzyme is mainly responsible for the conversion of ribonucleosides to deoxyribonucleoside triphosphates (dNTPs), which are essential for DNA polymerization and repair. Both regulatory subunit RRM1 and catalytic subunit RRM2 influence the cytotoxic action of gemcitabine. RRM1 overexpression through transfection of a lung cancer cell line resulted in gemcitabine resistance and the reduction of RRM1 expression through RNA interference

abrogated the induced gemcitabine resistance [30]. As for the RRM2 subunit, its overexpression is associated with resistance to gemcitabine and down regulation of RRM2 by siRNA enhanced gemcitabine cytotoxicity, both *in vitro* and *in vivo* in pancreatic adenocarcinoma [31].

The aberrant expression of genes associated with cellular survival and apoptosis upon treatment with gemcitabine is also implicated in resistance to this drug [32, 33]. Once gemcitabine is incorporated into DNA, the cell enters a process of cell death, mainly through apoptosis, in response to cytotoxic drug treatment [34, 35]. One of the main proteins involved in the cell death mechanism and apoptosis is p53 [36]. The expression of p53 plays an important role in apoptosis pathways, inducing cell cycle arrest and in the higher concentration ranges, p53 induces apoptosis. In sensitive malignant cells, a variety of anticancer drugs have been shown to produce extensive apoptosis, but it has been suggested that the inability of some cells to undergo apoptosis is similar to the mechanism of gemcitabine resistance. Human lung cancer expressing the mutation of the p53 gene does not undergo apoptosis after gemcitabine treatment [37].

1.2.3. Modifications of Gemcitabine

From the previous sections it can be inferred that, although gemcitabine is an effective treatment to patients with different types of cancer and mainly to treat pancreatic adenocarcinoma, it has low membrane permeability and is extensively degraded by CDA into an inactive metabolite in the liver. Moreover, the increasing levels of resistance also reduce gemcitabine cytotoxicity. Thus, a frequent administration schedule at high drug doses is required, and this leads to serious side effects. To date, various innovative approaches have been developed to overcome these disadvantages, including combination therapy to determine the utility of adding a second cytotoxic drug or radiotherapy to this treatment regimen, but clinical trials have shown modest improvements in disease-free survival, and did not result in statistically significant improvements in survival with reported survival rates reaching 20% to 40% at 1 year [38, 39]. The FDA has also approved the use of gemcitabine in combination with carboplatin, paclitaxel and cisplatin for the treatment of patients with ovarian, breast and non-small cell lung cancer (NSCLC), respectively.

A different strategy consists on chemically modifying gemcitabine, in order to enhance transport and cytotoxicity. These modifications can provide (i) protection against deamination, (ii) better storage and (iii) prolonged release in the cell, (iv) a possible use in the case of deoxycytidine kinase deficiency, and (v) transporter deficiency. These new gemcitabine-based systems have the potential to improve the clinical outcome of a chemotherapy strategy and make these new molecules into prodrugs (a biologically inactive derivative of a parent drug molecule that usually requires an enzymatic or chemical transformation within the body to release the active drug and has improved delivery properties in comparison to the parent molecule [40]).

Most modifications on the gemcitabine structure are performed at the 4-(N)- and 5'-positions, as these two functional groups have significant roles in the action of this drug: the inactivation of gemcitabine results from deamination on the 4-(N)-site, whereas the necessary phosphorylation to make it active occurs in the hydroxyl group at the 5'-position. Some of the new molecules resulting from the modification of gemcitabine and their most relevant properties are described below.

1.2.3.1. Modifications at the 4-(N)-site of gemcitabine

1.2.3.1.1. PEG – Gemcitabine

Polyethylene glycol (PEG, Figure 3) refers to a family of differently-sized polymers with high solubility in water and excellent biocompatibility that have been conjugated to several molecules, from antitumor agents, proteins, peptides or low molecular-weight drugs, due to a relevant number of advantages resulting from the PEGylation process [41]. This technique has become the leading approach to (a) increase plasma half-life of the PEGylated products, (b) provide enzyme protection and (c) accumulate the PEGylated product in tumor zones according to the "enhanced permeability and retention" effect (EPR) [42-44]. However, PEG can activate the complement system, which has been recently proposed as a major underlying or contributing cause of infusion reactions, referred to as complement activation-related pseudoallergy (CARPA), an anaphylactic-type reaction within the Type I category of hypersensitivity reactions (HSRs) [45]. Clinical trials of several derivatives of PEG coupled to anticancer drugs are already under way or have been completed [46].

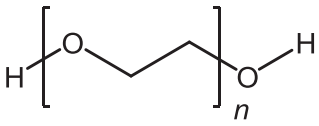

Polyethylene glycol

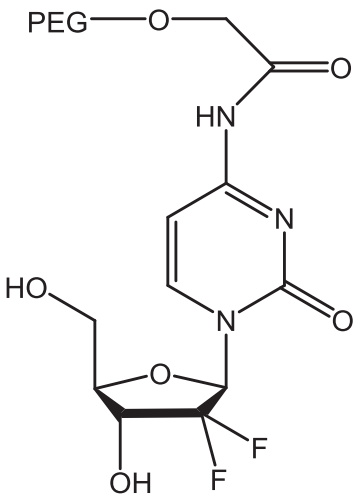

Figure 3: Chemical structures of polyethylene glycol (PEG) and of a PEG – gemcitabine conjugate.

Because of encouraging results from studies with other anticancer agents, and given that the anticancer effects of gemcitabine are limited by its rapid metabolization and consequently short half-life, as well as its low tumor uptake, the coupling of PEG to gemcitabine has been tested by

several research teams. In a recent paper, the synthesis of a PEG – gemcitabine construct, by conjugating the amino group at the 4-(N)-position of gemcitabine to an *N*-hydroxysuccinimide derivative of PEG, has been carried out (Figure 3) [47]. It is known that the cellular uptake of PEG-drug conjugates occurs through endocytosis and that conjugates are retained in transport vesicles which traffic along the endolysosomal scaffold, which are acidic in nature [48, 49]. The endolysosomal transport vesicles allow cleavage of the amide bonds between PEG and gemcitabine, thanks to the acidic nature of these vesicles, and thereby allow its prolonged release. Vandana's team was able to demonstrate a colocalization of PEG-gemcitabine in lysosome and endosome after 24 h incubation, and an enhanced retention in cancer cells after 3 days of incubation in comparison to parent gemcitabine, using confocal analysis. Moreover, pharmacokinetic studies have shown consistently higher (by 21-fold) bioavailability of PEG-gemcitabine over unmodified gemcitabine, after 1 h of intravenous administration in mice and, in MiaPaCA 2 and PANC-1 cells, PEG – gemcitabine was more effective in comparison to native gemcitabine.

1.2.3.1.2. Folate-PEG – Gemcitabine

Folate, or folic acid, has been used as a targeting agent in cancer nanotherapeutics, because its receptor is overexpressed in several types of cancers (lung, breast, kidney, and ovarian) [50-52], while in normal human tissues its receptors may have limited distribution. To improve the effect of PEG – gemcitabine, folic acid has been inserted into PEG – gemcitabine conjugates, where the drug was coupled through its 4-(N)-amino group to the carboxylic end of an aminocarboxylated PEG (NH_2-PEG-COOH), while folic acid was linked through its carboxylic function to the amino group of the polymer (

Figure 4). The active targeting and cytotoxic superiority of Folate-PEG – Gemcitabine, compared to the nontargeted PEG – gemcitabine, were investigated [53]. All conjugates were able to release the drug in a pH-dependent manner with no role played by enzymes, which confirms previous studies showing that the protection of the amino group of gemcitabine prevents enzymatic degradation [54]. Polymer conjugation of gemcitabine increased drug plasma half-life by reducing its kidney clearance, which was dependent on the polymer's molecular weight. Folic acid–PEG derivatives were also found as less toxic than PEG derivatives, which was explained by a slower entry into the cell by endocytosis and a cytotoxic activity only after the release of gemcitabine. Moreover, derivatives targeting folate receptors need a receptor-mediated endocytosis mechanism for cell penetration in cells that do not overexpress the folate receptor. In contrast, in KB-3-1 cells, which overexpress folate receptors, derivatives with folate are certainly less cytotoxic than parent gemcitabine but are more cytotoxic than gemcitabine only coupled to PEG [53].

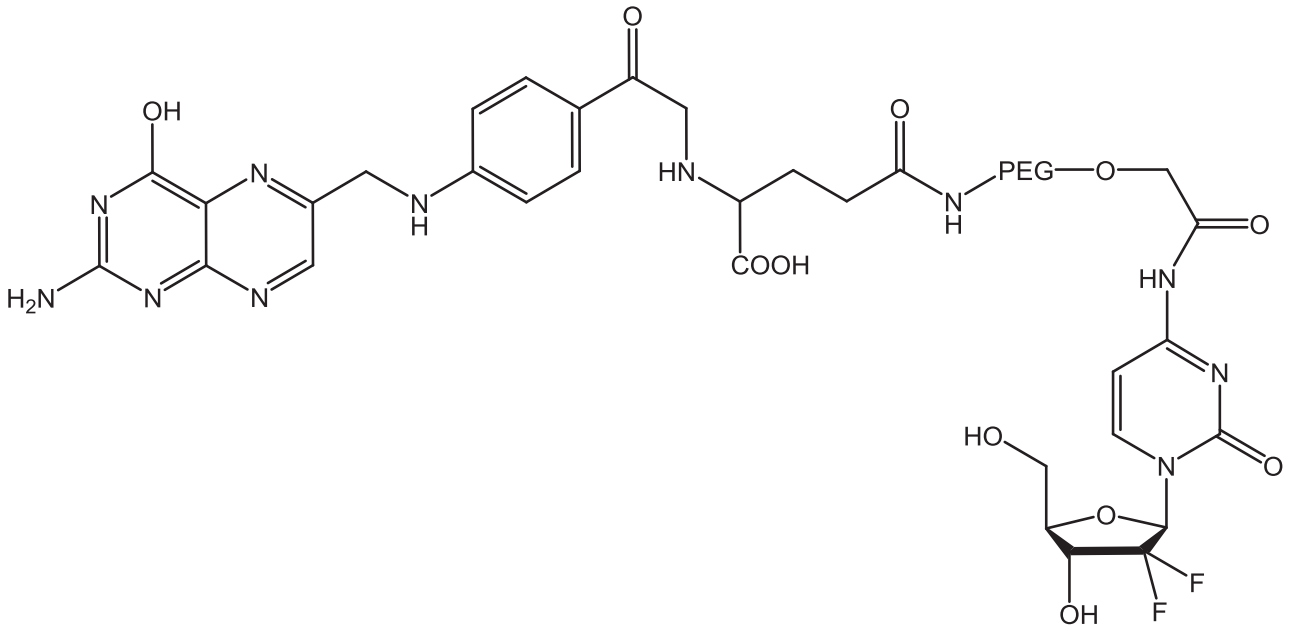

Figure 4: Chemical structure of a Folate-PEG – gemcitabine conjugate.

1.2.3.1.3. Valproic acid – Gemcitabine (LY2334737)

An orally available prodrug of gemcitabine has been developed, consisting of gemcitabine linked to valproic acid via an amide bond at the 4-(N)-position. This molecule is called LY2334737 (Figure 5), and is able to circumvent the rapid deamination of gemcitabine into dFdU, and thus bypass hydrolysis in enterocytes and portal circulation, avoiding the extensive first pass metabolism that occurs with unmodified gemcitabine, underlying its poor oral bioavailability due to an extensive deamination by CDA.

The stability of the prodrug was tested on a pH range from 1 to 8, to check the possibility of delivering an intact prodrug into systemic circulation after passing through the gastrointestinal tract following oral administration. LY2334737 degradation is pH-dependent, with about 21% degradation at pH 1 and no degradation between pH 6 to 8, after 4 h of incubation at 40 °C [55]. Circulating levels of LY2334737 are detectable several hours after oral administration. In addition, a gradual release of gemcitabine following cleavage of the amide bond should enhance efficacy, since more cancer cells should be exposed to a continuous effective cytotoxic level of gemcitabine. The researchers have found that, in mice bearing HCT-116 human colon tumor xenografts, a much smaller dose via oral administration has the same efficacy that a high dose administered via intraperitoneal injection. Phase I trials of LY2334737 either as monotherapy or in combination with other agents were carried out to determine the maximum tolerated dose and dose limiting toxicities of daily administration [56].

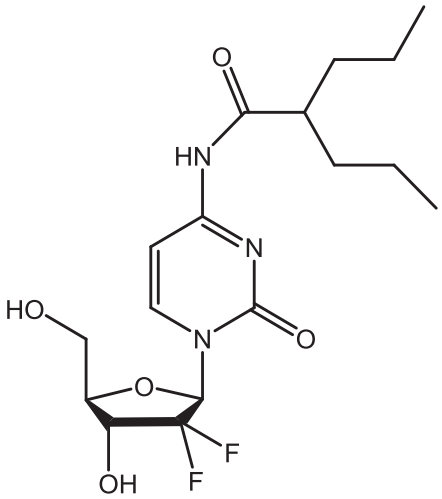

Figure 5: Chemical structure of LY2334737, a prodrug of gemcitabine tested in Phase I clinical trials.

1.2.3.1.4. Squalenoyl – Gemcitabine

Squalene is a triterpene that is an intermediate in the cholesterol biosynthesis pathway. Both *in vitro* and *in vivo* model experiments suggest a tumor-inhibiting role for squalene [57] and, therefore, it has been linked to various nucleoside analogues [58].

Couvreur's team was interested in the pharmacological activity of gemcitabine covalently coupled at 4-(N*)*-position with 1,1',2-tris-nor-squalenoic acid to obtain Sq-gemcitabine [4-(*N*)-tris-nor-squalenoyl-gemcitabine, SQdFdC] (Figure 6).

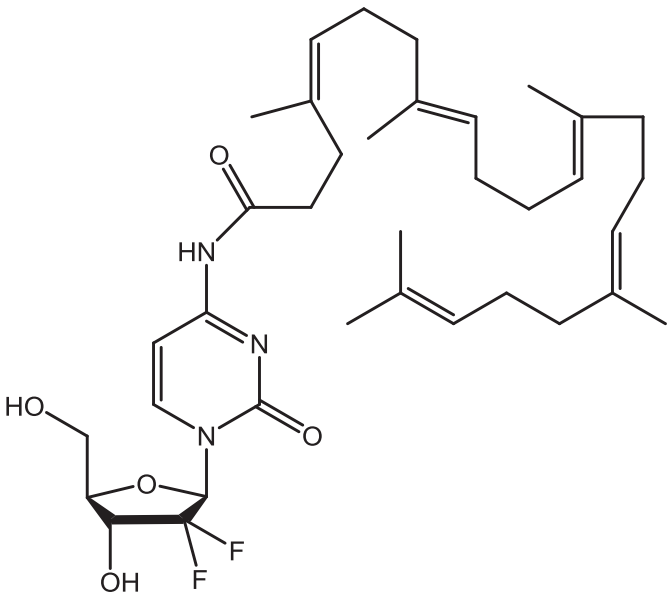

Figure 6: Chemical structure of squalenoyl – gemcitabine (SQdFdC).

Those authors investigated the anticancer activity of Sq-gemcitabine *in vitro* on resistant murine and human leukemia cells (L1210 10K and CEM/ARAC8C, respectively). L1210 10K cells were characterized by a lower expression of cytoplasmic dCK and CEM/ARAC8C by a deficiency in hENT1 transporters [59, 60], hence respectively representing two major resistance factors to gemcitabine. After 72 h of incubation at different concentrations, Sq-gemcitabine demonstrated 3.26 and 3.22-fold higher cytotoxicity compared to gemcitabine with L1210 10K and CEM/ARAC8C, respectively [60]. After intravenous injection of Sq-gemcitabine in aggressive leukemia-bearing mice, a significant increase in survival time compared to gemcitabine was obtained. This increase was attributed to the high degree of localization of Sq-gemcitabine in the liver and spleen, which are the major metastatic organs. Sq-gemcitabine was found to be more efficient than gemcitabine, suggesting the considerable potential of this treatment for leukemia.

Studies on human pancreatic adenocarcinoma models were also performed. Sq-gemcitabine showed higher antiproliferative and cytotoxic effects *in vitro* compared to parent gemcitabine, on chemoresistant tumor cells (Panc-1) and sensitive cell lines (Capan-1 and BxPc-3), which were associated with significant DNA synthesis inhibition, S-phase arrest, and higher induction of apoptosis (caspase 3 activation) [61].

While the mechanism of entry and metabolization of gemcitabine into cells is known, the cellular uptake mechanism of Sq-gemcitabine, its subcellular localization, and its metabolization pathway have been studied only recently. An *in vitro* passive entry in cancer cells (MCF-7: human breast adenocarcinoma) and a preferential accumulation in endoplasmic reticulum, thanks to the high lipophilic level of squalene, were observed [62]. This passive input may explain the efficacy of Sq-gemcitabine on cell lines deficient in active transporters [63].

Finally, two important elements have contributed to the efficiency of this new drug: (a) the storage of gemcitabine in the endoplasmic reticulum allowed it to be protected from deamination by the presence of squalene in the 4-(N*)*-position, and (b) the progressive cleavage to its parent form allowed the metabolization of the cancer compound.

1.2.3.1.5. Lipophilic Prodrugs

To protect against the deamination of gemcitabine, it was proposed to covalently link the amino group in the 4-(N)-position with saturated and monounsaturated fatty acids, namely, with those bearing long C18 and C20 chains. In 1998, Eli Lilly patented the synthesis of lipophilic gemcitabine derivatives (Figure 7), which showed better cytotoxicity than unmodified gemcitabine.

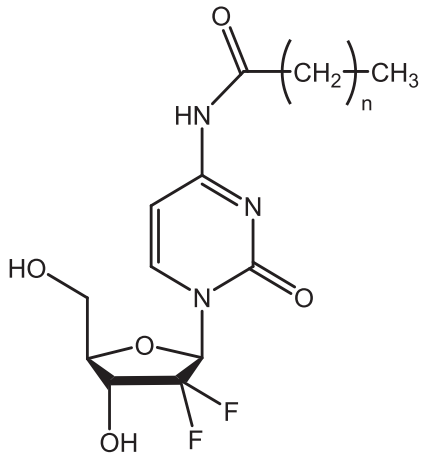

Figure 7: General structure of lipophilic 4-(N)-acyl – gemcitabine conjugates.

A few years later, the synthesis of a series of 4-(N)-acyl derivative prodrugs of gemcitabine was carried out, first to prevent diffusion through liposome bilayers and later to be encapsulated into other particles [64]. Liposomal formulations containing these lipophilic prodrugs of gemcitabine increased the drug entrapment efficacy with respect to conventional liposomes, but their encapsulation efficiency (EE) closely depended on the length of the 4-(N)-acyl chain, the phospholipids, and the presence of cholesterol. Better results were obtained by incorporating 4-(N)-lauroyl-gemcitabine (GemC12) and 4-(N)-stearoyl-gemcitabine (GemC18) in liposomes composed by DSPC/DSPG 9:1. Furthermore, while parent gemcitabine is rapidly converted into inactive metabolite by CDA which is widely distributed in plasma, C12 and C18 derivatives were both stable in plasma. After 24 h, more than 60% of unmodified GemC12 and GemC18 prodrugs were still present, whereas only 40% of unmodified gemcitabine was present after 8 h of incubation of the drug in plasma. The prodrugs were also stable the pH range 4−9, which confirms the stability of the acyl-drug amide linkage. *In vitro* studies have shown that cytotoxicity of free or encapsulated GemC12 and GemC18 derivatives were 2- and 7-fold (in KB and HT-29 cells line, respectively) greater than that of parent gemcitabine. Encapsulation of the C18 derivatives into liposomes produced an increase of plasma availability: the AUC was 50 times higher than for

unmodified gemcitabine, resulting in the increased accumulation in tumor cells and a high level of antitumoral efficacy in mice grafted with HT-29 and KB 396p cells [65].

The increase of anticancer activity observed with these lipophilic derivatives compared with parent gemcitabine was obtained at the expense of their solubility in aqueous media. Indeed, with their highly lipophilic properties, these compounds proved difficult to reconcile with intravenous administration, and hence encapsulation is necessary. The modification of lipophilic behavior and encapsulation could be considered a good and versatile antitumoral approach against several tumors which become less sensitive to the parent drug.

1.2.3.1.6. H–Gemcitabine: Hoechst conjugated to gemcitabine

Dasari and his team developed a new conjugate, composed of the DNA binding agent Hoechst conjugated to gemcitabine [66, 67]. H–Gemcitabine (

Figure 8) is designed to reduce the systemic toxicity of gemcitabine by targeting it to the necrotic core of tumors, and also protect against deamination of its 4-(N) amine via protection with an amide bond. H–Gemcitabine targets tumors via its Hoechst moiety, which binds extracellular DNA (E-DNA) present in the necrotic core of tumors. The authors showed that H–Gemcitabine is significantly more effective than free gemcitabine at treating xenograft human colon tumors in nude mice, and also has a maximum tolerated dose equivalent to that of gemcitabine [67].

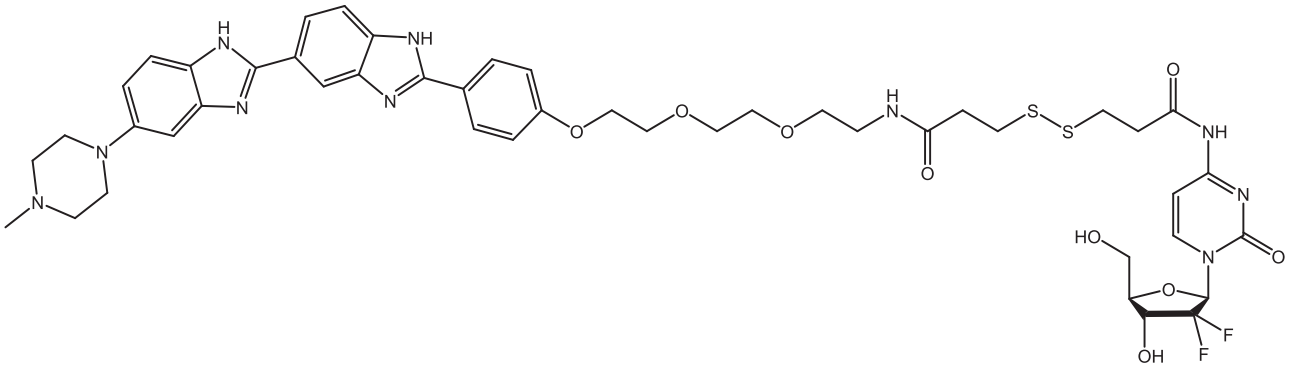

Figure 8: Chemical structure of Hoechst – Gemcitabine.

1.2.3.2. Modifications at the 5'-site of gemcitabine

1.2.3.2.1. CP–4126

In an attempt to enhance cellular uptake, prolong cell retention, and increase the half-life of gemcitabine with a less hydrophilic moiety, conjugation with a fatty acid side chain at the drug's 5'-site has also been carried out [68, 69]. In this connection, CP–4126 has been developed through esterification of the 5'-position of the nucleoside sugar moiety with elaidic acid, a monounsaturated fatty acid with a *trans*-double bond at carbon 9 (Figure 9).

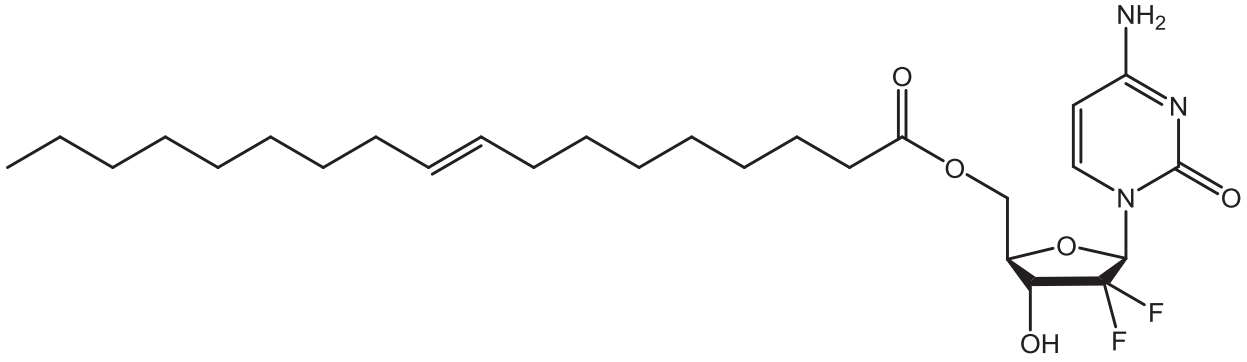

Figure 9: Chemical structure of gemcitabine derivative CP–4126.

Due to its different molecular design, CP–4126 is absorbed by cancer cells independent of hENT1 levels, which improves its efficacy in tumors with low or no hENT1 expression [70]. CP–4126 needs to be converted into gemcitabine by nonidentified esterases, releasing the fatty acid and allowing the free drug to be phosphorylated [71]. *In vitro* tests have shown that IC50 of gemcitabine increased up to 200-fold in deficient nucleoside transport cell lines, but there was no difference with CP–4126, suggesting a nucleoside transporter-independent transport in the cell of the fatty acid derivative [72]. Inside the cell, CP–4126 was localized in the membrane and the cytosolic fraction, leading to long retention after removal of the cell culture medium. This accumulation caused a slower and prolonged release of the gemcitabine from the lipophilic derivative. CP–4126 is active in cells with deficient nucleoside membrane transport [73], but on the other hand, activity of parent gemcitabine and CP–4126 was comparable in the cell lines without resistance, while in dCK deficient cells, both compounds were inactive, because CP–4126 depends, like free gemcitabine, on activation by dCK.

In contrast to parent gemcitabine, which was highly toxic via the oral route, CP–4126 was administered orally with various schedules and an efficient antitumor activity [74]. CP–4126 is currently in a phase II clinical trial with patients with solid tumors [71], to investigate the use of CP–4126 as a second-line treatment for advanced, metastatic pancreatic cancer in patients refractory

to first line gemcitabine treatment, where the resistance mechanism is likely due to impaired drug entry into tumor cells.

1.2.3.2.2. NEO6002

NeoPharm has synthesized a novel gemcitabine-cardiolipin conjugate via a succinate linker to enhance the uptake and efficacy by a prolonged release of gemcitabine in cancer cells [75]. Cardiolipin (CL) is a major membrane phospholipid specifically localized in mitochondria. At the cellular level, CL has been shown to have a role in the triggering of apoptosis [76]. The conjugate is called NEO6002 (Figure 10) and *in vitro* studies showed that this conjugate can improve cytotoxic efficacy and potentially overcome NT-deficient (nucleoside transporters) gemcitabine-resistant tumors, indicating a different internalization route of NEO6002 [77]. NeoPharm's studies on NEO6002 showed evidence of cytotoxicity against various cancer cell lines, including A549 (human lung), BxPC-3 (human pancreas), MX-1 (human breast), HT-29 (human colon), and P388 (murine leukemia) [78]. *In vivo* studies showed that mice treated with gemcitabine for six daily 27 µmol/kg-doses were all moribund, whereas no mouse treated with NEO6002 died. This suggested that NEO6002 was less toxic at equimolar dosage when compared to gemcitabine.

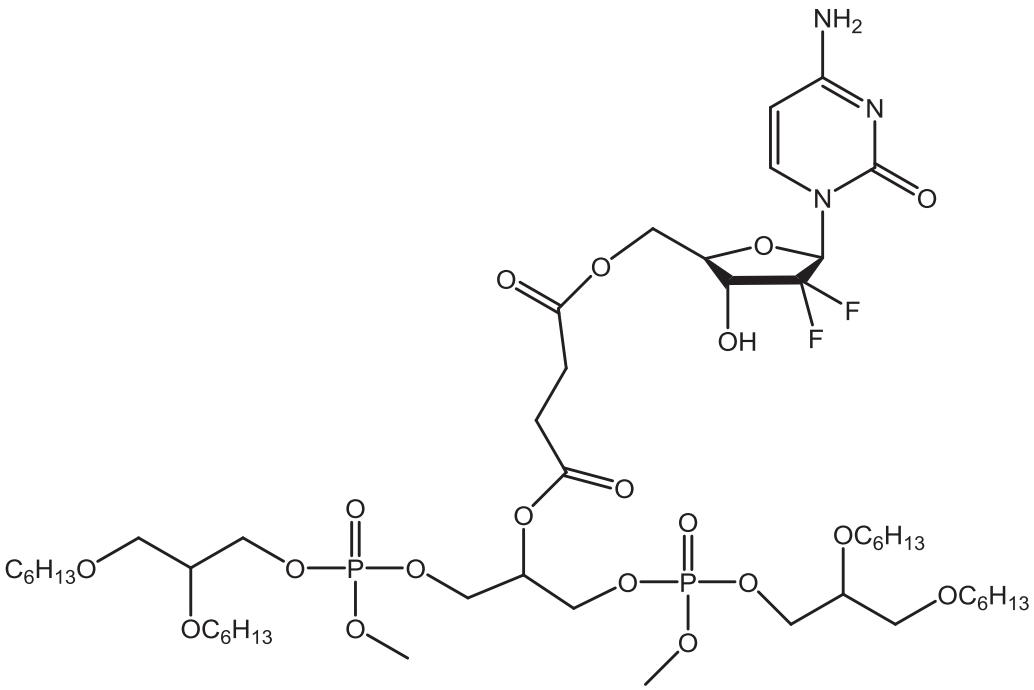

Figure 10: Chemical structure of NEO6002.

1.2.3.2.3. Phosphoramidate Gemcitabine

Because the obligatory phosphorylation is often the rate-limiting step in the activation process of many anticancer drugs and is therefore still one of the limiting factors for the therapeutic use of nucleoside analogues, the use of modified nucleotide prodrugs incorporating a phosphate protecting group, has led to the selective release of the monophosphorylated nucleoside analogue [79]. This modification was tested on gemcitabine to get (a) resistance to chemical degradation, (b) passive diffusion across cell membranes, and (c) release of the monophosphorylated metabolite, independent of kinase expression. These prodrugs were designed to undergo intracellular activation to generate an unstable phosphoramidate intermediate anion, followed by a spontaneous cyclization and P–N bond cleavage by water to liberate the nucleoside monophosphate [80].

In 2009, Perigaud *et al.* synthesized four derivatives of gemcitabine, *N*-(n-butylamino)-*O*-(*S*-pivaloyl-2-thioethyl)-*O*-5'-gemcitabine phosphoramidate diester (Gem-1), *N*-(isopropylamino)-*O*-(*S*-pivaloyl-2-thioethyl)-*O*-5'-gemcitabine phosphoramidate diester (Gem-2), *N*-(benzylamino)-*O*-(*S*-pivaloyl-2-thioethyl)-*O*-5'-gemcitabine phosphoramidate diester (Gem-3), and *N*-(benzylamino)-*O*-(*S*-(2,2-dimethyl-3-hydroxypropionyl)-2-thioethyl)-*O*-5'-gemcitabine phosphoramidate diester (Gem-4) (Figure 11). A better cytotoxicity level was obtained in preliminary *in vitro* tests with Gem-1, Gem-2, and Gem-3 compared to the parent gemcitabine in L1210 10K cell line (23.7 ± 1.2 μM, 18.3 ± 1.5 μM, 9.7 ± 9.0 μM, 36.7 ± 11.6 μM, respectively) [81].

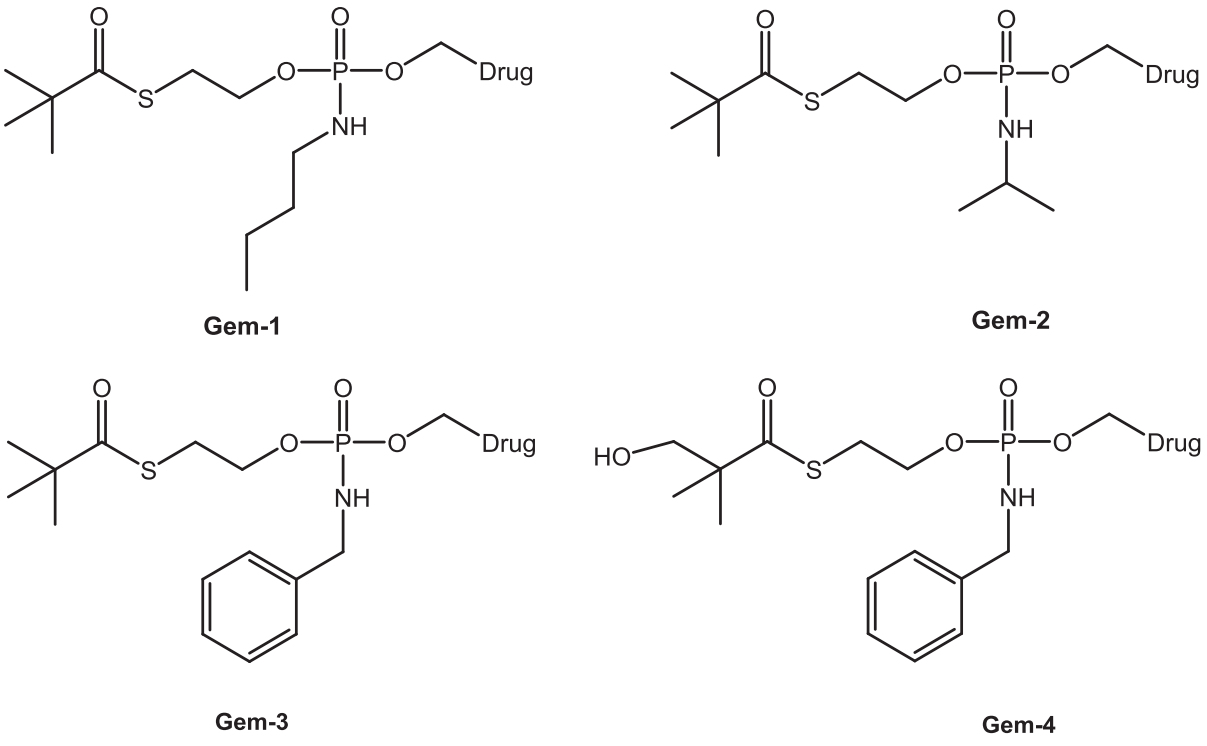

Figure 11: Chemical structures of gemcitabine derivatives Gem-1, Gem-2, Gem-3 and Gem-4.

The purpose of these modifications was to overcome resistance in tumors deficient in dCK by intracellular delivery of gemcitabine 5′-monophosphate after cell-membrane crossing by passive diffusion [82]. *In vitro* tests on many cancer cell lines have shown that the prodrugs are less active than unmodified gemcitabine in wildtype cell lines but more active than the parent drug in dCK deficient cell lines (AG6000 and CEM-dCK). However, after blocking the equilibrative nucleoside transport, the inhibition of tumor growth was no longer observed with the prodrugs, indicating that their antitumor activity was mediated by cell entry implying equilibrative nucleoside transport.

1.2.3.2.4. Gemcitabine prodrugs incorporating D-enantiomer amino acids

Gemcitabine prodrugs with D- and L-amino acids (Figure 12) were synthesized by Tsume's team. Their chemical stability in buffers, resistance to glycosidic bond metabolism, enzymatic activation, permeability in Caco-2 cells and mouse intestinal membrane and antiproliferative activity in cancer cells were determined and compared to that of parent gemcitabine [83].

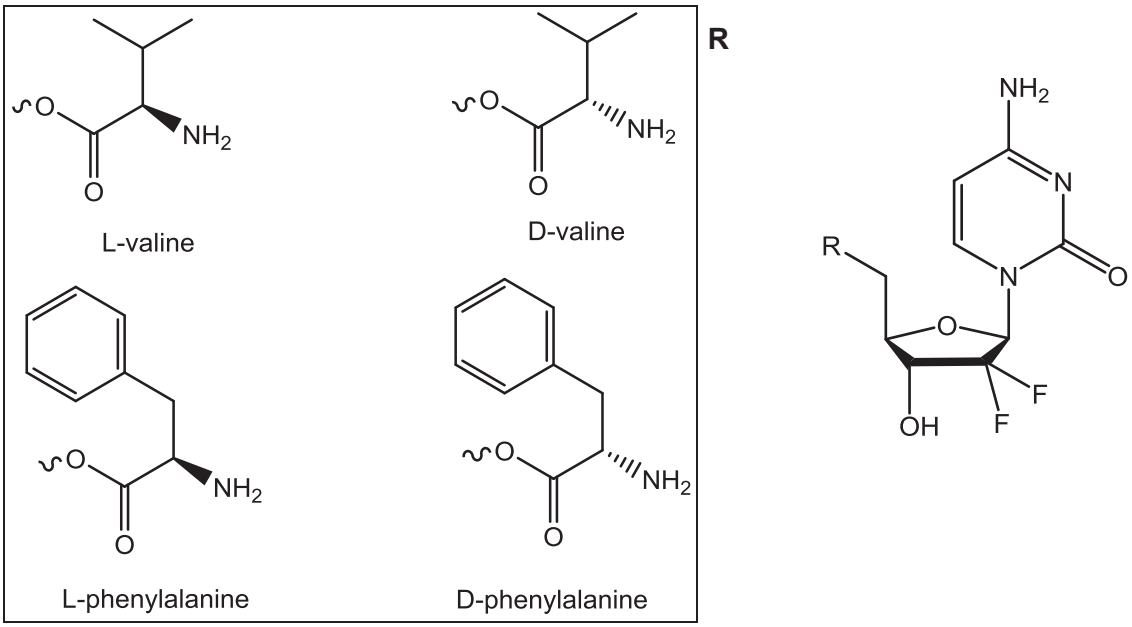

Figure 12: Gemcitabine prodrugs with D- and L-amino acids.

As expected, prodrugs containing D-amino acids were enzymatically more stable than their L-configuration counterparts. The activation of all gemcitabine prodrugs was 1.3 – 17.6-fold faster in cancer cell homogenate than their hydrolysis in buffer, suggesting enzymatic action. The enzymatic activation of amino acid monoester prodrugs containing D-amino acids in cell homogenates was 2.2-10.9-fold slower than for amino acid monoester prodrugs with L-amino acids. All prodrugs exhibited enhanced resistance to glycosidic bond metabolism by thymidine phosphorylase compared to parent gemcitabine. Also, these gemcitabine prodrugs showed

effective permeability in mouse jejunum to superior to gemcitabine. More importantly, the plasma concentration of D-amino acid gemcitabine prodrugs was considerably higher than that of L-amino acid gemcitabine prodrugs.

Overall, gemcitabine has become the standard treatment for pancreatic cancer, and is also widely used in combination for other solid cancers such as lung, bladder, ovary, or breast. The short half-life is not the only drawback; numerous tumors develop resistance mechanisms: resistance by a lack of transporters and resistance by a lack of kinase required for phosphorylation and thus activation are some examples. The chemical modification of a drug is a smart solution to try to override this resistance and improve the resulting pharmacokinetic parameters. Gemcitabine prodrugs have beneficial antitumoral effects by using independent nucleoside transport, by reducing the catabolic effect of CDA, by prolonging the release of the native or monophosphate gemcitabine, and finally by enhancing the cytotoxicity effect. Thus, gemcitabine modification seems to be an innovative and interesting approach to treat less-sensitive cancers. In this connection, this thesis explores the chemical modification of gemcitabine and subsequent conjugation to Cell-Penetrating Peptides (CPP), in an effort to facilitate the delivery of that drug into cancer cells, taking advantage of the fact that all CPP are able to efficiently pass through cell membranes while being non-cytotoxic and carrying a wide variety of cargos inside cells [84]. The main features of CPPs and their chemical synthesis methods are next described.

1.3. Cell-Penetrating Peptides

Today, the treatment and/or cure of genetic diseases, cancer or bacterial infections resistant to conventional antibiotics are some of the greatest challenges in the field of medicine. In this context, peptides and proteins have been the subject of considerable interest in medicine, research and drug development due to a wide variety of applications.

Within the wide variety of peptides used in today's medicine for innumerous applications, Membrane Active Peptides (MAPs) have some particular advantages over small molecules because they have higher specificity and affinity for therapeutic targets, but also in relation to proteins of greater molecular weight in terms of feasibility of synthesis, derivatization flexibility, low immunogenicity and physicochemical parameters compatible with their use as therapeutic agents [85]. MAPs include Cell-Penetrating Peptides (CPPs), capable of efficiently delivering deoxyribonucleic acid (DNA), proteins, or other molecules to the interior of a variety of cell types, via a receptor-independent mechanism while maintaining the integrity of the cell, and Anti-Microbial Peptides (AMPs), which interact with bacteria, fungi or parasites, inhibiting their activity by destabilizing their cell membranes.

CPPs have the intrinsic property to deliver therapeutic molecules (nucleic acids, drugs, imaging agents, etc.) into cells and tissues in a nontoxic manner. This has indicated that they may be potential components of future drugs and disease diagnostic agents. These versatile peptides are simple to synthesize, functionalize, and characterize yet are able to deliver covalently or noncovalently bound bioactive cargos (from small chemical drugs to large plasmid DNA) inside cells, primarily via endocytosis, in order to obtain high levels of gene expression, gene silencing, or tumor targeting, for example (Figure 13). Typically, CPPs are often passive and nonselective, and must be functionalized or chemically modified to create effective delivery vectors that succeed in targeting specific cells or tissues. Furthermore, the design of clinically effective systemic delivery systems requires the same attention to detail in both design of the delivered cargo and the cell-penetrating peptide carrier [84].

Several strategies have been developed to deliver therapeutic agents across cellular membranes, whose hydrophobic nature protects cells from an influx of exogenous molecules, including bioactive molecules such as peptides, proteins, and oligonucleotides. These include microinjection, electroporation, and liposome and viral-based vectors. However, these methods have various drawbacks, including low efficiency, high toxicity, penurious bioavailability, and poor specificity. An alternative strategy emerged from the unexpected finding that short sequences of some proteins exerted membrane-crossing properties, including the 16-mer peptide derived from the third helix homeodomain of *Antennapedia* (later named Penetratin) and the 11-mer derived from TAT protein. These two peptides served as the foundation for the development of CPPs as a new type of molecular vector able to promote the delivery of a variety of cargos.

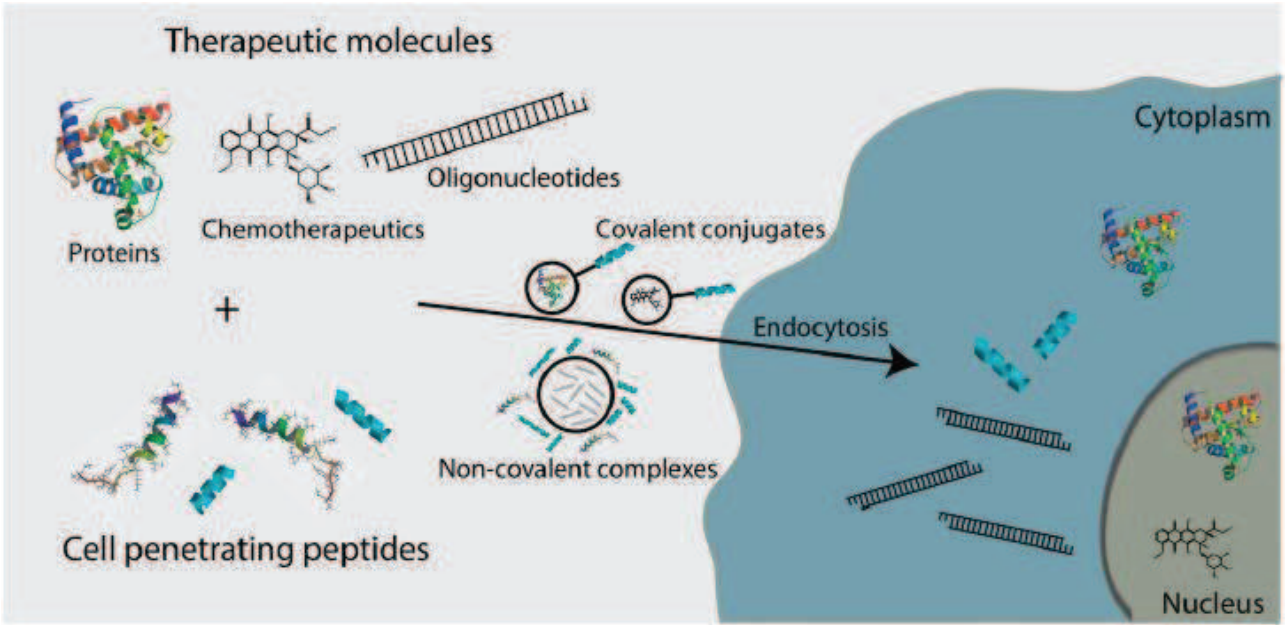

Figure 13: CPPs as delivery vectors – intracellular delivery of CPP-cargo complexes. Reproduced from [84]

In recent years, CPPs have been extensively studied and their main characteristics have been established: low cytotoxicity, ability to be taken up by a variety of cell types, dose-dependent efficiency, and no restriction with respect to the size or type of cargo [86]. In general, CPPs are relatively short peptides that consist of less than 40 amino acids and are able to enter cells by means of various mechanisms, including endocytosis, and are further able to assist in the intracellular delivery of covalently or noncovalently conjugated bioactive cargos.

Understanding the properties and similarities of these peptides is a key factor for the rational design and prediction of new CPPs. For example, almost every CPP sequence involves positively charged amino acids. In fact, a chain of arginines forms one of the most widely used CPPs, R9 [87]. The interactions of a given CPP with cell membranes can also be governed by its secondary structure, specifically helicity. It has been shown that peptides with an R-helical region can more efficiently enter cells [88].

When using CPPs as a delivery system, one must consider that drug delivery must often be highly specific. This has also become a major issue in the design of CPPs because they tend to enter cells nonselectively. The use of a specific drug alleviates this problem, but there are also ways to improve the delivery vector. For example, cell-specific peptide sequences have been shown to target breast cancer cells [89]. With these promising results, it is possible that CPPs could one day emerge as tissue-specific transport vectors for a variety of bioactive molecules [90, 91]. The greatest challenge will be the design of peptides that have specificity for specific glycosaminoglycans (GAGs), lipids or membrane proteins, and thus have the ability to select one internalization pathway over another to specifically deliver the cargo to cells or tissues and thereby promote its biological activity.

1.3.1. Cellular Uptake Mechanisms of CPPs

Although numerous studies report on the uptake mechanisms that transport CPPs across the plasma membrane, the exact pathways through which CPPs enter cells have not been absolutely resolved [92, 93]. Despite many similarities among CPPs, the mechanism of their uptake has been seen to vary considerably. The use of different experimental conditions can also affect the cellular uptake and translocation mechanism of CPPs, as evidenced by contradictory observations. For example, contradictory results are obtained through the use of different concentrations, cell types, incubation time, and various physiochemical parameters of the CPPs, including hydrophobicity and net charge [94-97]. Therefore, it is likely that CPPs without any cargo can be taken up by cells via multiple pathways, including direct penetration of the plasma membrane and endocytic uptake mediated by clathrin, caveolae, and/or other molecules, depending on the nature of the peptide/cell interaction (Figure 14).

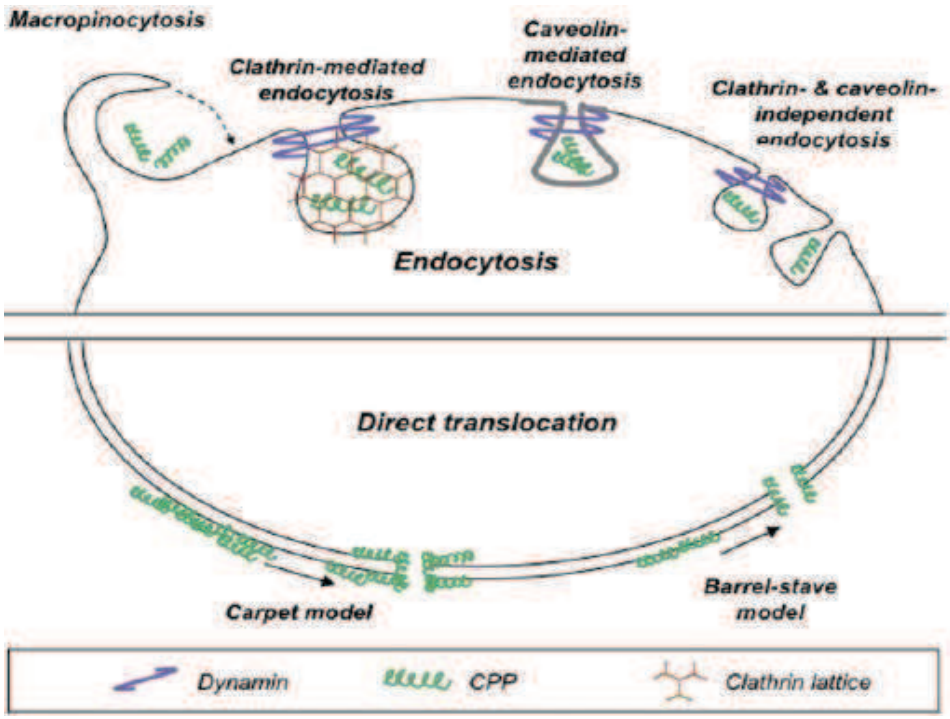

Figure 14: Different mechanisms of cellular uptake CPPs can use to penetrate into cells. Reproduced from [98].

1.3.2. Applications of CPPs

The ability to introduce drugs and other active biomolecules into cells led to investigating the potential use of CPPs as therapeutics. A large number of preclinical studies have reported on the successful applications of complexes of CPPs attached to therapeutic cargos in cancer, muscular dystrophy, cardiology, antiprion diseases, and both viral and bacterial infections [84].

For this thesis, CPPs applications in cancer therapy are the most relevant. Therapeutics that make use of CPPs have been reported in numerous studies over the last two decades. Properly developed CPPs and their conjugates with therapeutics offer a very promising pathway to deliver lower concentrations of toxic drugs to critical tissues such as tumors, heart, etc. One drawback in the use of chemotherapy is the evolution of drug resistance within the cell population. CPP-drug constructs have great potential to increase the solubility, biodistribution, and pharmacokinetic profiles of currently approved chemotherapeutic drugs. Small chemotherapeutic drugs have also been delivered by CPPs (doxorubicin, methotrexate, cyclosporine A, paclitaxel) [98]. CPP-doxorubicin conjugates were demonstrated to exhibit a higher apoptotic efficiency compared with free doxorubicin in the MDA-MB 231 cell line due to the different apoptotic pathways utilized by the CPP construct [99].

In summary, CPPs are cell-penetrating peptides that can efficiently traverse the plasma membrane of both cells and tissues and are successfully used as delivery vectors for therapeutic molecules. After efficient cellular internalization, CPPs are able to release their cargo into the cytosol in order to promote the desired biological effect. When coupled to a cargo, CPPs use endocytosis as the main cellular translocation mechanism. There are several ways to increase the uptake and stability of CPP-cargo complexes *in vivo*, for example, chemical modifications of the structure of known CPPs or rational design of novel CPPs. Further investigations into the structure and mechanisms of uptake of CPP-cargo complexes will be required to evaluate CPPs as potential delivery tools for biomolecules in *in vitro* and *in vivo* models. Prior to use, CPPs must undergo both pharmacological and toxicological studies *in vivo*. Considering evidence from numerous studies, CPPs have the potential to become a universal tool to carry therapeutic molecules across cellular membranes without a risk of toxicity or inflammatory reactions.

For the research developed within scope of this thesis, peptides Penetratin (RQIKIWFQNRRMKWKK) and pVEC (LLIILRRRIRKQAHAHSK) were selected. Penetratin was selected because of its historical significance: it was one of the first CPPs to be discovered and has been extensively studied, including in cancer research [100, 101]. The second peptide, pVEC, equally displays an excellent penetration capability and has been applied to cancer treatment as well [89, 102, 103]. pVEC was chosen for this project due to its sequence similarity to Penetratin, in an attempt to determine the importance of the sequence and size of the peptides in their activity.

1.3.3. Solid Phase Peptide Synthesis (SPPS)

Given the importance and the enormous therapeutic potential of peptides, there is a growing need to obtain them in the necessary quantities and purity degrees for their application in the clinics. Although peptides can be extracted from biological matrices (cells, tissue or even organisms for example), and can also be attained recurring to recombinant DNA expression techniques in microorganisms, these approaches do not yield, in a general sense, peptides in quantities sufficient enough nor with the degree of purity required for therapeutic use.

The chemical synthesis of peptides is the only methodology that allows structural modifications of peptides with a look toward the improvement of their therapeutic index, whether it is through incorporation of unnatural amino acids or other chemical alterations. Additionally, the chemical synthesis generally provides peptides in an even larger scale and with a higher degree of final purity. Therefore, several methodologies have been developed to chemically synthesize peptides. Initially, this type of synthesis was exclusively carried out in solution phase. However, this methodology presents several disadvantages – it is extremely costly, time consuming, complex (each intermediary needs to be isolated and purified) and has low returns. In an effort to overcome these limitations, in 1963, Robert Bruce Merrifield introduced **Solid Phase Peptide Synthesis (SPPS)**, a new method of synthesizing peptides that presents innumerable advantages relative to the peptide synthesis in solution. The peptide is built on an insoluble solid support and the reaction vessel contains a filter and is, normally, connected to a vacuum system. This allows the removal of side products formed and excess of reagents and solvents by washing and filtration. Consequently, the elongation of the peptide up until the sequence is complete is done in a continuous way, and the isolation and purification of the peptide is carried out only once, after cleaving the peptide (separating it from the solid support).

Briefly, in order to synthesize peptides, α-amino acids (AA) are sequentially linked together through the formation of an amide bond (peptide bond). The condensation reaction must be regioselective, being absolutely necessary to suppress the reactivity of functional groups other than those involved in the formation of the peptide bond, that is, the carboxyl group of AA1, the α-amino group of AA2 and reactive functional groups possibly present in side chains of amino acids must be blocked in some way. The reactivity of the α-amino group is suppressed by a temporary protecting group, removed after each coupling (usually 9-fluorenylmethoxycarbonyl (Fmoc) or tert-butoxycarbonyl (Boc)), and the carboxyl group of AA1 as well as any other reactive functional groups in AA side chains are blocked by “permanent” protection, respectively, through the bond linking the peptide to the solid support or the peptide bond or by “permanent” protecting groups (*tert*-butyl (^{t}Bu) or benzyl (Bzl)), respectively. These “permanent” protecting groups are removed when the peptide sequence is completed and the peptide is subjected to a chemical treatment to cleave it from the solid support [104].

Also, and because the reaction between an amino group and a carboxyl group is thermodynamically but not kinetically favored, it is necessary to properly activate the carboxyl group. This activation is achieved with coupling agents, also known as condensation or activating agents. Otherwise, an undesired acid-base reaction will occur leading to the formation of a salt, instead of the intended condensation reaction, bonding the two amino acids through an amide bond.

By convention, the sequential order of amino acids in a peptide is presented in the $N_t \rightarrow C_t$ sense, i.e., with the *N*-terminal amino acid (N_t, with the free α-amino group) on the left and the C-terminal amino acid (C_t, with the free carboxyl group) on the right. However, chemical synthesis is performed in the $C_t \rightarrow N_t$ sense (contrary to the biosynthetic route for protein synthesis in ribosomes). So, in SPPS, a peptide is constructed following cycles of activation and coupling of *N*-protected amino acids and deprotection steps, starting with the C_t amino acid through the N_t amino acid (Figure 15). When the sequence is complete, a chemical cleavage is performed to remove the "permanent" protecting groups and to separate the peptide from the solid support.

In addition to the innumerous advantages of the SPPS methodology (it is much is faster, simpler – and therefore cheaper – and has better yields than peptide synthesis in solution), the SPPS approach was quickly and easily automated (also by Merrifield and collaborators in 1965). Since then, new equipments have been developed, aiming at producing peptides faster and more efficiently. Some equipments can even synthesize different peptides simultaneously (in a small or median scale). One example of these equipments is the Symphony X Multiplex Peptide Synthesizer, developed by Protein Technologies, Inc. ©, which is a 24-channel peptide synthesizer that can run different sequences, scales and protocols on multiple reactors all at the same time, or run up to 12 reaction vessels with preactivation (Figure 16).

Nevertheless, and although SPPS has evolved a considerable extent, there are still some challenges to overcome when synthesizing peptides, including racemization problems, the aggregation of peptide chains as the sequence gets longer, the intramolecular interactions that make the peptide coil on itself, and other steric hindrance problems. Recently, heat provided by microwave radiation (MW) has been used to try to surpass aggregation problems. Since the first serious experiments for synthesizing peptides with the help of microwaves in 1992 [105], the Microwave Assisted Peptide Synthesis (MAPS) or MW-SPPS approach has evolved greatly and has been incorporated in some automated systems, such as the Liberty1 Microwave Peptide Synthesizer© developed by CEM Corporation (Figure 17). Additionally, with this approach, coupling reactions are much faster and, in many cases, the synthesis yield and the peptides' purity are also higher. However, some side reactions can be favored as well as the chemical modification of some amino acids (cysteine, histidine and aspartic acid are more prone to undergo racemization and other modifications).

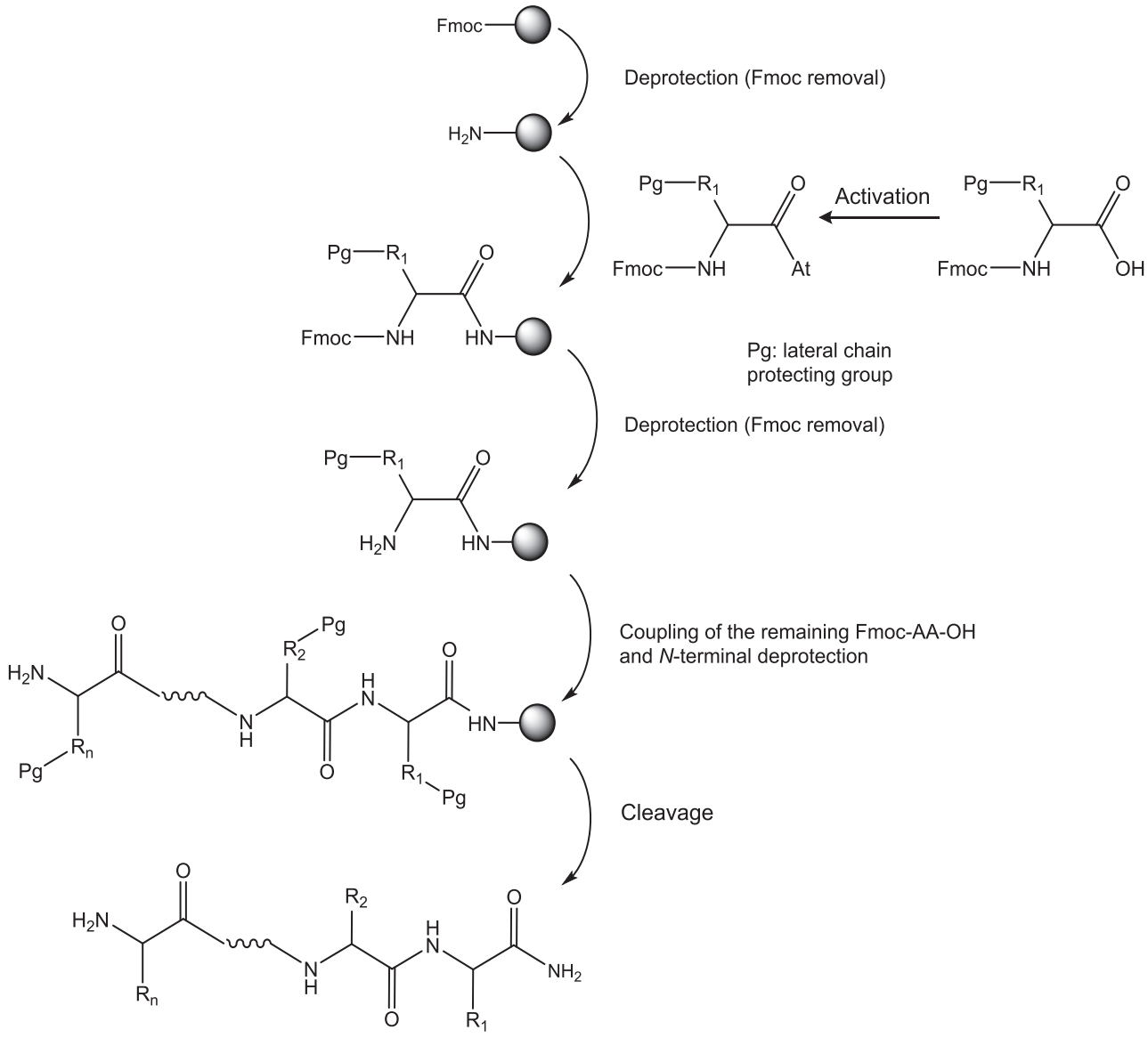

Figure 15: General procedures in SPPS, following the Fmoc/^{t}Bu orthogonal protection scheme.

Figure 16: Symphony X Multiplex Peptide Synthesizer ©, available in our laboratory.

Figure 17: CEM Liberty1 Microwave Peptide Synthesizer™, used in this project.

In summary, the SPPS methodology is faster, simpler, cheaper and more efficient than peptide synthesis in solution. Moreover, the current technology and the use of MW radiation make peptide synthesis even faster and higher yielding. Nowadays, numerous peptide sequences can be easily obtained, containing unnatural amino acids or some structural modification if necessary for their application. These modified peptides cannot be provided by the biosynthetic pathway. Thus, SPPS has allowed peptides to have a greater prominence and importance in several and diverse areas, from biomedical engineering and the development of new drugs to nanotechnology.

In this project, all peptides were synthesized as C-terminal amides, following standard SPPS procedures, with an orthogonal Fmoc/^{t}Bu protection scheme. Peptides were synthesized both manually and recurring to a CEM Liberty1 Microwave Peptide Synthesizer™ (Figure 17).

2. EXPERIMENTAL

2.1. Reagents, Solvents and Equipments

All solvents used in this study were of analytical grade. Reagents and solvents were purchased from Novabiochem (Fmoc-amino acids and Fmoc-Rink Amide MBHA resin), Merck (TFA and other solvents), Sigma-Aldrich (coupling agents, piperidin, *N*-ethyl-*N,N*-diisopropylamine (DIPEA) and 3-(tritylthio)propionic acid) and Carbosynth Ltd. (Berkshire, UK) (gemcitabine hydrochloride).

Compounds' purity and conjugates' time-dependent kinetics studies were determined by high-performance liquid chromatography with diode array detection (HPLC-DAD) on a Merck-Hitachi LaChrom Elite equipment, with quaternary pump, automatic and thermostated by Peltier effect injector and a diode detector. A reverse phase Purospher star RP C-18 (octadecylsilane) column (125 x 4.0 mm), with a particle diameter of 5 µm, was used. The elution was performed with a variable gradient of acetonitrile (ACN) in water containing 0.05% trifluoroacetic acid (TFA), at a 1 mL/min flow and detection at variable wavelength (220 or 270 nm).

Drug-CPP conjugates were purified by Reverse Phase Medium-Pressure Liquid Chromatography (RP-MPLC), using a C18 Vydac® 218TP stationary phase, by Grace Vydac.

The mass spectrometry analyses were performed on a Thermo Scientific LTQ Orbitrap XL spectrometer, with electrospray ionization and both quadrupole ion trap (ESI-IT MS) and Orbitrap detection (Materials Centre of the University of Porto, CEMUP).

After purification and characterization, peptides and conjugates were lyophilized in a BenchTop Pro 9L with omnitronics from SP Scientific (Department of Chemistry and Biochemistry of Faculty of Sciences of University of Porto).

Cell viability assays were conducted using flat bottom 96-well plates by TPP Techno Plastic Products (Switzerland) and a microplate reader by Bio-tek Instruments Inc. (Powerwave XS, Winooski, EUA).

2.2. Peptide Synthesis by SPPS

2.2.1. Manual Synthesis

2.2.1.1. Experimental setup

Manual syntheses took place in a polypropylene syringe with a polyethylene porous filter adapted to a vacuum system to eliminate the excess of reagents and the solvents used to wash the resin after each reaction step. A *Teflon*™ rod was used to manually stir the resin beads throughout the syntheses (Figure 18).

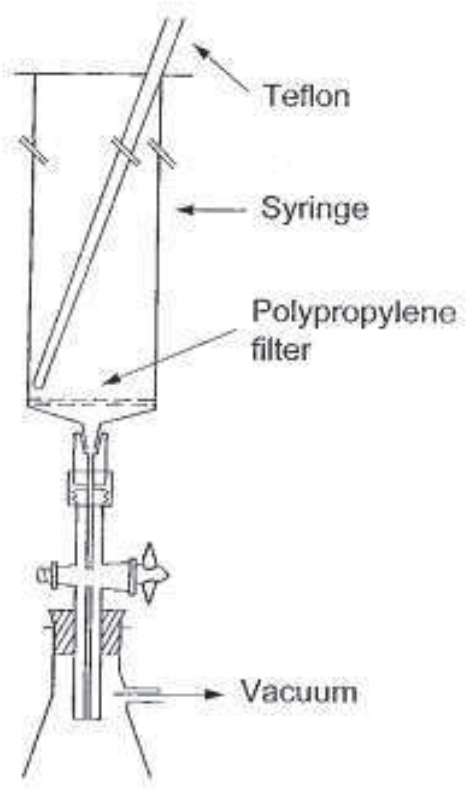

Figure 18: Experimental setup for manual SPPS.

2.2.1.2. Preparation of the resin

The resin used in the syntheses was the Fmoc-Rink Amide MBHA, a polystyrene-based polymer functionalized with 4-methylbenzhydrylamine (MBHA) groups, further modified with an N-Fmoc protected (R,S)-2-{4-[amino(2,4-dimethoxyphenyl)methyl]phenoxy}acetic acid linker (Rink or Knorr linker) (Figure 19). The resin had a 0.60 mmol/g loading capacity and syntheses were performed at 0.2 mmol scale, so 0.33 g of resin were required for each synthesis. The dry resin was transferred into the syringe and was conditioned in *N,N*-dimethylformamide (DMF) for 20 min. After that time, DMF was rejected and the resin was swelled in dichloromethane (DCM) for another 15 min.

The initial deprotection step (release of the free amino group of the Rink linker) was carried out using 20% piperidine in DMF (3 mL, 1 x 1 min + 1 x 20 min). After the deprotection, the resin was washed with DMF (3 mL, 3 x 1 min) and DCM (3 mL, 3 x 1 min) and a Kaiser test was performed. Upon a positive Kaiser test (dark blue resin beads and solution), release of the free amine groups is confirmed and, therefore, the construction of the peptide chain can be initiated.

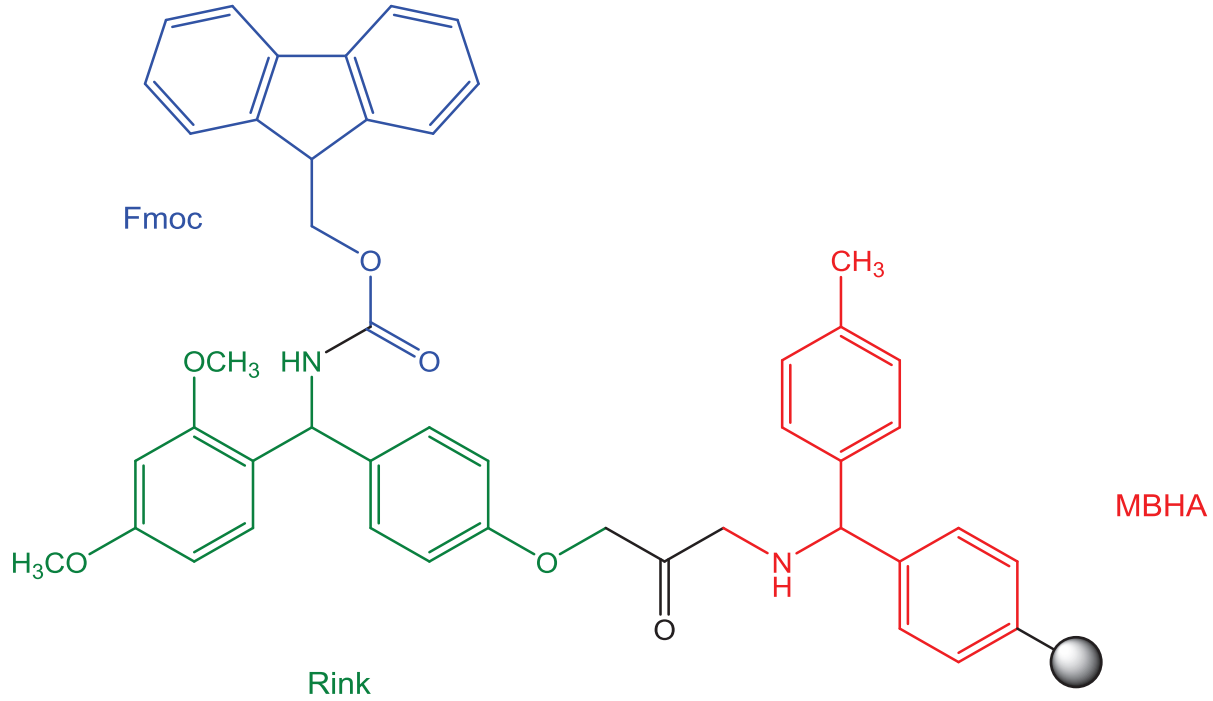

Figure 19: Chemical structure of the Fmoc-Rink Amide MBHA resin (polystyrene base polymer represented by the grey sphere).

.

2.2.1.3. Kaiser Test

The Kaiser (or ninhydrin) test is a qualitative assay used to detect the presence or absence of free primary amino groups, revealing whether a coupling or deprotection step was successful. It is based on a colorimetric reaction that occurs between ninhydrin (yellow) and free primary amino groups, leading to the formation of a blue chromophore known as Ruhemann's purple (Figure 20).

Kaiser tests were carried out by transferring a few dry resin beads to a small glass tube and adding the test reagents A and B in a 3 to 1 proportion (6 drops of reagent A and 2 drops of reagent B). After homogenization, the test tube was placed in an oven at 110 ºC and after 3 minutes the color of the resin beads and solution was assessed. After coupling one N-Fmoc protected amino acid, the peptidyl-resin should not react with ninhydrin, and so it should remain yellow (negative test). However, as a successful deprotection step removes the Fmoc group, leaving the amine group available to react with ninhydrin, the peptidyl-resin and the solution should turn (dark) blue (positive test). When the test indicated a step wasn't completed, that step was repeated.

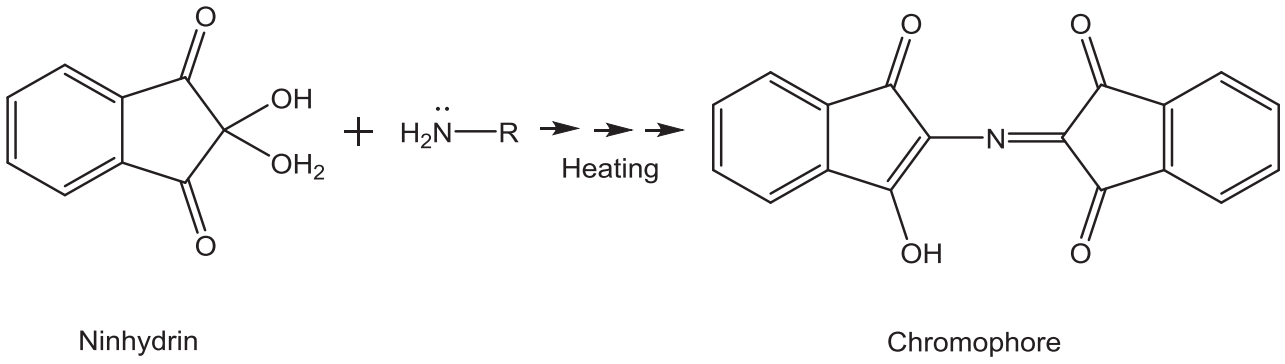

Figure 20: Ninhydrin general reaction with primary amines, resulting in the formation of a chromophore.

The preparation of reagents A and B used in the Kaiser tests undertaken was as follows:

Reagent A: a solution of phenol (40 g) was prepared in 10 mL of ethanol (EtOH). Next, 2 mL of an aqueous solution of KCN (16.5 mg/25 mL) were mixed with 100 mL of freshly distilled pyridine. Finally, the two solutions were mixed together.

Reagent B: solution of 5 g of ninhydrin in 100 mL of EtOH (this solution was protected from light).

2.2.1.4. Coupling of Amino Acids and Deprotection Cycles

Prior to coupling, amino acids were activated in solution for approximately 5 min before being transferred to the syringe to react with the resin or peptidyl-resin. This activation was accomplished by preparing a solution of Fmoc-AA-OH (5 eq.), coupling agent *O*-(benzotriazol-1-yl)-*N,N,N′,N′*-tetramethyluronium hexafluorophosphate (HBTU, 5 eq.) and base DIPEA (10 eq.) in DMF. Solvents are used in only sufficient volumes to ensure the proper solvation of the amino acids and the peptidyl-resin beads, which is a crucial condition for efficient chain assembly. The activated amino acid solution was then transferred to the reaction vessel to react with the previously deprotected resin or peptidyl-resin for 1 h, under stirring. After this time, the peptidyl-resin was washed with DMF (3 mL, 3 x 1 min) and DCM (3 mL, 3 x 1 min) to eliminate the excess of reagents, solvents and side products and a Kaiser test was performed to confirm the efficiency of the coupling. When the Kaiser test was negative, the following deprotection step was carried out, using the deprotection solution (20% piperidine in DMF (3 mL, 1 x 1 min + 1 x 20 min). Once deprotection was completed, the resin was washed again with DMF (3 mL, 3 x 1 min) and DCM (3 mL, 3 x 1 min) and another Kaiser test was performed. When the deprotection was confirmed by a positive Kaiser test, the next Fmoc-AA-OH was coupled following the same aforementioned conditions. The peptide sequence was completed by repeating the cycles of coupling of N-Fmoc amino acids and deprotection steps.

The procedures for the coupling and deprotection steps are given in detail in Table 1:

Table 1: General steps of Fmoc/^{t}Bu SPPS.

Step	Reagents/Solvents	Operation	Time (min)	Repetitions
Deprotection (removal of Fmoc group)	20% piperidine in DMF (v/v)	Deprotection	1 20	1 1
	DMF	Wash	1	3
	DCM	Wash	1	3
	Kaiser test	Control	3	1
Coupling of Fmoc-amino acids	Fmoc-AA-OH (5 eq) HBTU (5 eq) DIPEA (10 eq)	Coupling	60	1
	DMF	Wash	1	3
	DCM	Wash	1	3
	Kaiser test	Control	3	1

2.2.2. SPPS Assisted by Microwave Energy

A Liberty1 Microwave Peptide Synthesizer (CEM Corporation) was used to synthesize both Cys-Penetratin and Cys-pVEC peptides, using a 0.1 mmol scale and Fmoc-Rink Amide MBHA resin (loading capacity: 0.60 mmol/g). The resin was conditioned by solvating in DMF for 30 min and transferred to the equipment's reaction vessel.

In order to try to obtain better yields, double couplings were programmed for the amino acid residues tryptophan, glutamine, serine and arginine, as well as for the first amino acid of each sequence (lysine for both peptides). The experimental conditions for the coupling and deprotection steps are detailed in Table 2.

Table 2: Experimental conditions for SPPS on the CEM Libery1 Peptide Synthesizer.

Step	Reagents/Solvents	Microwave Power (W)	Temperature (ºC)	Time (s)
Removal of Fmoc group from the resin	Deprotection solution	35	75	30 x 2
Removal of Fmoc group from the AA		35	75	180
Fmoc-AA-OH coupling	Fmoc-AA-OH (0.2 M in DMF) Activator solution Activator base solution	30[a]	75[a]	300[a]

[a] 25 W, 50 ºC and 240 s for Fmoc-Cys(Trt)OH; 25 W, 75 ºC and 300 s for Fmoc-Arg(Pbf)-OH.

In the MW-assisted synthesis of the target peptides, the composition of the deprotection, coupling activator and coupling base solutions were as follows:

***Deprotection solution*:** 20% piperidine (v/v), HOBt·H_2O 0.1 M in DMF

***Activator solution*:** HBTU, HOBt 0.5 M in DMF

***Activator base solution*:** DIEA 2.0 M in NMP

2.3. Cleavage: separating the peptide from the resin and removing the side chain protecting groups

When the peptidic sequence was completed and after the final deprotection, the peptidyl-resin was subjected to a chemical treatment that cleaves the bond linking the peptide to the resin beads. First, a cleavage cocktail (cocktail R) was prepared in the hood, containing 90% TFA, 5% thioanisole, 3% 1,2-ethanedithiol and 2% anisole (v/v). Then, the dry peptidyl-resin was transferred to 15 mL Falcon tubes in 100 mg portions and 1 mL of cleavage cocktail was added to each portion. The tubes were left under orbital stirring for 2.5 h at room temperature. After that time, the peptide should be soluble in the solution and so the content of the tubes was filtered on a D4 funnel previously rinsed with TFA, and the resin beads were washed with TFA. The filtrate, containing the soluble peptide, was transferred to new Falcon tubes in 1 mL portions and 14 mL of cold *tert*-butyl methyl ether were added to each tube. After slightly shaking the tubes, they were cooled to -22 ºC for about 8 minutes and then centrifuged at 3500 rpm for 7 minutes at -5 ºC. The ether was carefully rejected and “fresh” ether was added again. The addition of ether and centrifugation were repeated 3 more times and finally the tubes were left in a vacuum desiccator until the crude peptide was dry. Dry peptide pellets were then solubilized in 10% aqueous acetic acid and analyzed by HPLC-DAD and HPLC hyphenated with ESI-IT MS (LC-MS).

2.4. Structural modification of Gemcitabine

In order to conjugate gemcitabine with the CPPs, the hydrochloride salt of the drug was chemically modified to compound **(4)** according to a recently described protocol [67]. Firstly, gemcitabine had to be modified to *N*-[3-(*S*-trityl)sulfanyl]propanoylgemcitabine **(3)**, after which the trityl (Trt) protecting group was removed, producing the free thiol, i.e. yielding *N*-(3-sulfanyl)propanoylgemcitabine **(4)** (Figure 21). Compound **(4)** was then used for either the direct coupling with the Cys-modified CPPs (route e) in Figure 21) (***Strategy A***) or for subsequent S-derivatization with 2,2-disulfanyldipyridine to afford compound **(7),** that was next coupled to the Cys-modified CPPs (route d) in Figure 21) to produce the target conjugates **(5)** (***Strategy B***). Detailed procedures are next described.

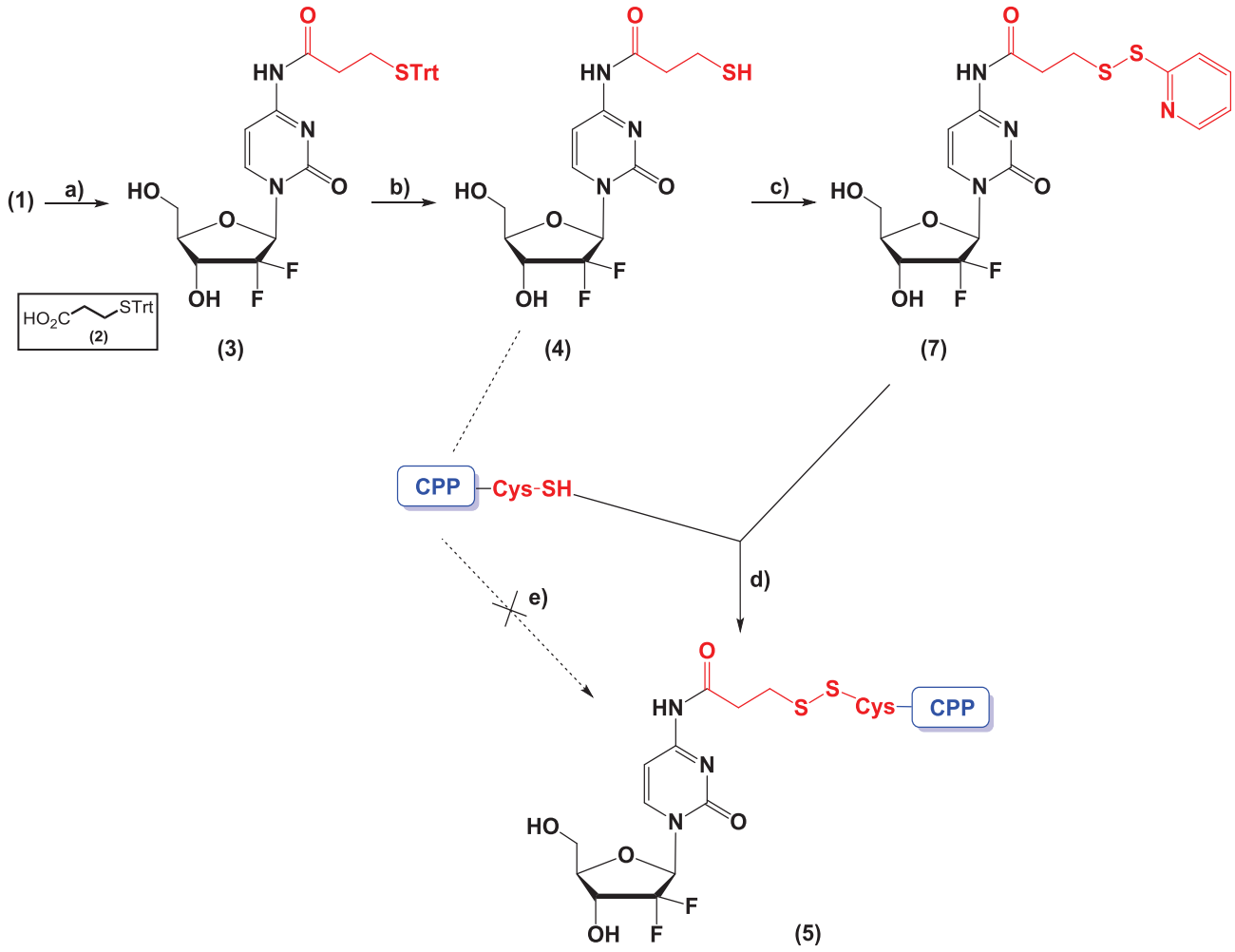

Figure 21: Synthesis of new CPP-Gemcitabine conjugates **(5)**. a) 3-(*S*-trityl)sulfanylpropanoic acid **(2)**, TBTU, DIEA, DMF, 0 ºC - rt, 24h, (45%); b) DCM/TFA 1:1, Et_3SiH 0 ºC, 1h (95%); c) 2,2-disulfanyldipyridine **(6)**, MeOH, AcOH, rt, 24h (60%); d) DMF, rt, 24 h (95% for Pen; 60% for pVEC); e) 5% DMSO in H_2O/ACN (3:1), pH 8 (dil. NH_4OH), 24h.

2.4.1. Synthesis of *N*-[3-(*S*-trityl)sulfanyl]propanoylgemcitabine (3)

Briefly, 3-(*S*-trityl)sulfanylpropanoic (0.24 g, 0.6 mmol) was dissolved in 2 mL of anhydrous DMF. The reaction mixture was brought to 0 ºC and then *O*-(Benzotriazol-1-yl)-*N,N,N',N'*-tetramethyluronium tetrafluoro borate (TBTU) (0.26 g, 0.8 mmol) was added to this solution followed by 0.2 mL (1.3 mmol) of DIPEA. After 30 min, gemcitabine hydrochloride (0.2 g, 0.7 mmol) was added to the reaction mixture, which was stirred for another 30 min at 0 ºC and then allowed to warm to room temperature and stirred for 24 h, and monitored by TLC. The reaction mixture was washed with DCM 3 times and the solvents were evaporated under reduced pressure. Liquid–liquid extraction followed by liquid chromatography on silica-gel using DCM/propanone (Me_2CO) 1:1 (v/v) as eluent were performed to purify the crude product. Compound **(3)** was obtained with a 45% yield.

2.4.2. Synthesis of *N*-(3-sulfanyl)propanoylgemcitabine (4)

Compound **(3)** (0.4813 g, 1 eq) was brought to 0 ºC and 2.0 mL of a TFA:DCM (1:1 v/v) solution were added followed by triethylsilane (TES) (2.4 eq). The mixture was stirred for 2 h, and the solvents were then removed under reduced pressure. The crude product was washed with *tert*-butyl methyl ether 3 times and dried under reduced pressure. Compound **(4)** was obtained with a 95% yield and analyzed by HPLC at 2 different wavelengths and by ESI-IT MS.

2.5. First approach to the synthesis of the conjugate Gemcitabine –Linker–Penetratin: *Strategy A*

To obtain the desired conjugates, a protocol described by Albericio *et al*. for the formation of a disulfide bridge between the modified drug and the Cys-modified peptide was followed [106]. To that purpose, compound **(4)** and the peptide Cys-Penetratin were dissolved in H_2O/ACN (3:1 v/v, 4 mL) containing 5% dimethylsulfoxide (DMSO), and the pH was adjusted to 8.0 with dilute NH_4OH. The reaction mixture was stirred at room temperature and monitored by HPLC (elution in gradient mode, 0 – 100% ACN in water with 0.05% TFA). After 26 h of reaction, the solvents were removed under reduced pressure and the crude product was washed with methanol (MeOH). Once the product was dried in a vacuum desiccator, it was analyzed by HPLC at 2 different wavelengths and LC-ESI/MS and found not to correspond to the target conjugate.

2.6. Synthesis of the Gemcitabine–Linker–CPP conjugates: *Strategy B*

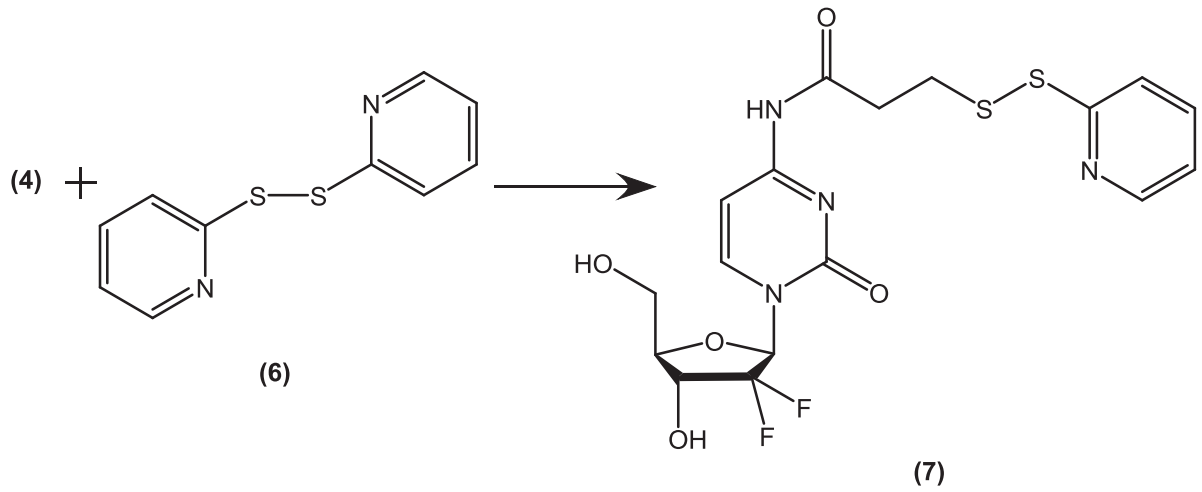

Figure 22: Synthesis of Gemcitabine-dithiopyridine **(7)**.

N-(3-sulfanyl)propanoylgemcitabine **(4)** was converted into *N*-{3-[*S*-(2-sulfanyl)pyridyl]sulfanyl} propanoylgemcitabine **(7)** following a protocol described by Dasari *et al*. [67]. Briefly, compound **(4)** (0.038 g, 0.1 mmol) and 2,2'-disulfanyldipyridine **(6)** (0.054 g, 0.25 mmol) were dissolved in anhydrous MeOH (2.5 mL) containing glacial acetic acid (1.8 µL, 0.03 mmol). The reaction mixture was stirred at room temperature for 24 h and monitored by TLC. The crude product was purified by column chromatography on silica-gel, using DCM/MeOH 7:1 as eluent (60% yield), and its structure subsequently identified as compound **(7)** by HPLC and ESI-IT MS.

To obtain the conjugates, compound **(7)** (0.022 g, 0.047 mmol) and Cys–CPPs (0.056 g, 0.024 mmol) were dissolved in anhydrous DMF with triethylamine (3.3 µL, 0.024 mmol). The reaction mixture was stirred under an argon atmosphere and monitored by HPLC. After 24 h, the reaction was stopped and the crude product was analyzed by HPLC and LC/ESI-MS (95% yield for conjugation with Cys-Pen and 60% for Cys-pVEC).

2.7. Purification of the conjugates

Drug-peptide conjugates were solubilized in the minimum volume required of 10% aqueous acetic acid and purified by Reverse Phase Medium-Pressure Liquid Chromatography (RP-MPLC), using ACN in water with 0.05% TFA as eluent, in gradient mode (15 – 40%). The collected fractions were analyzed by HPLC to determine which contained the conjugate with a purity greater than 92%. These fractions were subsequently pooled and lyophilized.

2.8. Stability studies

2.8.1. Calibration curve

A phosphate-buffered saline (PBS) with pH = 7.4 was prepared and seven gemcitabine standard solutions with different concentrations (100.0, 85.0, 70.0, 55.0, 40.0, 20.0, and 10.0 μg/mL) were prepared in that buffer to trace the calibration curve. These solutions and the PBS control ([Gemcitabine] = 0 μg/mL) were analyzed by HPLC, using ACN in water with 0.05% TFA as eluent, in gradient mode (0 – 100%), for 30 minutes, at a flow rate of 1 mL/min and detection at λ = 220 and 270 nm. The calibration curve was traced using the absorption values of the peak relative to gemcitabine.

2.8.2. Study of conjugates' stability at physiological pH and temperature

To determine the extension of the hydrolysis of the conjugates' bonds, both Gemcitabine–Linker–Penetratin and Gemcitabine–Linker–pVEC conjugates were dissolved in PBS (200.0 μg/mL) and left under magnetic agitation for 6 days at 37 ºC, with periodic uptake of aliquots that were subjected to HPLC analysis, with detection at 220 and 270 nm.

This study was repeated for the Gemcitabine–Linker–Penetratin conjugate, in the same conditions, for 22 days.

2.9. *In vitro* growth inhibition assays

2.9.1. Cell cultures

2.9.1.1. Cell cultures conditions

All the manipulations involving cell cultures were performed in a vertical laminar flow cabinet biosafety level 2A (ADS *Laminaire*). Cell cultures were always incubated at a temperature of 37 ºC in a humidified atmosphere with 5% CO_2.

2.9.1.2. Cell lines

Three different cell lines were tested in this study: Caco-2 (heterogeneous human epithelial colorectal adenocarcinoma), MKN-28 (human gastric cancer) and HT-29 (human colon adenocarcinoma). The cells were grown as monolayer in cell culture plates and maintained in cell culture medium. Cells were always exponentially growing, having conducted its subculture by trypsinization, once or twice a week.

Caco-2 and HT-29 cells were kindly provided from Faculty of Medicine of University of Porto (FMUP) and MKN-28 cells were provided by the Institute of Molecular Pathology and Immunology of the University of Porto (IPATIMUP, Porto, Portugal).

2.9.1.3. Culture medium

Caco-2 cells were maintained in Minimum Essential Medium (MEME), supplemented with 15% of inactivated fetal bovine serum (FBS), 2 mL of glutamax (L-alanyl-L-glutamine), 1% antibiotic/antimycotic solution (100 units/mL penicillin, 100 µg/mL streptomycin and 2.5 µg/mL of amphotericin B). To inactivate FBS, the serum was in a water bath at 56 ºC for 1 h.

MKN-28 and HT-29 cells were maintained in complete culture medium RPMI 1640 AQmedia containing 10% heat-inactivated FBS, 1% antibiotic/antimycotic solution (100 units/mL penicillin, 100 µg/mL streptomycin and 2.5 µg/mL of amphotericin B).

2.9.1.4. Trypsinization of the cell lines

The trypsinization consisted on the detachment of the monolayer cells upon the action of a trypsin solution. Briefly, after removing the cell culture medium, the cells were washed with PBS and the trypsin solution was added. After 1 min, the excess of trypsin was removed and the cells were then incubated for about 5 min at 37 ºC, until the cells are detached from the culture plate. Trypsin action was terminated by the addition of culture medium, through the inhibitors present in FBS.

2.9.1.5. Evaluation of cell viability

Cell viability was evaluated with the vital stain, trypan blue. After trypsinization, the total number of viable cells was determined for all cell lines. For this purpose, 50 µL of cell suspension were added to 50 µL of trypan blue and the number of viable cells (not colored, because of their ability to exclude the stain) was determined in a Neubauer chamber. The number of viable cells was expressed per mL of cellular suspension.

2.9.1.6. Maintaining cells in exponentially growth phase

After trypsinization, cell density was adjusted to 1.5 x 10^5 viable cells/mL, in culture medium.

2.9.2. Sulforhodamine B (SRB) assay: evaluation of the antiproliferative activity of the compounds

The effect of the compounds on the growth of the three cell lines was evaluated according to the procedure adopted by the National Cancer Institute (NCI, USA) in the "*In vitro Anticancer Drug Discovery Screen*" that uses the protein-binding dye Sulforhodamine B (SRB) to assess cell growth [107, 108]. This is a micromethod that uses 96-well plates and evaluates the effect of compounds on exponentially growing cells after continuous exposure for 48 h, through the quantification of the cellular protein content by the protein dye SRB.

The cell lines were inoculated in flat bottom 96-well plates (100 µL/well) at the density that ensures the exponential grow, and incubated for 24 h before the addition of the compounds, to allow the cells to adhere and stabilize. Five different concentrations were tested for each compound: 100.0; 50.0; 25.0; 12.5 e 6.3 µM (100 µL/well), which were prepared by serial dilution (1:2) in culture medium. In the control cells, the addition of compound was replaced by the addition of culture medium.

After a 48 h incubation with the compounds, the cells were fixated with a solution of trichloroacetic acid (TCA) 50% for 60 min at 4 ºC, followed by a wash step with H_2O. The plates were completely dried, and the cells were then dyed with a SRB solution (0.4% in 1% acetic glacial acid) (50 µL/well) for 30 min, at room temperature. The excess of SRB was removed and the plates were washed with a solution of 1% acetic acid. Plates were dried once again and the bound SRB was solubilized in Tris-HCl buffer (10 mM in H_2O, pH 10.5) (100 µL/well). The absorbance was measured at 492 nm in a microplate reader. Cellular proliferation was expressed as the percentage of optic density (OD) relative to the OD of the control cells.

3. RESULTS AND DISCUSSION

3.1. Peptide Synthesis

3.1.1. Manual Synthesis of Cys-Penetratin

After the manual synthesis of the peptide Penetratin, modified with an N-terminal cysteine residue (Cys-Pen) to allow the posterior conjugation to modified gemcitabine, the peptide was cleaved from the resin following the protocol described in the Experimental section. Once dried in the vacuum desiccator and then solubilized in 10% aqueous acetic acid, the crude product was analyzed by HPLC and LC-ESI/MS (Figure 23 and Figure 24). The sequence and exact mass of the Cys-Pen and the m/z ratios of its adducts with H^+ detected by ESI-IT MS are presented in Table 3.

Table 3: Sequence and exact mass of the Cys-Penetratin peptide and m/z ratios of its adducts with H^+ detected by ESI-IT MS.

Peptide	Sequence	Exact Mass (Da)
Cys-Penetratin	C-RQIKIWFQNRRMKWKK	2347.3147
Adducts	m/z	
$(P + 2H)^{2+}$	1175.4606	
$(P + 3H)^{3+}$	783.9737	
$(P + 4H)^{4+}$	588.2303	
$(P + 5H)^{5+}$	470.7842	
$(P + 6H)^{6+}$	392.4869	
$(P + 7H)^{7+}$	336.5602	

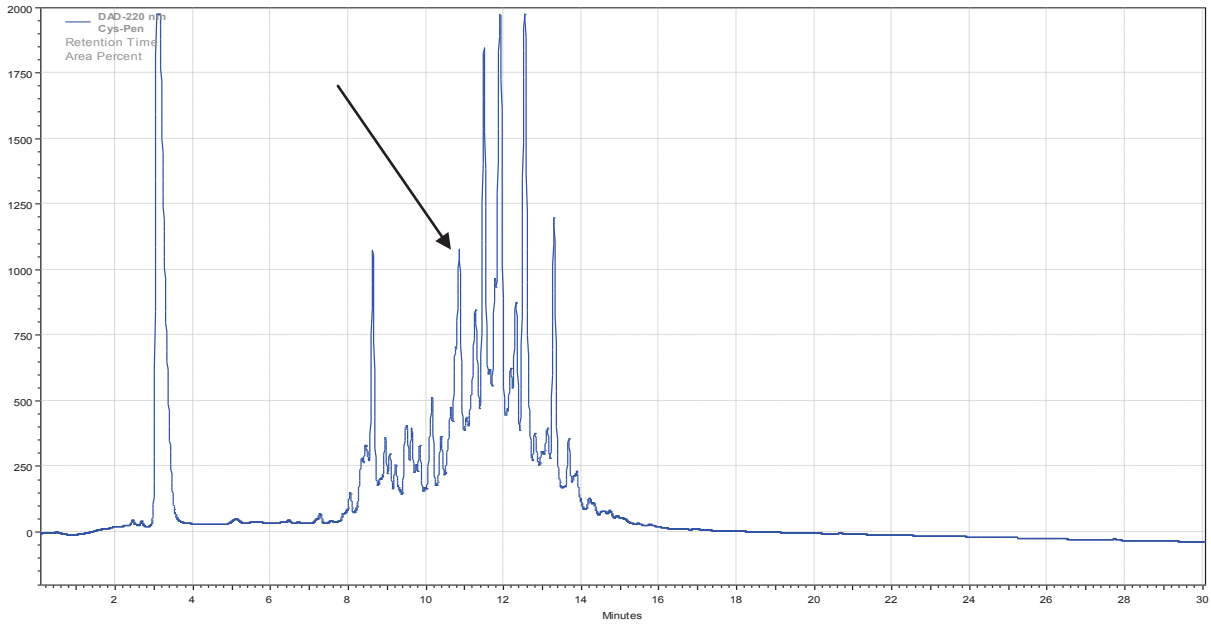

Figure 23: Chromatogram of the crude product obtained in the manual synthesis of Cys-Penetratin, acquired with a HPLC-DAD system, with a C18 column, using ACN in water with 0.05% TFA as eluent, in gradient mode (0 – 100%), for 30 minutes, at a flow rate of 1 mL/min and detection at λ = 220 nm. The arrow indicates the chromatographic peak that was identified as the target peptide by LC-ESI/Orbitrap MS (mass spectrum on Figure 24).

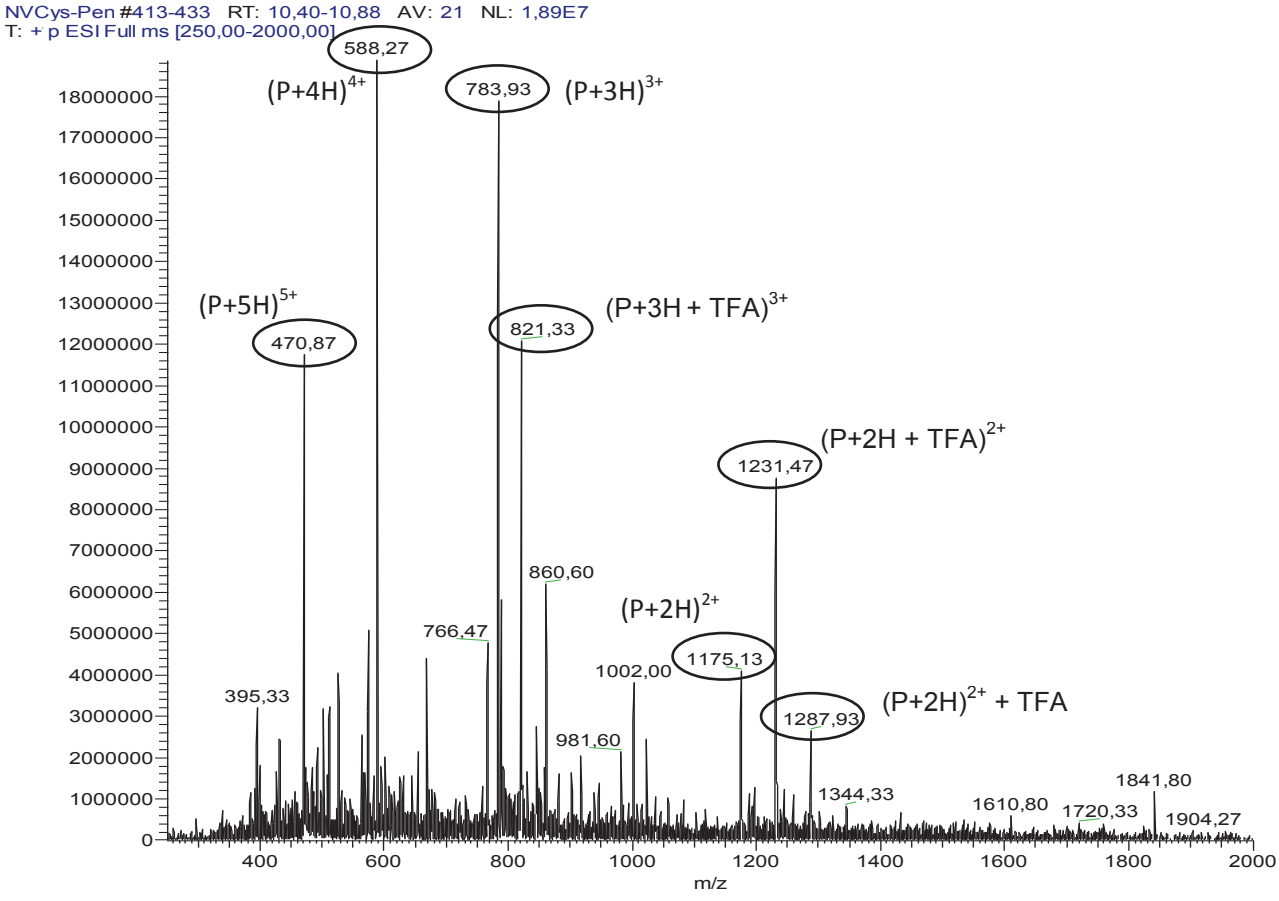

Figure 24: Mass spectrum (LC-ESI/Orbitrap MS, positive mode) of the Cys-Penetratin peptide (manual synthesis).

Together, these results show that the manual synthesis of this peptide results in a very complex combination of different products. The HPLC chromatogram shows the formation of various compounds and the MS reveals that the intended peptide (r_t = 10.4 min), detected as different protonated and TFA adducts, was a minor product of the synthesis whose isolation was not viable.

The manual synthesis of this peptide was repeated, but similar results (not shown) were obtained.

3.1.2. Manual Synthesis of Cys-pVEC

The peptide pVEC was also synthesized manually, bearing the same *N*-terminal modification (insertion of a cysteine residue) for subsequent coupling to modified gemcitabine. After cleaving and drying the crude product, it was analyzed by HPLC (chromatogram presented in Figure 25). Similarly to the previous synthesis of the Cys-Penetratin peptide, the manual synthesis of the Cys-pVEC peptide (C-LLIILRRRIRKQAHAHSK) resulted in a very complex crude product, as verified in the HPLC chromatogram. Again, it was not viable to isolate this peptide from crude product, and its further characterization by LC-ESI/MS was considered unnecessary.

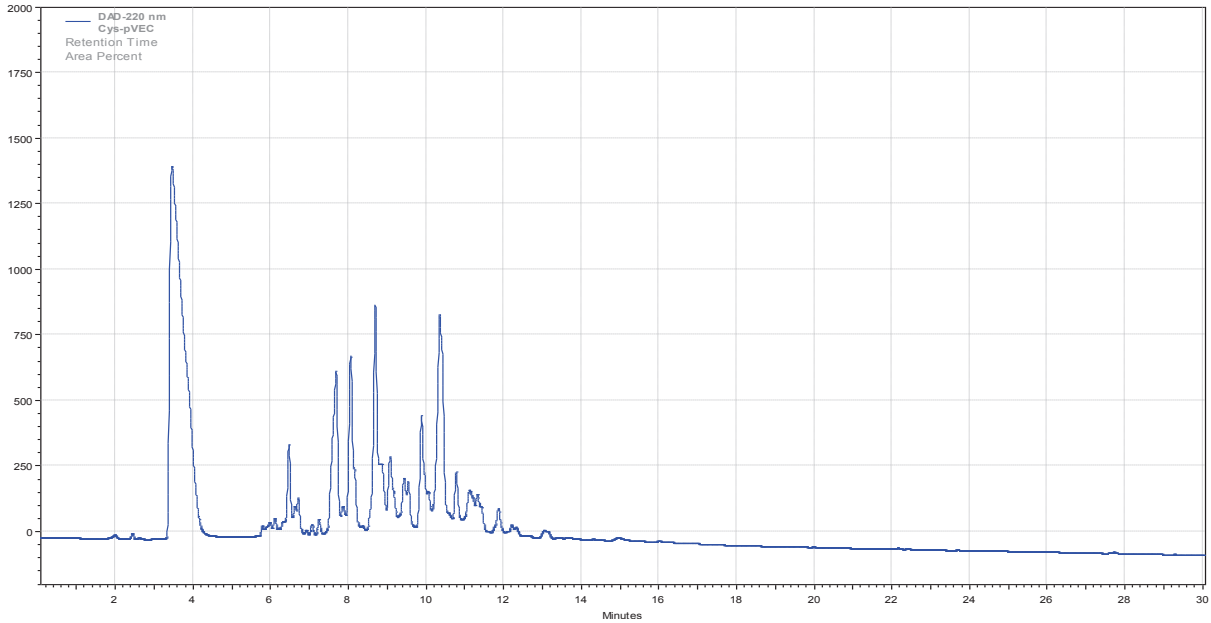

Figure 25: Chromatogram of the product of the manual synthesis of the peptide Cys-pVEC, acquired with a HPLC-DAD system, with a C18 column, using ACN in water with 0.05% TFA as eluent, in gradient mode (0 – 100%), for 30 minutes, at a flow of 1 mL/min and detection at λ = 220 nm.

In the view of the fact that the manual synthesis of these peptides was not successful, it was decided to carry out their synthesis by resorting to the CEM Liberty1 peptide synthesizer, with microwave radiation, available in the laboratory, as next described.

3.1.3. Automated MW-assisted Synthesis of Cys-Penetratin

The peptide Cys-Penetratin was synthesized in the CEM Liberty1 peptide synthesizer, assisted with microwave radiation. The peptide was cleaved from the solid support, and after the work-up described in the Experimental Section, it was solubilized in 10% aqueous acetic acid and analyzed by HPLC and LC-ESI/MS. The chromatogram and mass spectrum obtained are presented in Figure 26 and Figure 27, respectively.

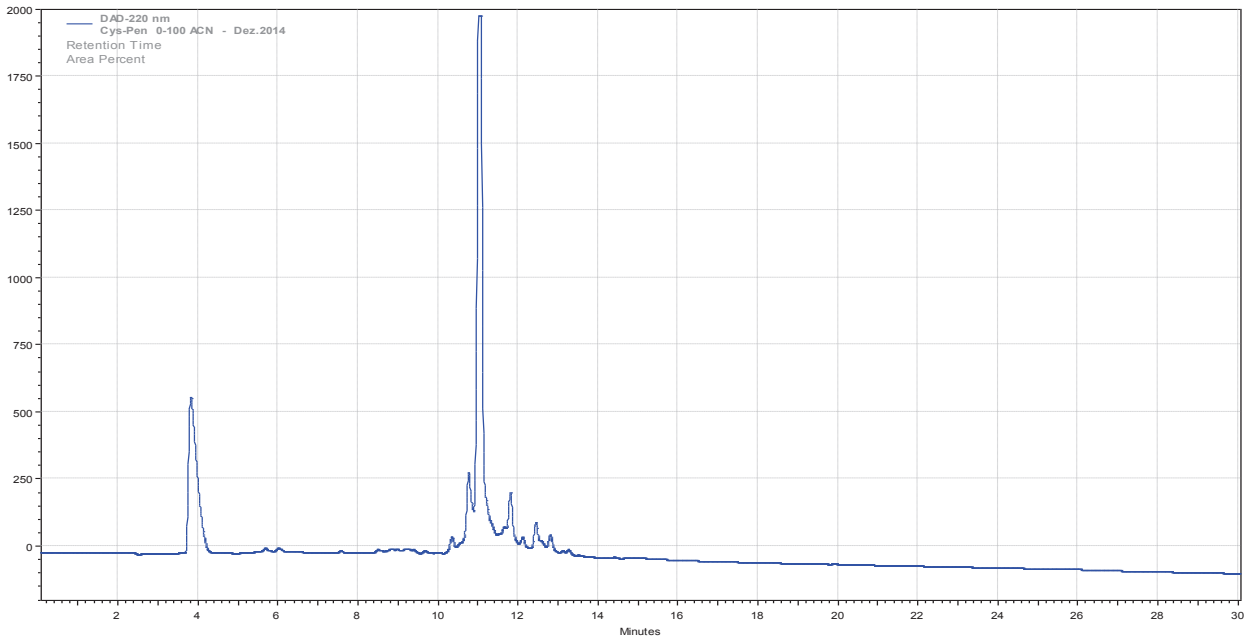

Figure 26: Chromatogram of the product of the synthesis of the peptide Cys-Penetratin in the CEM Liberty1 MW-assisted synthesizer, acquired with a HPLC-DAD system, with a C18 column, using ACN in water with 0.05% TFA as eluent, in gradient mode (0 – 100%), for 30 minutes, at a flow of 1 mL/min and detection at λ = 220 nm.

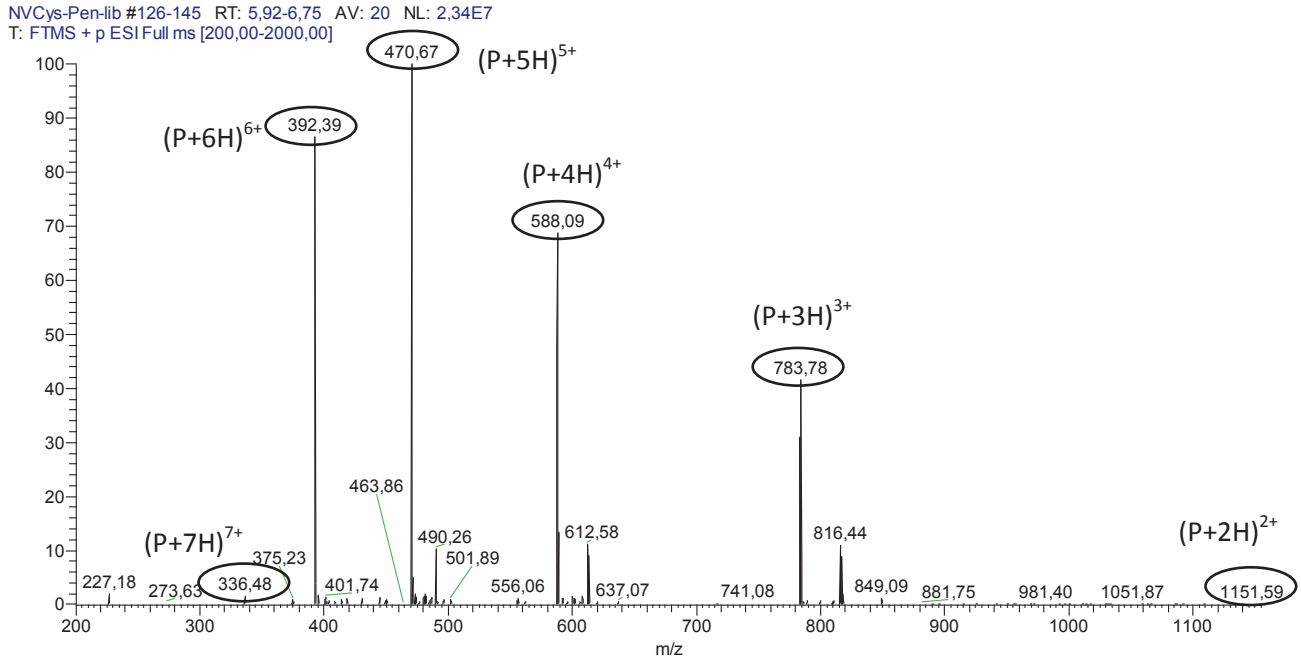

Figure 27: Mass spectrum (LC-ESI/MS Orbitrap, positive mode) of the Cys-Penetratin peptide (MW-assisted synthesis).

HPLC analysis revealed that the automated synthesis of the Cys-Pen peptide results in a much simpler crude product, with a distinct main compound (r_t = 11 min), whose LC-ESI/MS analysis confirmed as the target peptide, which has an exact mass of 2347.3147 Da. In fact, several peaks can be observed in the mass spectrum of the crude product, corresponding to different protonation states of the Cys-Pen peptide.

3.1.4. Automatic MW-assisted Synthesis of Cys-pVEC

The peptide Cys-pVEC was also synthesized in the CEM Liberty1 synthesizer and analyzed by HPLC and LC-ESI/MS after cleavage from the solid support and subsequent work-up (Figure 28 and Figure 29). The sequence and exact mass of the Cys-pVEC peptide and the m/z ratios of its adducts with H^+ detected by ESI-IT MS are presented in Table 4.

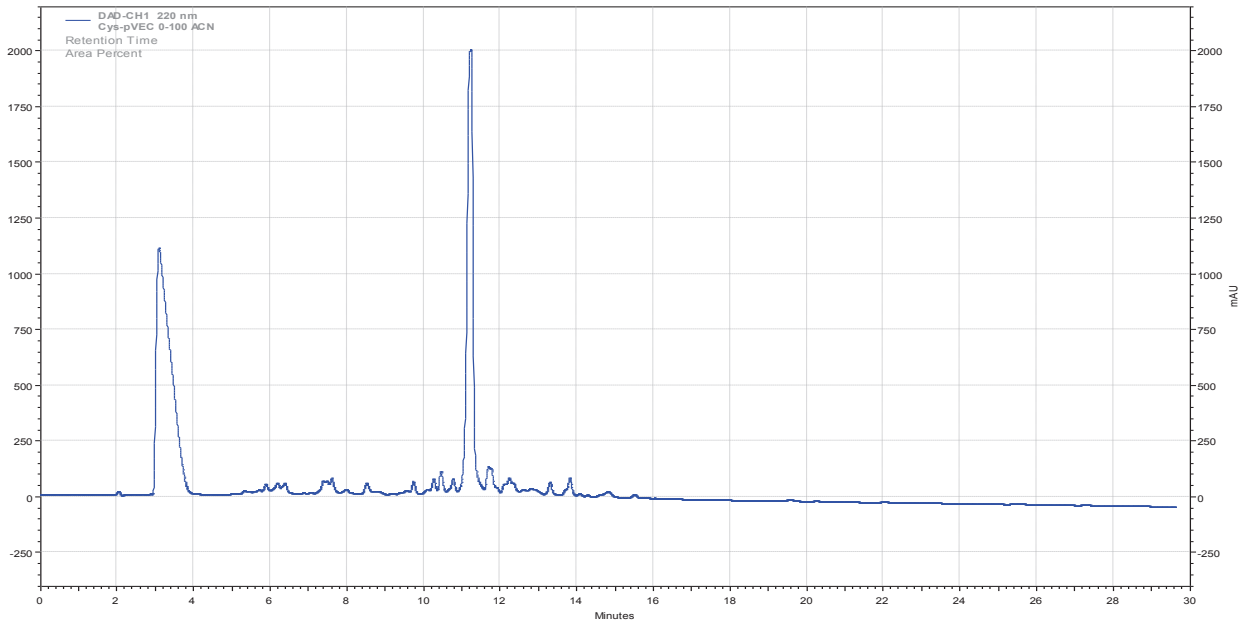

Figure 28: Chromatogram of the product of the synthesis of the peptide Cys-pVEC in the CEM Liberty1 MW-assisted synthesizer, acquired with a HPLC-DAD system, with a C18 column, using ACN in water with 0.05% TFA as eluent, in gradient mode (0 – 100%), for 30 minutes, at a flow of 1 mL/min and detection at λ = 220 nm.

The HPLC chromatogram confirmed the formation of a main product, with rt = 11.2 min, which was identified as the target Cys-pVEC peptide by LC-ESI/MS analysis. It is possible to observe several peaks in the mass spectrum, corresponding to different protonation states of the peptide.

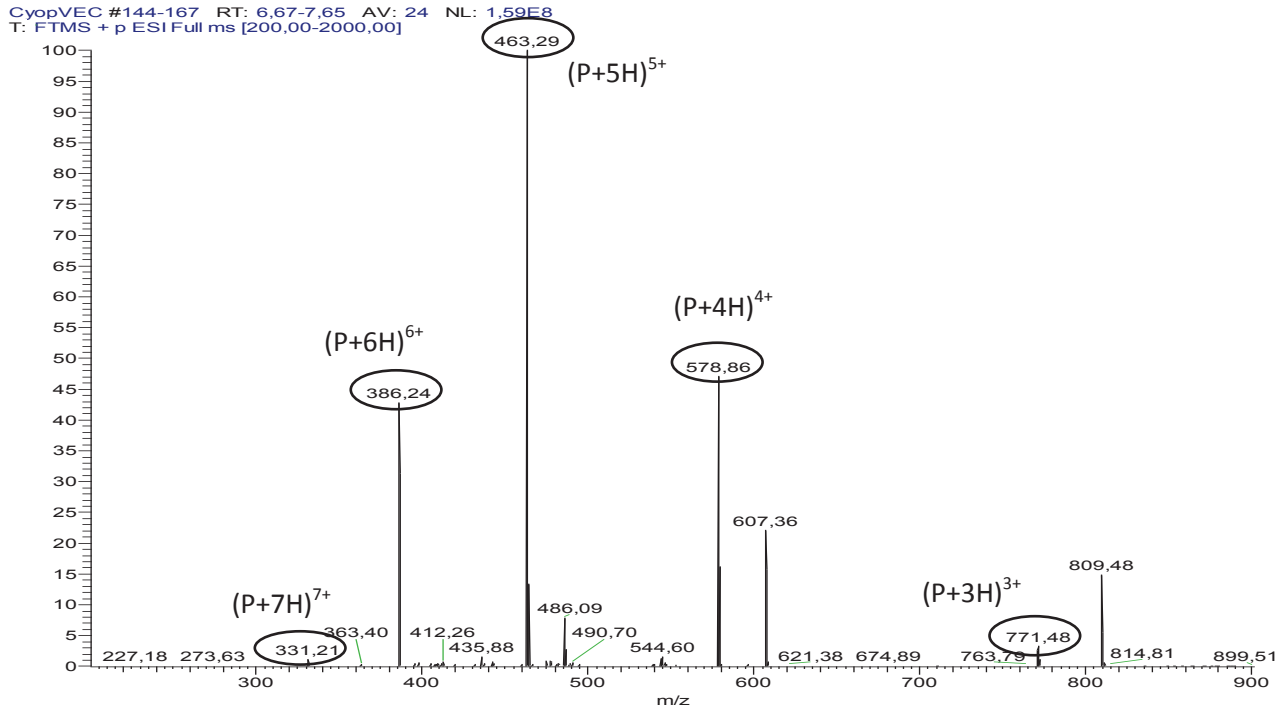

Figure 29: Mass spectrum (LC-ESI/MS Orbitrap, positive mode) of the Cys-pVEC peptide (MW-assisted synthesis).

Table 4. Sequence and exact mass of the Cys-pVEC peptide and m/z ratios of its adducts with H^+ detected by ESI-IT MS.

Peptide	Sequence	Exact Mass (Da)
Cys-pVEC	C- LLIILRRRIRKQAHAHSK	2311.4012
Adducts	m/z	
$(P + 2H)^{2+}$	1156.9401	
$(P + 3H)^{3+}$	771.6267	
$(P + 4H)^{4+}$	578.9700	
$(P + 5H)^{5+}$	463.3760	
$(P + 6H)^{6+}$	386.3134	
$(P + 7H)^{7+}$	331.2686	

The success of both syntheses using the CEM Liberty1 synthesizer demonstrates the importance of the microwave radiation to synthesize these peptides. This approach afforded both peptides with excellent purity grades, dismissing the need to purify them. The heat provided by the MW decreases the coiling of the peptide chain on itself as it grows and the aggregation between chains (caused by intramolecular and intermolecular interactions, respectively) at the same time as it reduces the time required for the condensation and deprotection reactions to occur.

3.2. Structural modification of Gemcitabine

After synthesizing the target CPPs, modified with an N-terminal cysteine residue, gemcitabine was also chemically modified, as described in the Experimental section, to enable its conjugation to the Cys-CPPs through a disulfide bond. To this end, the synthetic route displayed in Figure 21 was followed, pursuing synthesis of *N*-[3-(*S*-trityl)sulfanyl]propanoylgemcitabine **(3)**, *N*-(3-sulfanyl)propanoylgemcitabine **(4)** and *N*-{3-[*S*-(2-sulfanyl)pyridyl]sulfanyl}propanoylgemcitabine **(7)**, the latter being next coupled to the Cys-modified CPPs to produce the target CPP-gemcitabine conjugates. Results from the syntheses of compounds **(3)**, **(4)** and **(7)** are next described.

3.2.1. Synthesis of *N*-[3-(*S*-trityl)sulfanyl]propanoylgemcitabine (3)

The synthesis of compound **(3)** was carried out as described in the Experimental Section, and an ESI-IT MS analysis of the isolated product was performed. The mass spectrum obtained is represented in Figure 30, and confirms the expected structure for compound **(3)**, which was obtained with 45% yield.

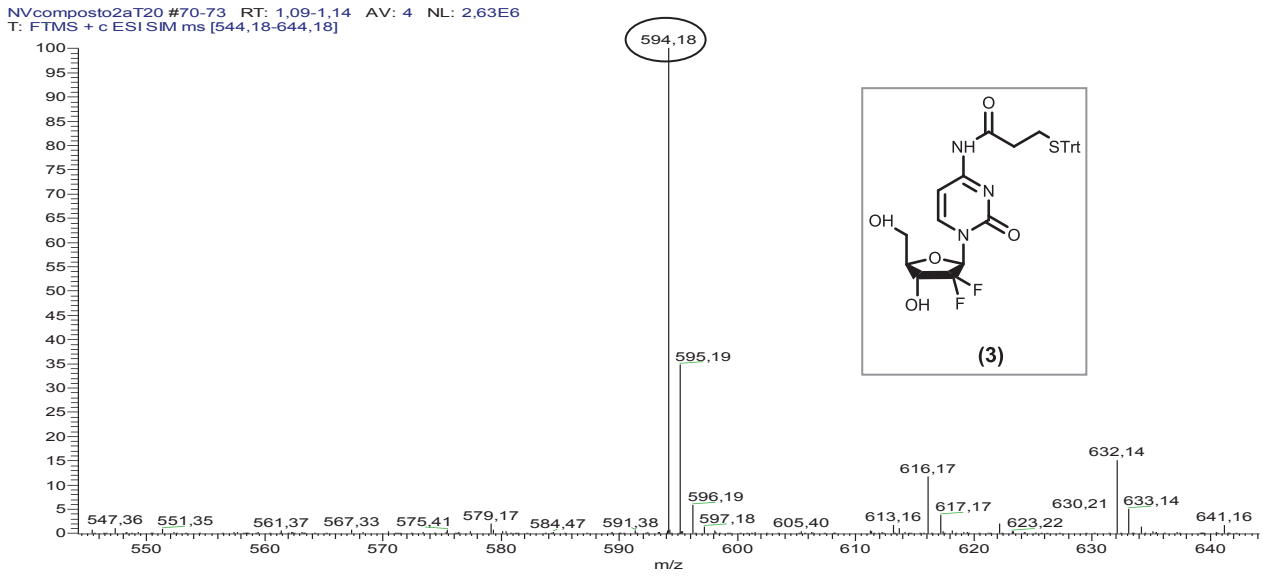

Figure 30: Mass spectrum (LC-ESI/MS Orbitrap, positive mode) of compound **(3)**.

3.2.2. Synthesis of *N*-(3-sulfanyl)propanoylgemcitabine (4)

The synthesis of compound (4) was carried out as described in the Experimental Section. The isolated product was analyzed by HPLC-DAD and by ESI-IT MS. The resulting chromatogram and mass spectrum are represented in Figure 31 and Figure 32, respectively. While the HPLC chromatogram revealed the formation of a major product, with a retention time of 14.2 min, ESI-IT MS analysis confirmed this product to have the molecular mass expected for compound **(4)**, whose molecular weight is 351.3248 g/mol. Still, some traces of unreacted gemcitabine were also detected in the mass spectrometry analysis (gemcitabine molecular weight is 263.20 g/mol).

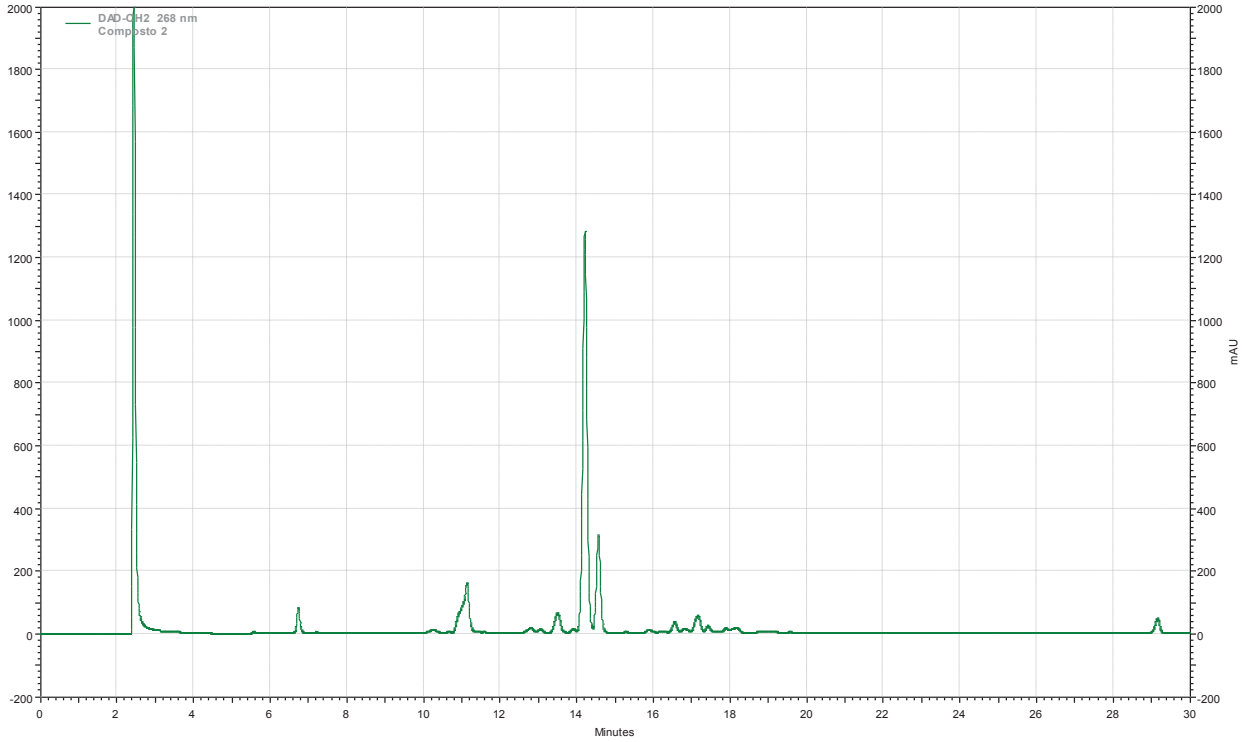

Figure 31: Chromatogram of compound **(4)**, acquired with a HPLC-DAD system, with a C18 column, using ACN in water with 0.05% TFA as eluent, in gradient mode (0 – 100%), for 30 minutes, at a flow of 1 mL/min and detection at λ = 270 nm.

In face of successful synthesis of **(4)**, and of the relatively low amount of impurities of the product isolated, this was subsequently used without further purification for direct conjugation with the Cys-Pen peptide (see 3.3.1).

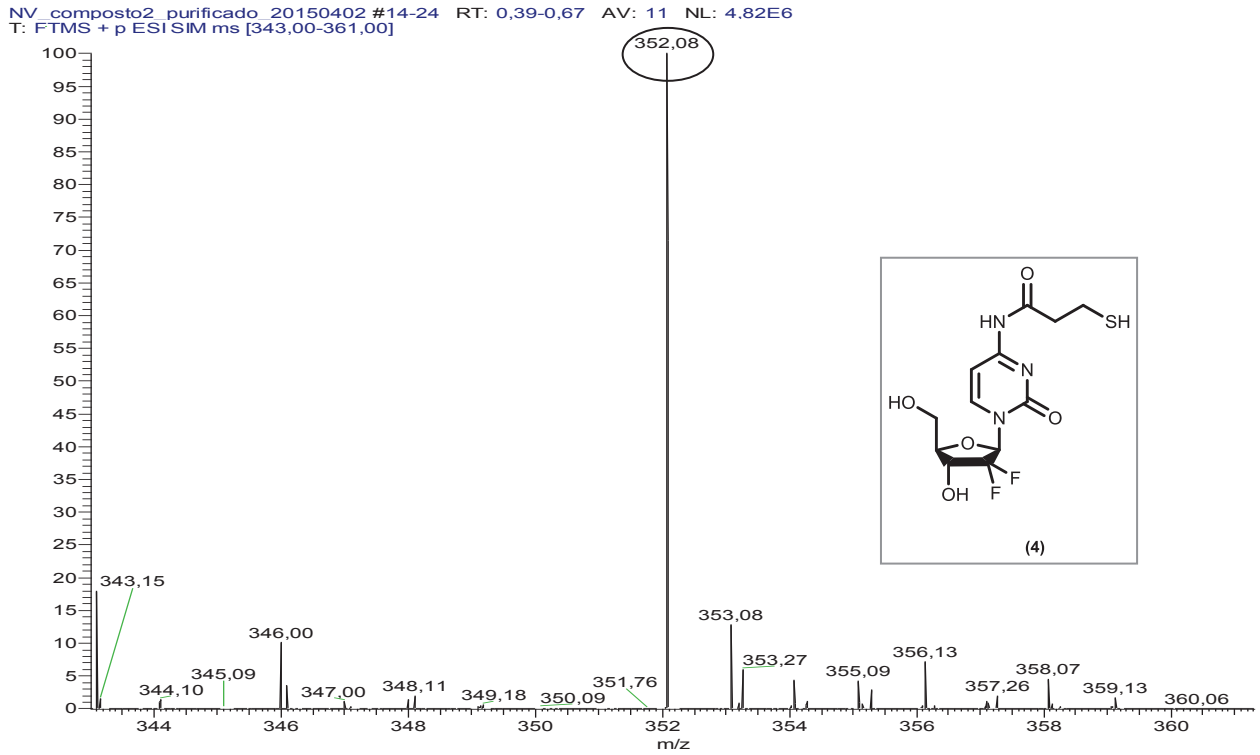

Figure 32: Mass spectrum (LC-ESI/MS Orbitrap, positive mode) of compound **(4)**.

3.2.3. Synthesis of *N*-{3-[*S*-(2-sulfanyl)pyridyl]sulfanyl}propanoyl-gemcitabine (7)

Compound **(7)** was produced by reacting *N*-(3-sulfanyl)propanoylgemcitabine **(4)** with 2,2-disulfanyldipyridine, as described in the Experimental Section. The isolated product was analyzed by HPLC and by ESI-IT MS, yielding the chromatogram and mass spectrum presented in Figure 33 and Figure 34, respectively. Results obtained confirmed that compound **(7)**, whose molecular weight is 460.4708 g/mol, was the main product of this synthesis (r_t observed in the HPLC = 13.1 min). Compound **(7)** was next used for conjugation with both Cys-Pen and Cys-pVEC peptides (see 3.2.2. and 3.3.3.).

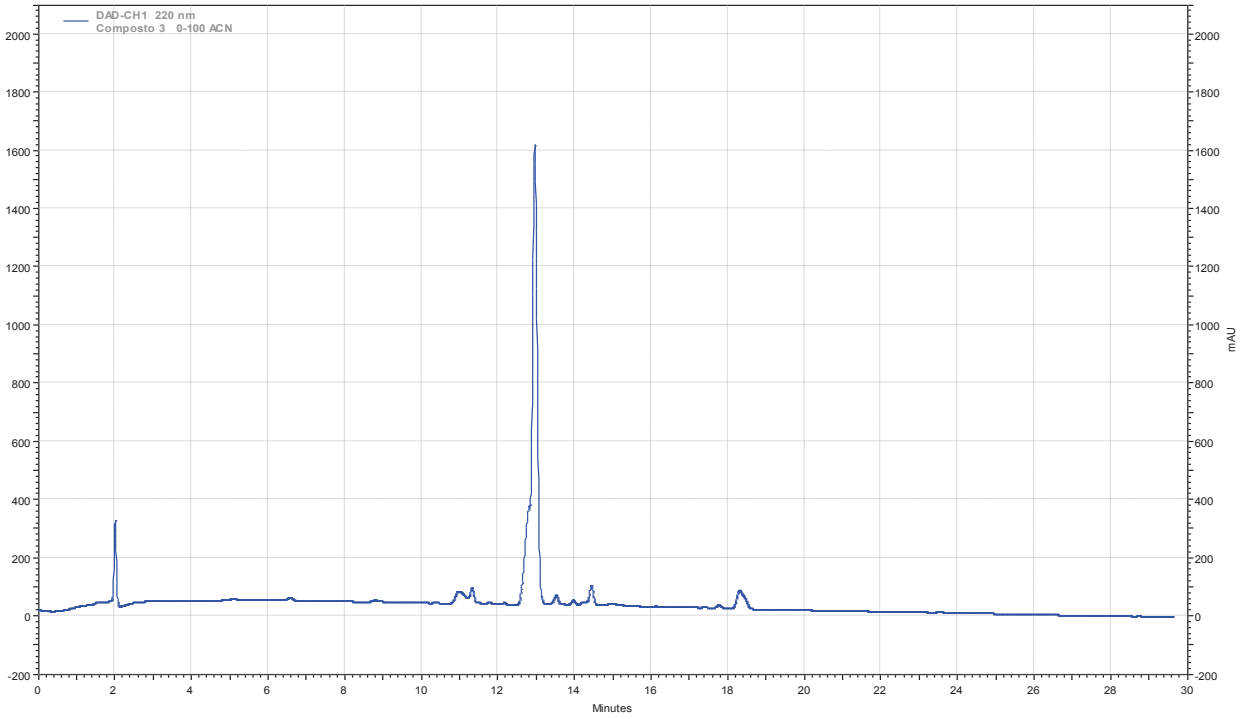

Figure 33: Chromatogram of compound **(7)**, acquired with a HPLC-DAD system, with a C18 column, using ACN in water with 0.05% TFA as eluent, in gradient mode (0 – 100%), for 30 minutes, at a flow of 1 mL/min and detection at λ = 220 nm.

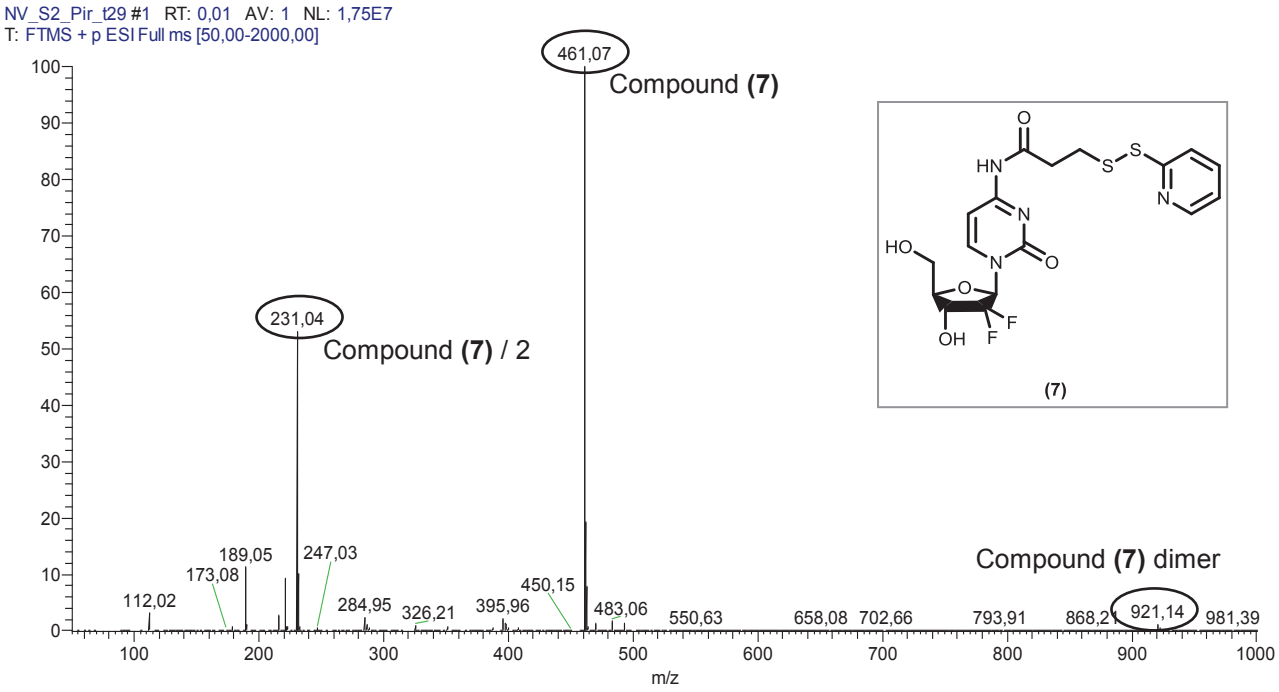

Figure 34: Mass spectrum (ESI-IT MS Orbitrap, positive mode) of compound **(7)**.

3.3. Synthesis of the Drug-CPP Conjugates

3.3.1. *Strategy A* – direct conjugation of compound (4) with Cys-Penetratin

Conjugation of compound **(4)** with the Cys-Pen peptide was attempted as described in the Experimental section. The course of the reaction was monitored by HPLC at two different wavelengths (220 and 270 nm) and the final product was analyzed by both HPLC and LC-ESI/MS. HPLC monitoring of reaction progress revealed that some kind of complex process was taking place, instead of a clean conversion of starting material(s) into the expected single product (data not shown). Figure 35 depicts the HPLC chromatogram of the starting Cys-Pen peptide, whereas Figure 36 and Figure 37 reproduce the chromatograms of the final reaction mixture with detection at 220 and 270 nm, respectively. The apparent formation of a major product was detected in the HPLC analysis with detection at 220 nm, by observation of a peak with a retention time of 13.1 min (Figure 36). In turn, HPLC analysis with detection at 270 nm revealed some release of gemcitabine (r_t = 6.8 min) from degradation of the starting compound **(4)**.

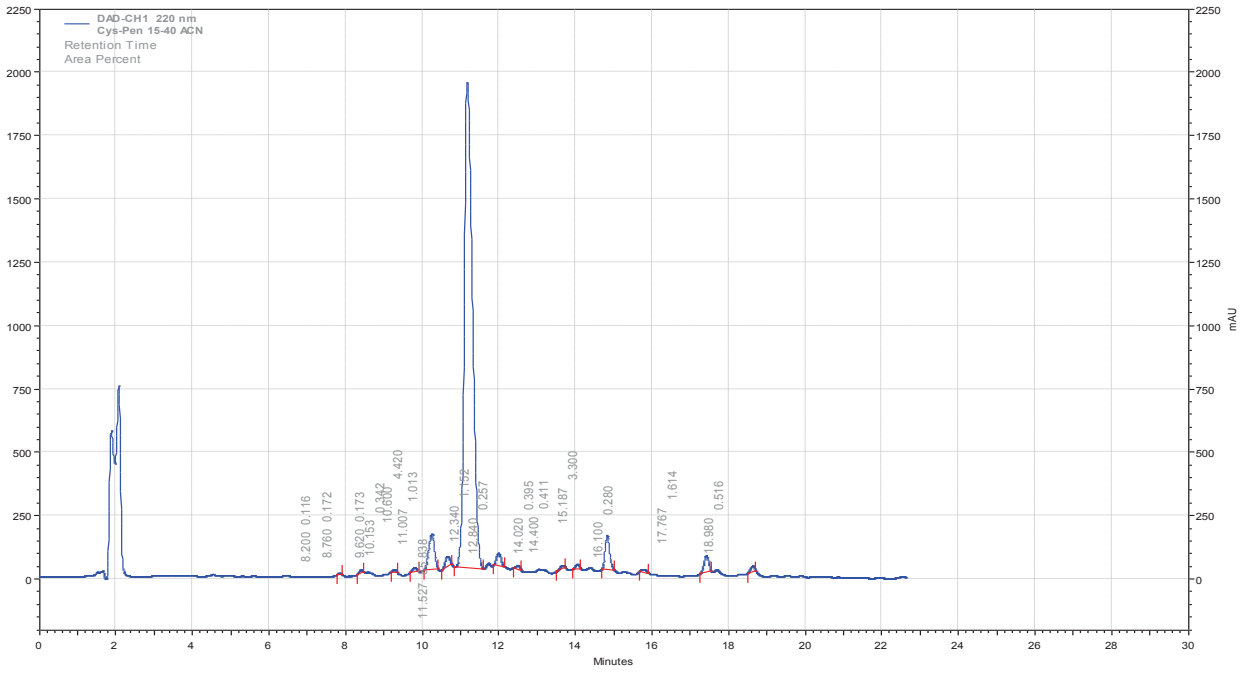

Figure 35: Chromatogram of the Cys-Penetratin peptide, acquired with a HPLC-DAD system, with a C18 column, using ACN in water with 0.05% TFA as eluent, in gradient mode (15 – 40%), for 30 minutes, at a flow of 1 mL/min and detection at λ = 220 nm.

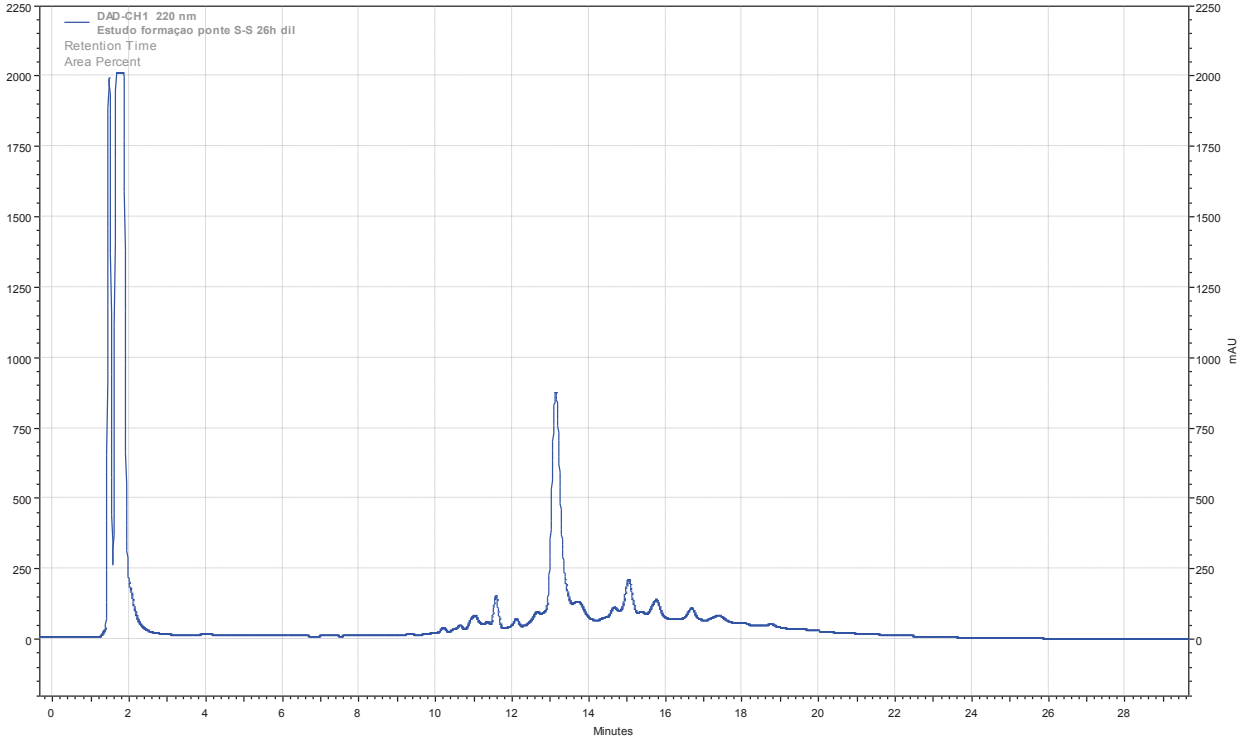

Figure 36: Chromatogram of the reaction mixture obtained in the attempt of producing the target Gemcitabine–Linker–Penetratin conjugate, following strategy A; data acquired with a HPLC-DAD system, with a C18 column, using ACN in water with 0.05% TFA as eluent, in gradient mode (15 – 40%), for 30 minutes, at a flow of 1 mL/min and detection at λ = 220 nm.

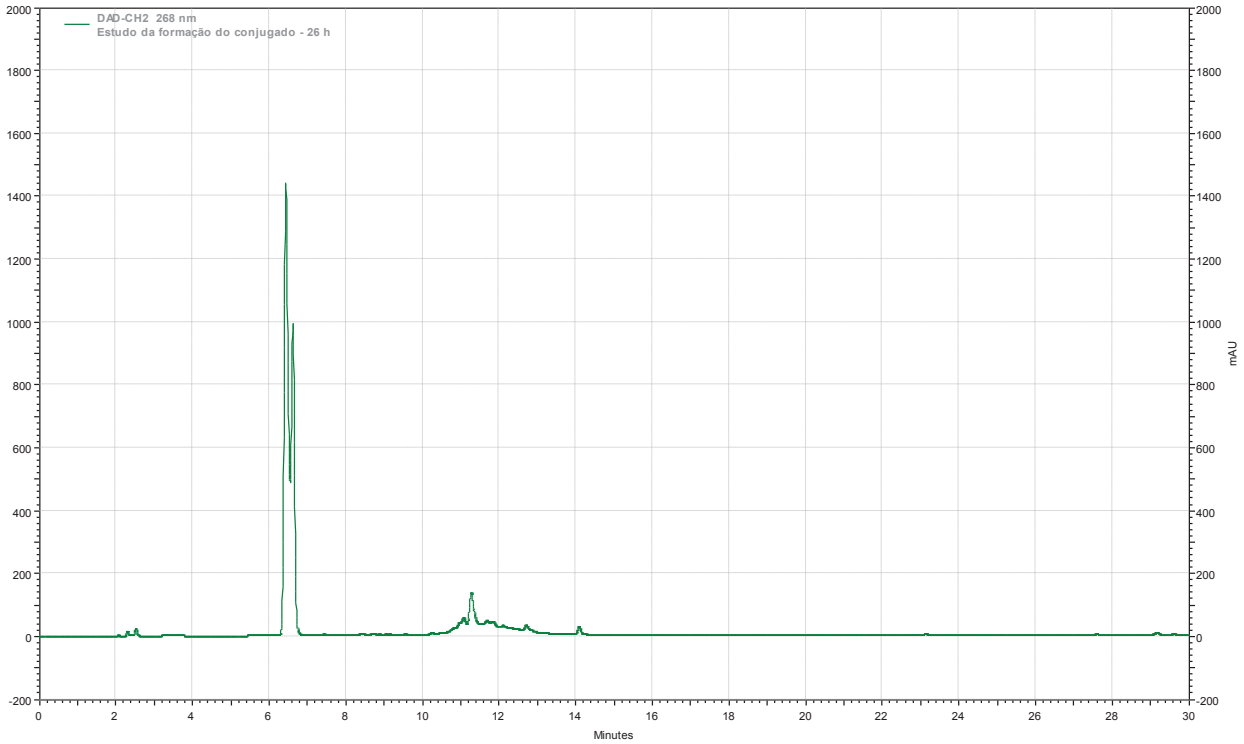

Figure 37: Chromatogram of the reaction mixture obtained in the attempt of producing the target Gemcitabine–Linker–Penetratin conjugate, following strategy A; data acquired with a HPLC-DAD system, with a C18 column, using ACN in water with 0.05% TFA as eluent, in gradient mode (15 – 40%), for 30 minutes, at a flow of 1 mL/min and detection at λ = 270 nm.

The mass spectrum from the LC-ESI/MS analysis of the mixture is presented in Figure 38, and shows that none of the ions observed correspond to the exact mass of the target conjugate (Figure 43), or of any of its protonated adducts (whose m/z ratios are presented in Table 5).

Release of parent gemcitabine from its derivative (4) was also confirmed by LC-ESI/MS analysis (not shown).

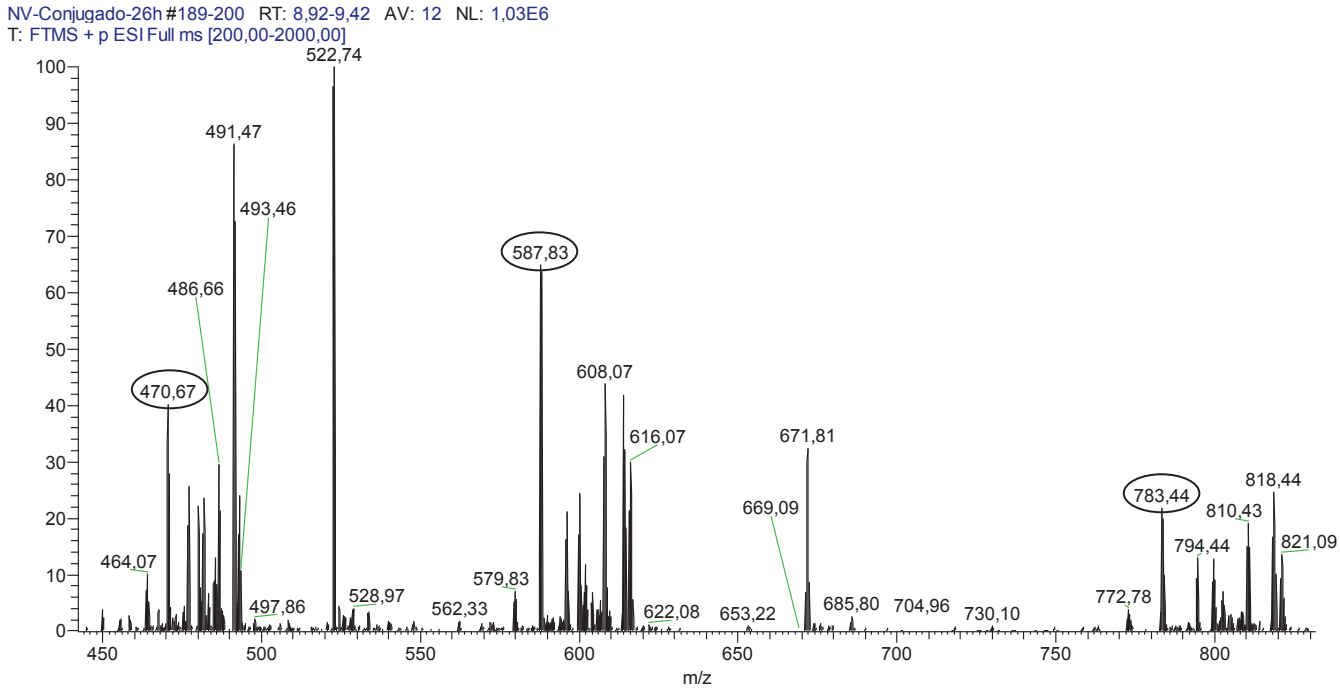

Figure 38: Mass spectrum (LC-ESI/MS Orbitrap, positive mode) relative to the most intense peak of the HPLC, highlighting three adducts of the Cys-Penetratin peptide.

Table 5: Exact mass of the Gemcitabine–Linker–Penetratin conjugate and m/z ratios of its adducts with H^+.

Conjugate	Exact Mass (Da)
Gemcitabine–Linker–Penetratin	2696.3691
Adducts	m/z
$(C + 2H)^{2+}$	1349.1846
$(C + 3H)^{3+}$	899.7897
$(C + 4H)^{4+}$	675.0923
$(C + 5H)^{5+}$	540.2738
$(C + 6H)^{6+}$	450.3949
$(C + 7H)^{7+}$	386.1956
$(C + 8H)^{8+}$	338.0461

3.3.2. *Strategy B* – conjugation of compound (7) with Cys-Penetratin

Compound **(7)** and the Cys-Penetratin peptide were conjugated as described in the Experimental section, and the reaction progress monitored by HPLC (not shown), taking the chromatogram of the starting Cys-Pen peptide (Figure 39) as reference. The final product was analyzed by HPLC and LC-ESI/MS, with results depicted in Figure 40 and Figure 41, respectively.

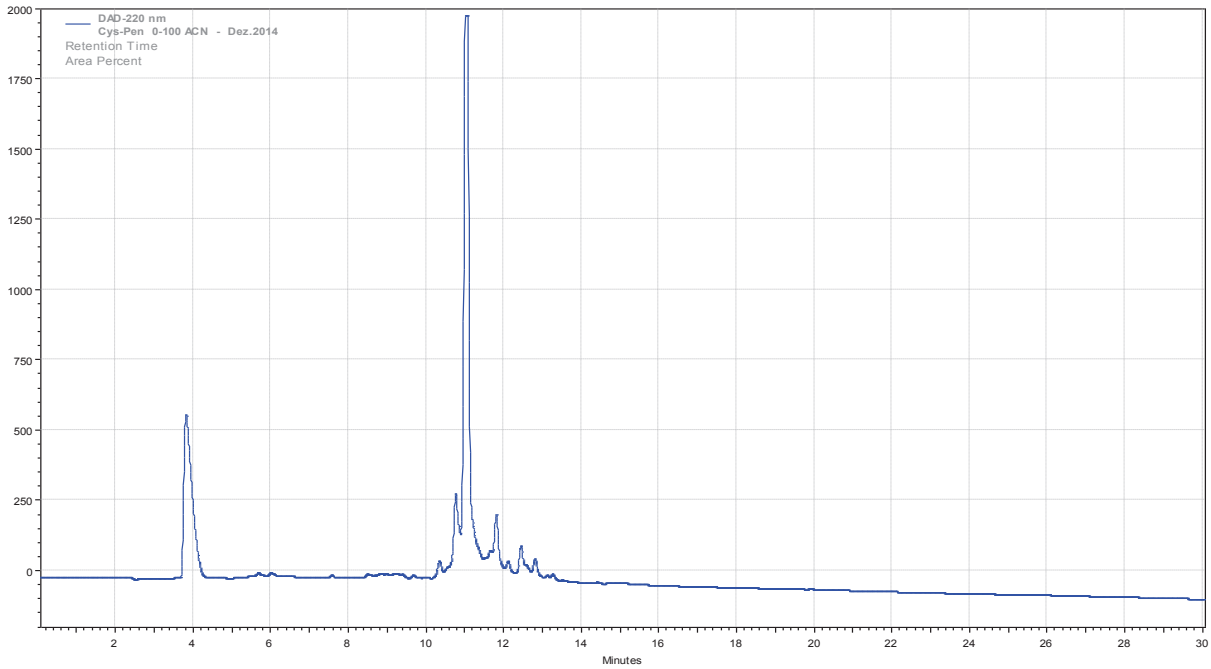

Figure 39: Chromatogram of the Cys-Penetratin peptide, acquired with a HPLC-DAD system, with a C18 column, using ACN in water with 0.05% TFA as eluent, in gradient mode (0 – 100%), for 30 minutes, at a flow of 1 mL/min and detection at λ = 220 nm.

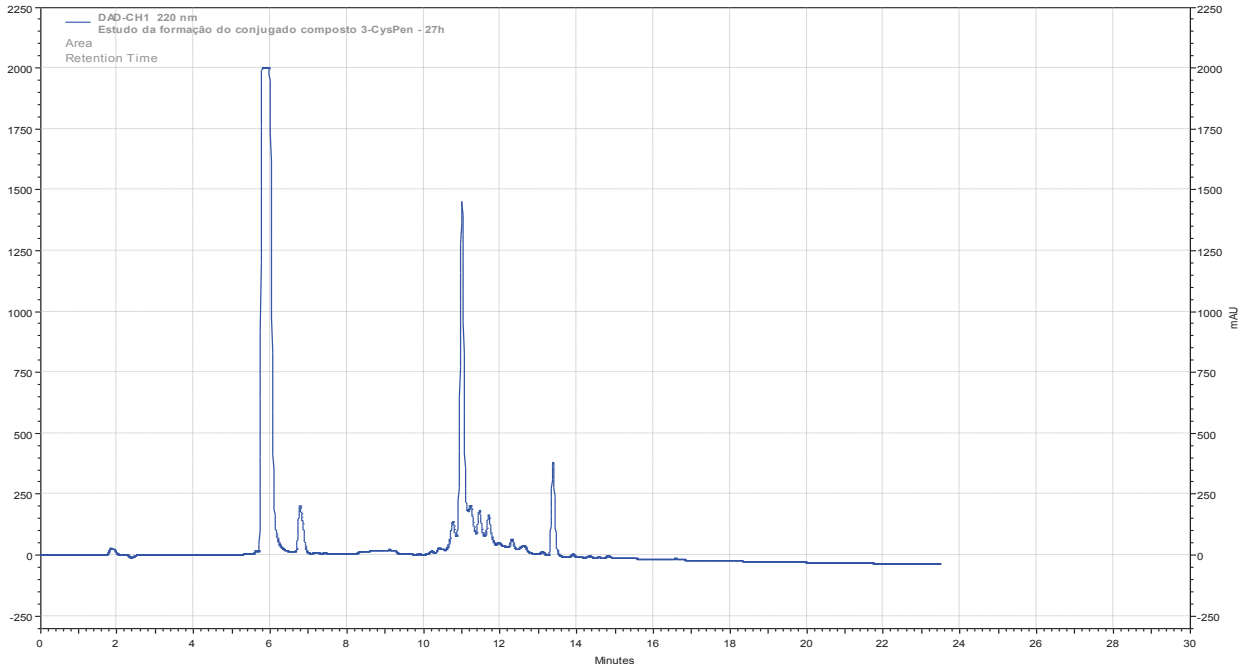

Figure 40: Chromatogram of the crude Gemcitabine–Linker–Penetratin conjugate, acquired with a HPLC-DAD system, with a C18 column, using ACN in water with 0.05% TFA as eluent, in gradient mode (0 – 100%), for 30 minutes, at a flow of 1 mL/min and detection at λ = 220 nm.

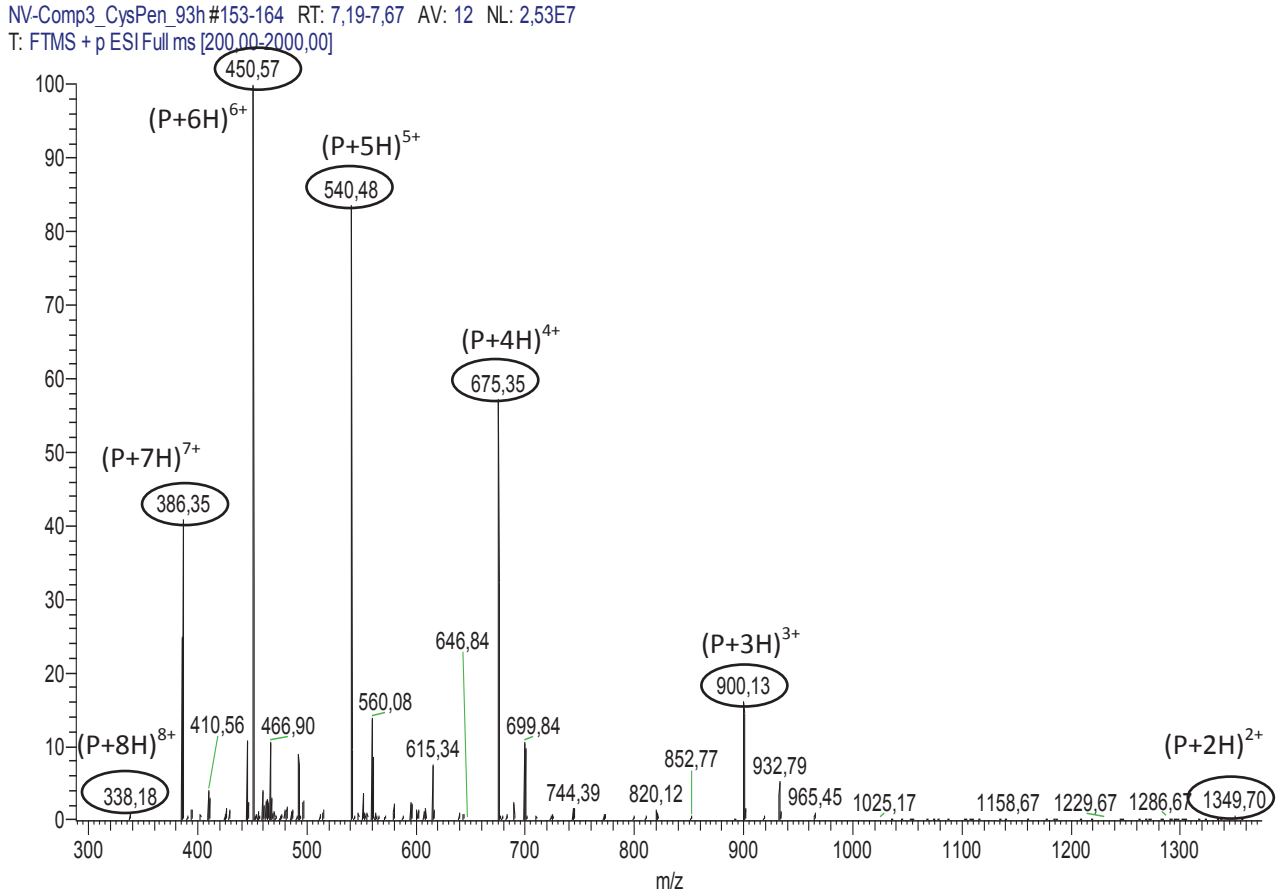

Figure 41: Mass spectrum (LC-ESI/MS Orbitrap, positive mode) of the Gemcitabine–Linker–Penetratin conjugate.

The chromatogram depicted on Figure 40 shows that the main product of this synthesis has a retention time of 11.1 min, whereas the mass spectrum on Figure 41 display several ions whose m/z values match those expected for different protonation states of the target conjugate (Table 5). It was also possible to detect unreacted compound **(7)** (which has a retention time of 13.3 min in the HPLC), both as a monomer (m/z = 461.08) and as a dimer.

The Gemcitabine–Linker–Penetratin conjugate was purified by RP-MPLC, using ACN in water with 0.05% TFA as eluent, in gradient mode (15 – 40%) and was obtained 100% pure (Figure 42).

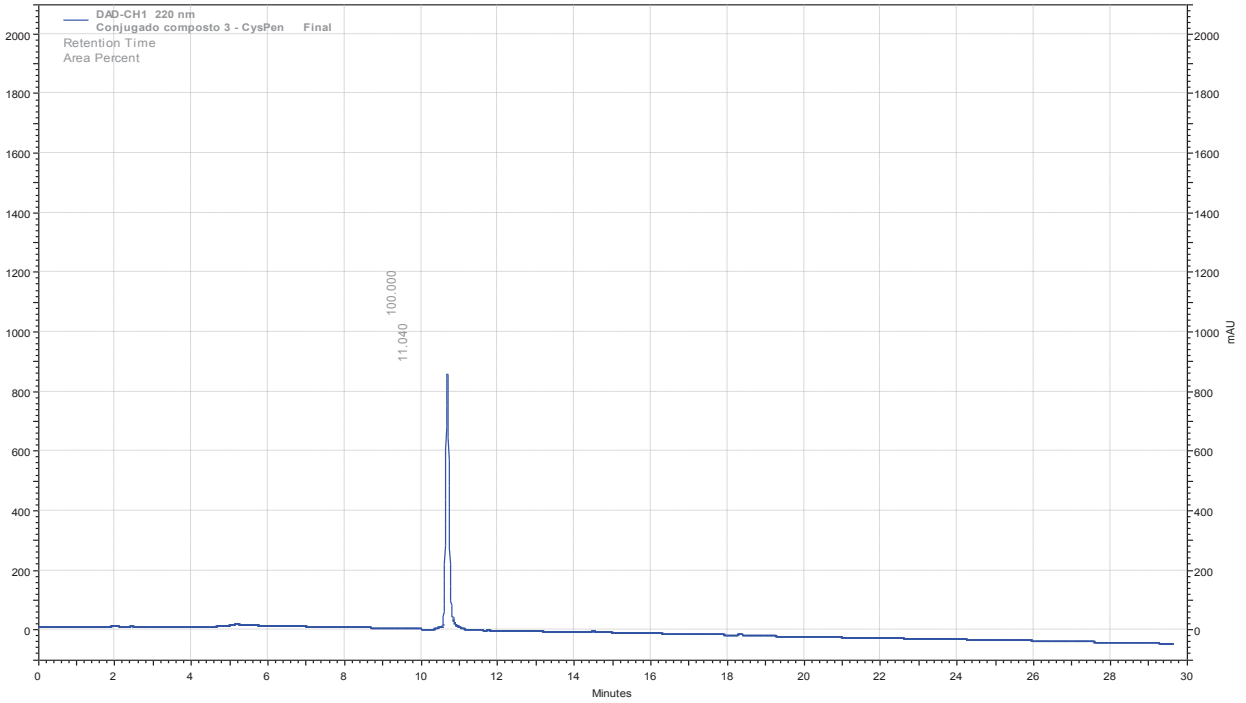

Figure 42: Chromatogram of the Gemcitabine–Linker–Penetratin conjugate after purification, acquired with a HPLC-DAD system, with a C18 column, using ACN in water with 0.05% TFA as eluent, in gradient mode (0 – 100%), for 30 minutes, at a flow of 1 mL/min and detection at λ = 220 nm.

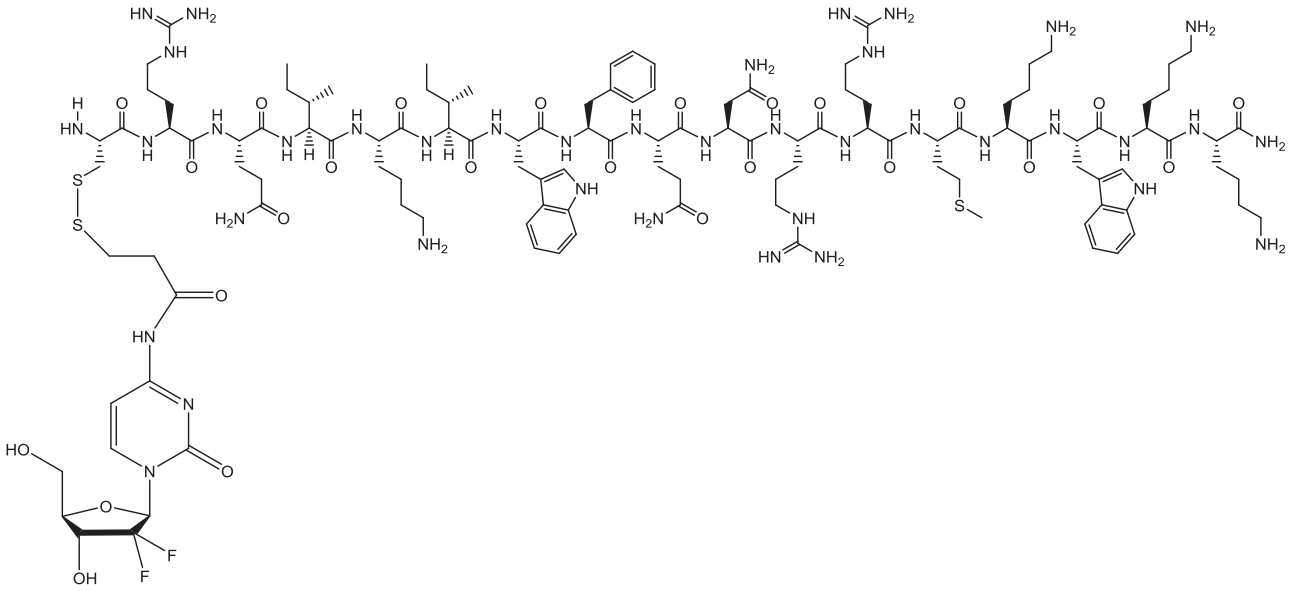

Figure 43: Chemical structure of the Gemcitabine – Linker – Penetratin conjugate (exact mass 2696.3691 Da).

3.3.3. *Strategy B* – conjugation of compound (7) with Cys-pVEC

Since conjugation strategy B successfully produced the target Gemcitabine–Linker–Penetratin conjugate, the same protocol was applied to the synthesis of the Gemcitabine–Linker–pVEC conjugate. As before, the reaction progress was monitored by HPLC (not shown), taking the chromatogram of the Cys-pVEC peptide (Figure 44) as reference. The final conjugate was analyzed by HPLC and LC-ESI/MS, with results as depicted in Figure 45 and Figure 46, respectively.

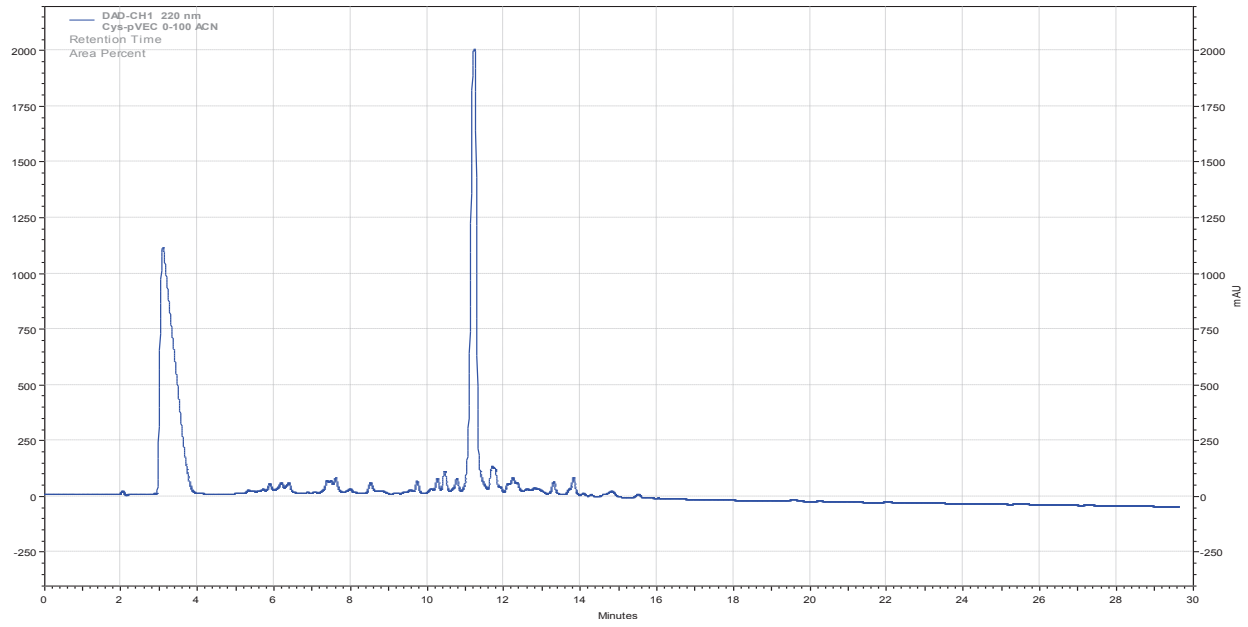

Figure 44: Chromatogram of the Cys-pVEC peptide, acquired with a HPLC-DAD system, with a C18 column, using ACN in water with 0.05% TFA as eluent, in gradient mode (0 – 100%), for 30 minutes, at a flow of 1 mL/min and detection at λ = 220 nm.

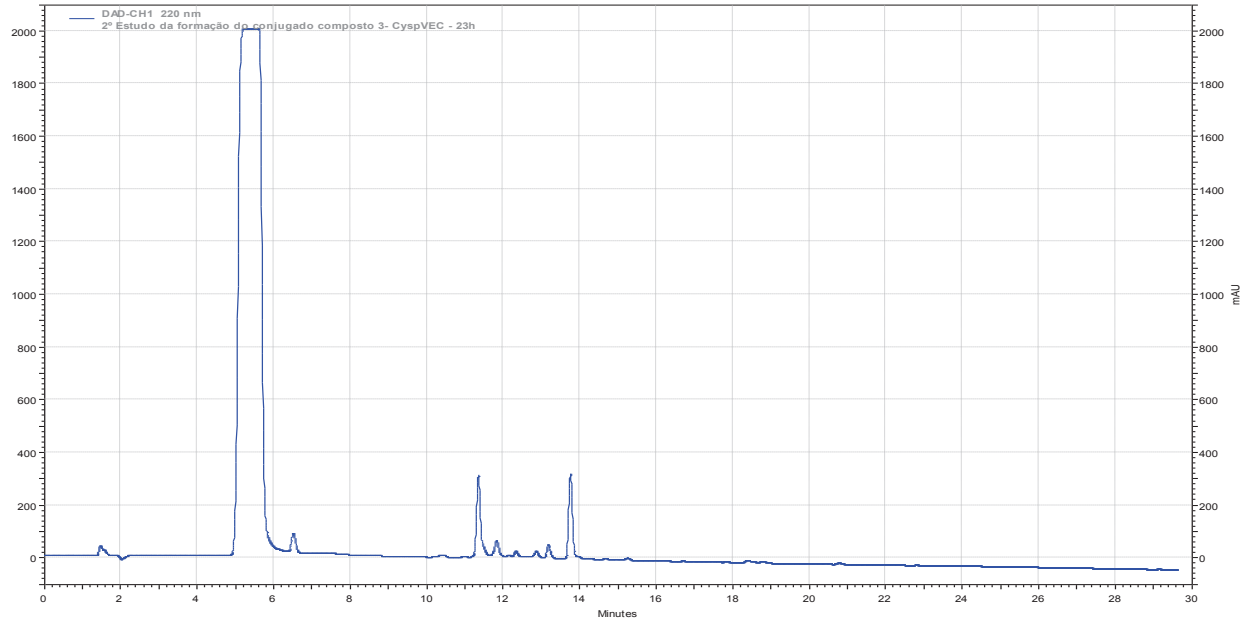

Figure 45: Chromatogram of the Gemcitabine–Linker–pVEC conjugate, acquired with a HPLC-DAD system, with a C18 column, using ACN in water with 0.05% TFA as eluent, in gradient mode (0 – 100%), for 30 minutes, at a flow of 1 mL/min and detection at λ = 220 nm.

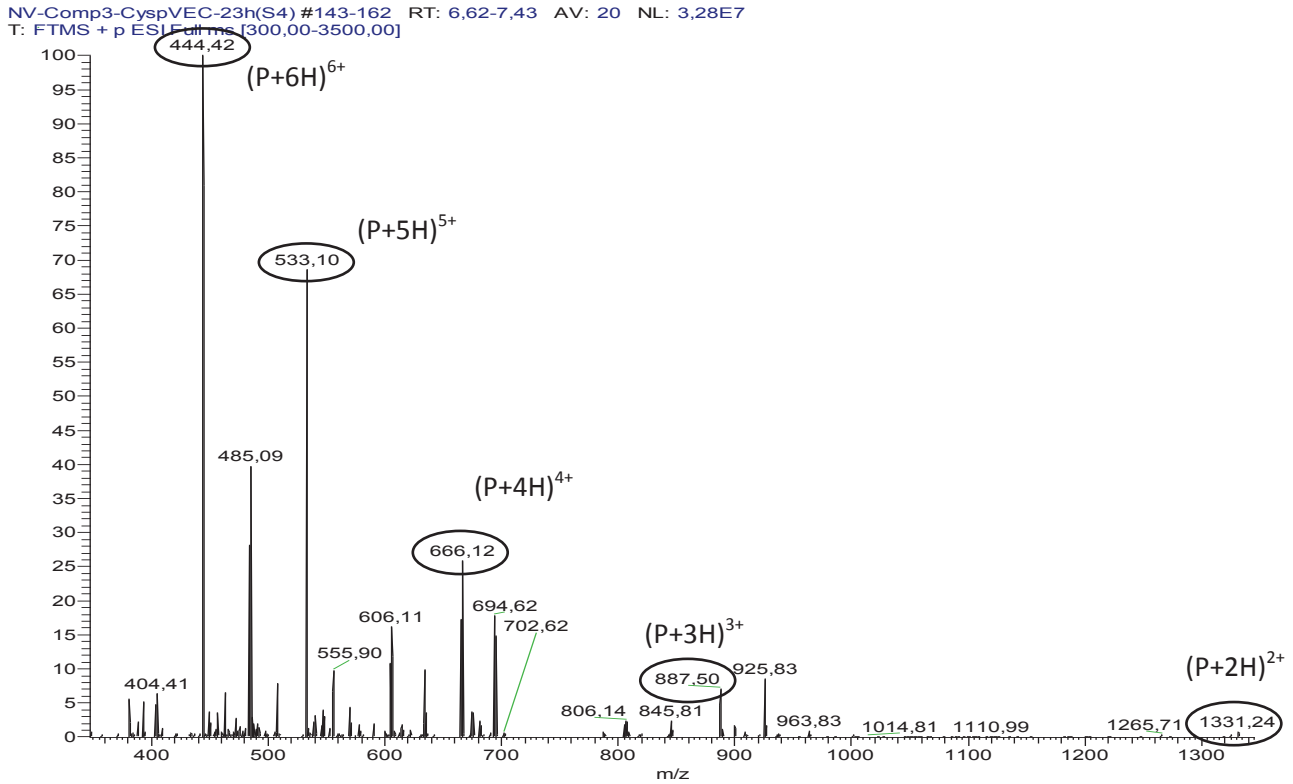

Figure 46: Mass spectrum (LC-ESI/MS Orbitrap, positive mode) of the Gemcitabine–Linker–pVEC conjugate.

Once again, it was possible to confirm that the target Gemcitabine–Linker–pVEC conjugate (Figure 47) was successfully synthesized, though the crude product was not as pure as that obtained in the synthesis of the Gemcitabine-Penetratin conjugate. The Gemcitabine–Linker–pVEC conjugate presented a retention time of 11.3 min (Figure 45) and the ions displayed in its mass spectrum (Figure 46) presented m/z values that matched those of its different protonation adducts (Table 6). Again, unreacted compound (7) could be detected by ESI-IT MS (m/z = 461.08) (HPLC retention time of 13.8 min).

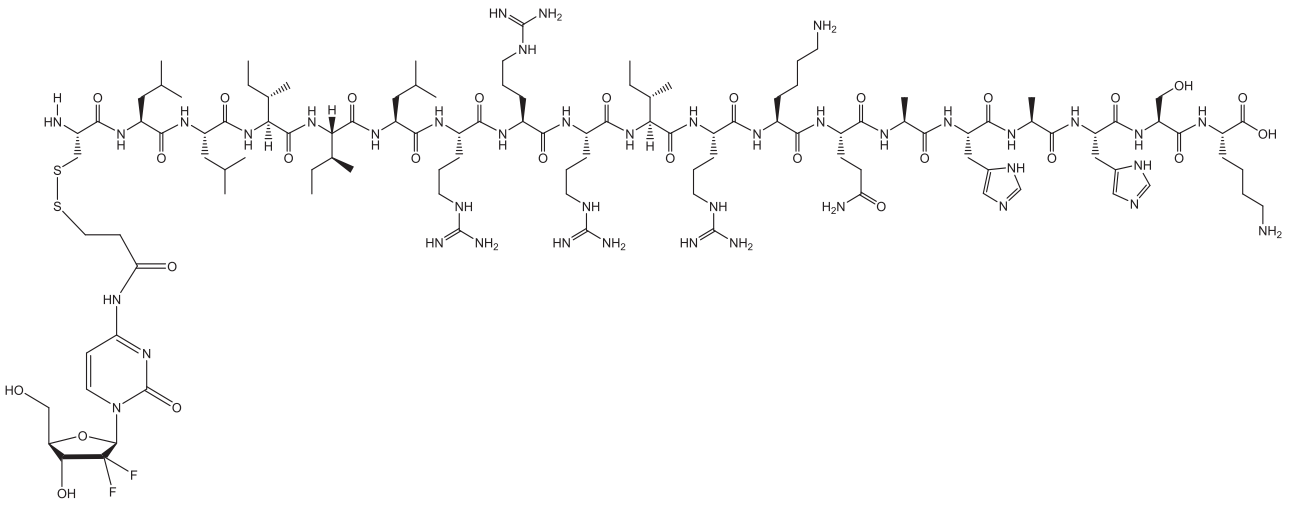

Figure 47: Chemical structure of the Gemcitabine – Linker – pVEC conjugate.

Table 6: Exact mass of the Gemcitabine–Linker–pVEC conjugate and m/z ratios of its adducts with H^+.

Conjugate	Exact Mass (Da)
Gemcitabine–Linker–pVEC	2660.4556
Adducts	m/z
C + $2H^+$	1331.2278
C + $3H^+$	887.8185
C + $4H^+$	666.1139
C + $5H^+$	533.0911
C + $6H^+$	444.4093
C + $7H^+$	381.0651

This conjugate was purified by RP-MPLC, using ACN in water with 0.05% TFA as eluent, in gradient mode (15 – 40%) and was obtained with 94% purity (Figure 48).

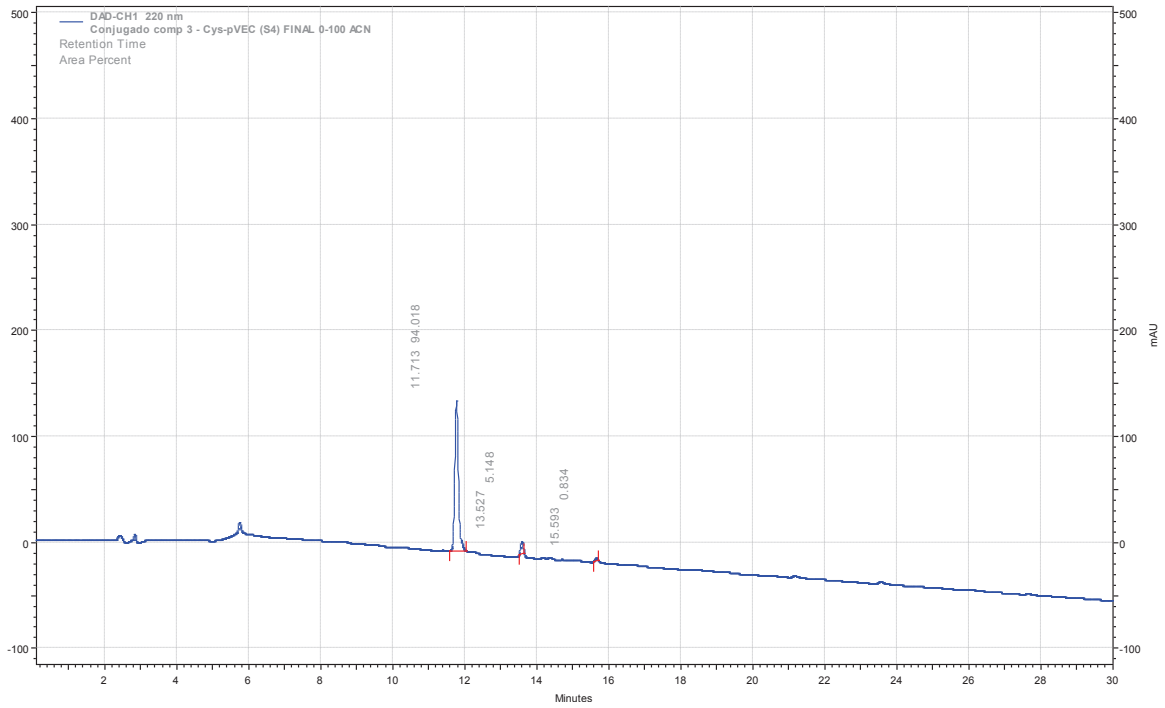

Figure 48: Chromatogram of the Gemcitabine–Linker–pVEC conjugate after purification, acquired with a HPLC-DAD system, with a C18 column, using ACN in water with 0.05% TFA as eluent, in gradient mode (0 – 100%), for 30 minutes, at a flow of 1 mL/min and detection at λ = 220 nm.

3.4. Studies on the stability of Drug-CPP conjugates

In order to determine how stable were the conjugates' hydrolysable bonds (Figure 49), at physiological pH and temperature, the stability of both Gemcitabine–Linker–Penetratin and Gemcitabine–Linker–pVEC conjugates was tested in PBS, pH 7.4, at 37 ºC for 6 days. HPLC analyses, with detection at 220 and 270 nm, were performed periodically to detect both the release of free gemcitabine and the hydrolysis of the conjugates. To this end, a calibration curve of gemcitabine was built prior to hydrolysis studies. Relevant graphs and chromatograms are presented further below.

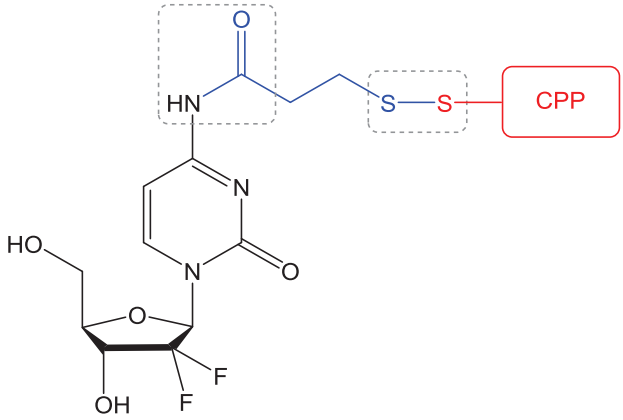

Figure 49: Schematic representation of the Peptide-Drug conjugates, highlighting the hydrolysable bonds.

3.4.1. Calibration curve

A calibration curve of gemcitabine was initially traced to determine if the correlation between the concentration of gemcitabine and the area under its chromatographic peak, detected at 270 nm, was linear. The linear correlation was confirmed as demonstrated by the graphic depicted in Figure 50.

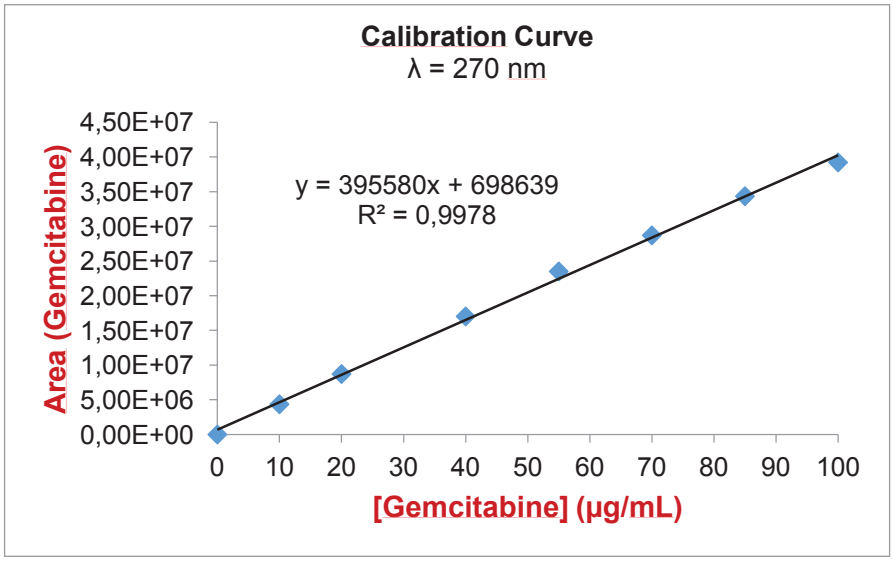

Figure 50: Calibration curve by HPLC analysis of gemcitabine solutions with different concentrations, with detection at λ = 270 nm.

3.4.2. Time-dependent kinetics of the conjugates' hydrolysis

After 6 days in PBS, pH 7.4, 37 ºC, chromatographic analyses reveals that the conjugates suffer minimal degradation, and have different kinetic profiles, as shown by the [Gemcitabine] = f(time) and [Conjugate] = f(time) graphical representations (Figure 51 and Figure 52; HPLC chromatograms performed periodically are included in the Supplementary Information section).

The Gemcitabine–Linker–pVEC conjugate produces a significant and exponential release of free gemcitabine, making most of the previously conjugated drug available within the first 48 h. On the other hand, the Gemcitabine–Linker–Penetratin conjugate releases gemcitabine more slowly and linearly over time, demonstrating a different behavior when it comes to the hydrolysis of the conjugates' bonds, based only on peptide sequence.

After analyzing these results, the time-dependent kinetics of the hydrolysis of the Gemcitabine–Linker–Penetratin conjugate was studied for 22 days, in the same conditions.

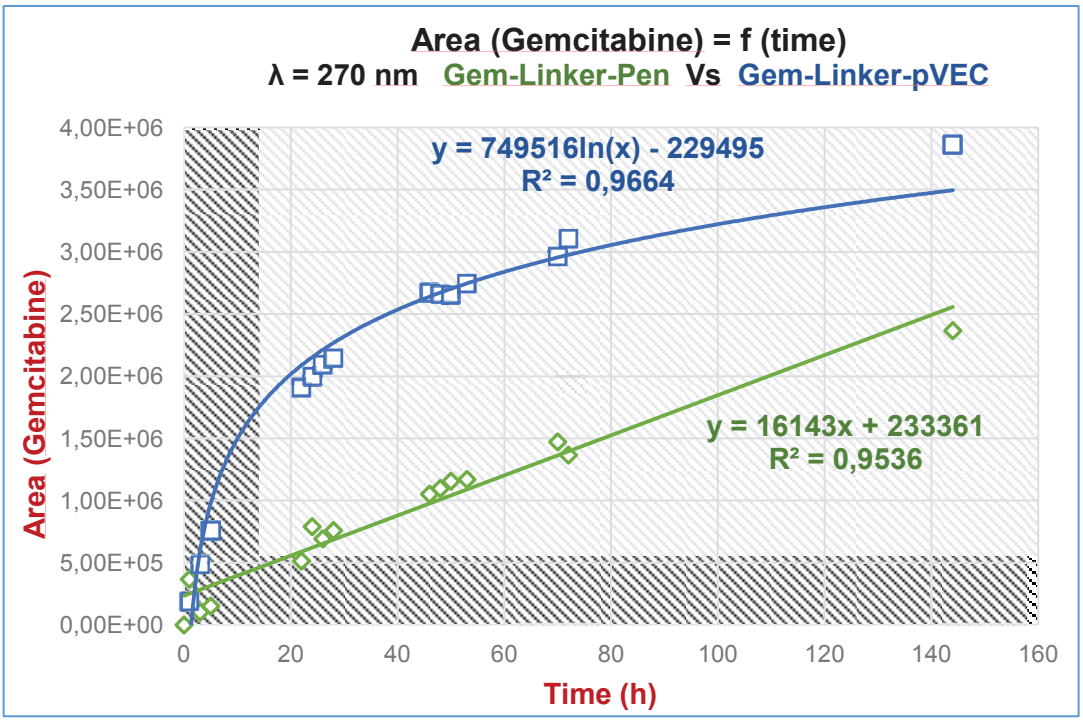

Figure 51: Graphical representation of the time-dependent release kinetics of free gemcitabine from the hydrolysis of Gemcitabine–Linker–Penetratin and Gemcitabine–Linker–pVEC conjugates in PBS (pH 7.4) at 37 ºC (λ = 270 nm).

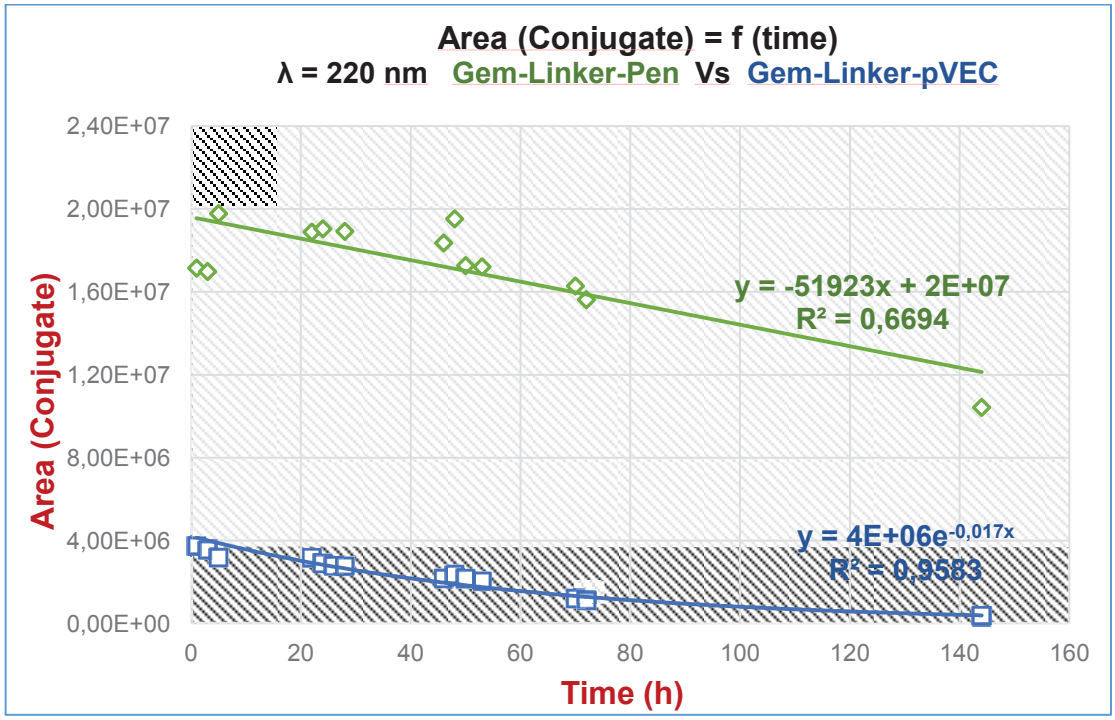

Figure 52: Graphical representation of the time-dependent kinetics of Gemcitabine–Linker–Penetratin and Gemcitabine–Linker–pVEC conjugates' hydrolysis in PBS (pH 7.4) at 37 ºC (λ = 220 nm).

3.4.3. Time-dependent kinetics of the Gemcitabine–Linker–Penetratin conjugate (over 22 days)

After 22 days, the degradation of the Gemcitabine–Linker–Penetratin conjugate is evident. However, the release of free gemcitabine from hydrolysis of this conjugate still doesn't present an adequate profile for drug release under the tested conditions, considering its higher chemical stability over a long period of time (Figure 53 and Figure 54).

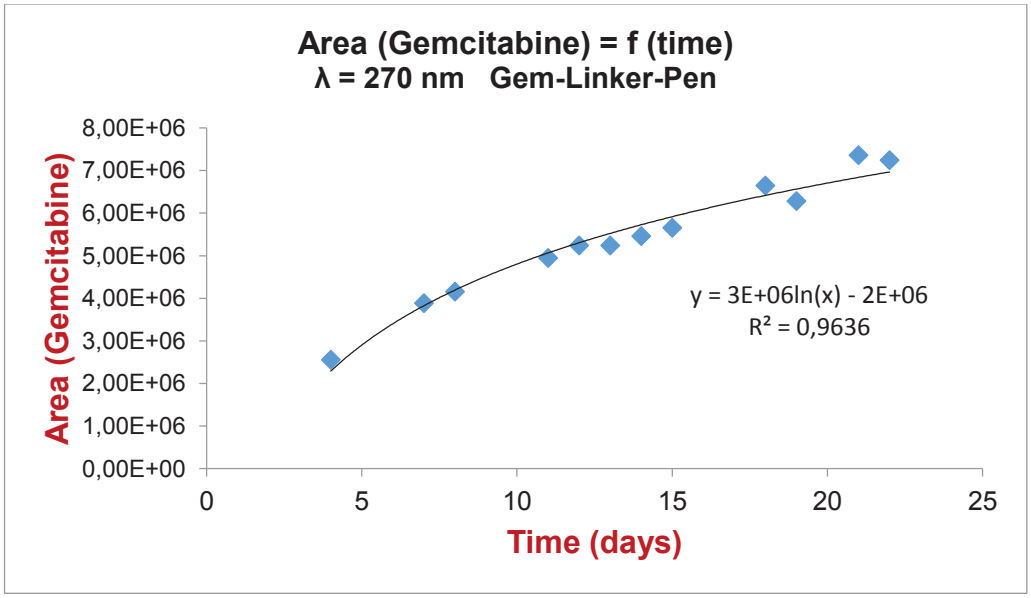

Figure 53: Graphical representation of the 22 days study on the time-dependent release kinetics of free gemcitabine from the hydrolysis of Gemcitabine–Linker–Penetratin conjugate in PBS (pH 7.4) at 37 ºC (λ = 270 nm).

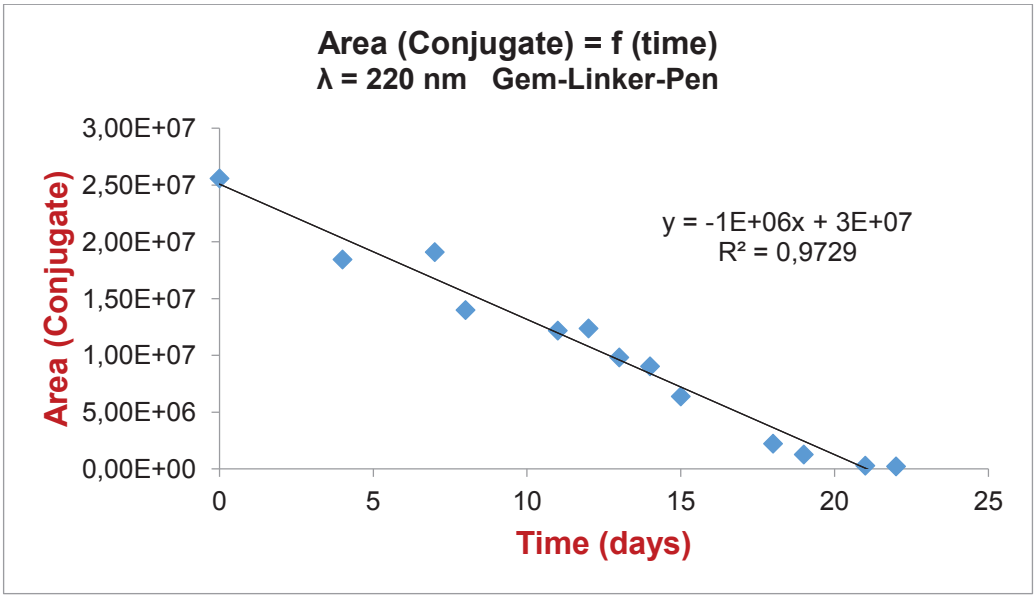

Figure 54: Graphical representation of the 22 days study on the time-dependent kinetics of Gemcitabine–Linker–Penetratin conjugate's hydrolysis in PBS (pH 7.4) at 37 ºC (λ = 220 nm).

3.5. Antiproliferative activity of the conjugates – SRB assay

After synthesizing the conjugates and determining their stability under physiological conditions, a preliminary study to evaluate the conjugates' antiproliferative activity was performed against three different cell lines: MKN-28 (human gastric cancer), Caco-2 (heterogeneous human epithelial colorectal adenocarcinoma) and HT-29 (human colon adenocarcinoma). Cells treated only with gemcitabine served as the control of this experiment. The Gemcitabine–Linker–pVEC conjugate was not tested against HT-29 cells because there was not a sufficient mass of this conjugate. Results are shown in Figure 55 and Table 7.

Table 7: Summary of the results of the antiproliferative activity of the compounds, with indication of the IC50 (μM).

	IC50 (μM) (Mean ± SEM)		
Compound	**MKN-28 (stomach)**	**Caco-2 (colon)**	**HT-29 (colon)**
Drug	> 100	> 100	32.23 ± 10.45
Drug-Pen	48.11 ± 9.30	67.04 ± 4.15	38.78 ± 21.09
Drug-pVEc	> 100	> 100	-

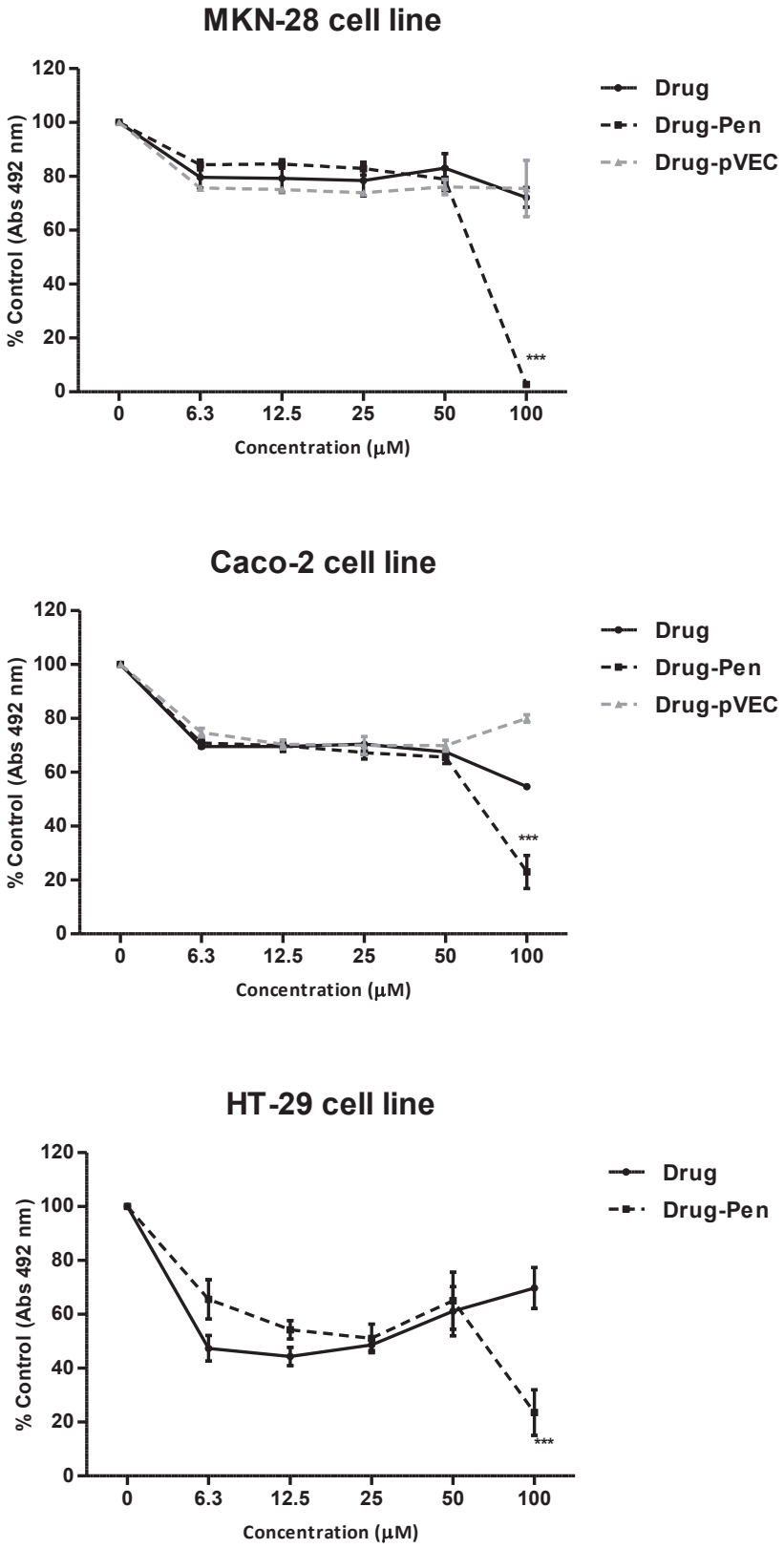

Figure 55: Effect of Gemcitabine–Linker–Penetratin and Gemcitabine–Linker–pVEC conjugates and free gemcitabine on the growth of different human tumoral cell lines evaluated by Sulforhodamine B assay. Cells were treated with a broad concentration range (6.3 – 100.0 μM) of each compound for 48 h. Each value represents the mean ± SEM (n = 3 – 6). **p <0.001, ***p <0.0001 (significant decrease vs control).

The Gemcitabine-CPP conjugates synthesized in this work were designed to act as new prodrugs of this chemotherapeutic agent, mainly by increasing the delivery of gemcitabine inside cells, where enzymatic hydrolysis will yield free gemcitabine, capable of inhibiting DNA synthesis.

After analyzing the results of this initial screening of biological activity, there are some preliminary conclusions can be taken: (a) Gemcitabine–Linker–pVEC conjugate displays an effect on cell viability comparable to free gemcitabine, (b) Gemcitabine–Linker–Penetratin can reduce cell viability to a more significant extent than the other compounds, although in the highest concentration tested (100 μM), this conjugate is close to cytotoxicity limits, and (c) Gemcitabine seems to have a greater activity in cells originated from the human colon than from the human stomach.

However, this study only gave the first insight into these conjugates' activity *in vitro* and a more exhaustive understanding of these conjugates' behavior, both *in vivo* and *in vitro*, is of major importance.

4. CONCLUSIONS AND FUTURE PERSPECTIVES

At the end of this dissertation project, it can be concluded that all of the proposed goals were accomplished. Both Cys-Penetratin and Cys-pVEC peptides were successfully synthesized by MW-SPPS with excellent purity, after the manual synthesis approach proved ineffective. This showed the importance of the heat provided by the microwave radiation to successfully synthesize these particular peptides.

Gemcitabine was also modified to bare a thiol group (compound **4**) or a dithiopyridine group (compound **7**) and was successfully conjugated to both CPPs. Gemcitabine–Linker–Penetratin and Gemcitabine–Linker–pVEC conjugates were obtained with an excellent purity grade and with acceptable yields.

The conjugates' stability studies demonstrated a different gemcitabine release profile for the two conjugates, with Gemcitabine–Linker–pVEC yielding free gemcitabine exponentially and after a short period of time, with more than 50% of gemcitabine being detected after 48 h, while Gemcitabine–Linker–Penetratin is more stable under the tested physiological conditions. Also, the preliminary *in vitro* assays on the antiproliferative activity of the conjugates indicated that cells treated with the Gemcitabine–Linker–Penetratin conjugate had greater growth inhibition percentages.

So as to continue this project, the next steps will require an optimization of the experimental conditions to modify gemcitabine, as well as optimizing the necessary purifications. As for testing the biological activity of the conjugates, both normal cells and cells with higher specificity for gemcitabine should be used in the next assays.

Overall, this investigation project proved to be a very promising new strategy/approach. In the future, different CPPs and different drugs could be conjugated in order to improve cancer (and even other diseases) treatments and diminish side effects.

5. BIBLIOGRAPHY

1. Web Page by National Cancer Institute: *Targeted Cancer Therapies*. Accessed November 11th, 2015; available from: http://www.cancer.gov/about-cancer/treatment/types/targeted-therapies/targeted-therapies-fact-sheet

2. Bianchi, V., Borella, S., Calderazzo, F., Ferraro, P., Bianchi, L. C. and Reichard, P. (1994), *Inhibition of ribonucleotide reductase by 2'-substituted deoxycytidine analogs: possible application in AIDS treatment,* Proceedings of the National Academy of Sciences, 91 (18), 8403-8407.

3. Ozols, R. F. (2005), *Gemcitabine and Carboplatin in Second-Line Ovarian Cancer,* Seminars in Oncology, 32, Supplement 6 4-8.

4. Albain, K. S., Nag, S. M., Calderillo-Ruiz, G., Jordaan, J. P., Llombart, A. C., Pluzanska, A.*, et al.* (2008), *Gemcitabine plus paclitaxel versus paclitaxel monotherapy in patients with metastatic breast cancer and prior anthracycline treatment,* J CLIN ONCOL, 26 (24), 3950-3957.

5. Akcali, Z., Calikusu, Z., Sakalli, H. and Ozyilkan, O. (2008), *Gemcitabine and cisplatin treatment of advanced-stage non-small-cell lung cancer in patients given cisplatin on day 8,* Tumori, 94 (4), 474-80.

6. Carmichael, J., Fink, U., Russell, R., Spittle, M., Harris, A., Spiessi, G.*, et al.* (1996), *Phase II study of gemcitabine in patients with advanced pancreatic cancer,* British journal of cancer, 73 (1), 101.

7. Web Page by National Cancer Institute: *FDA Approval for Gemcitabine Hydrochloride*. Accessed November 11th, 2015; available from: http://www.cancer.gov/about-cancer/treatment/drugs/fda-gemcitabine-hydrochloride#Anchor-PanCan

8. Web Page by lilly.com: *Highlights of prescribing information for GEMZAR (gemcitabine for injection), for intravenous use*. Accessed November 11th, 2015; available from: http://pi.lilly.com/us/gemzar.pdf

9. Web Page by FDA, USA: *GEMZAR® (Gemcitabine HCl) for injection - description*. Accessed November 11th, 2015; available from: http://www.fda.gov/ohrms/dockets/ac/06/briefing/2006-4254b_11_04_KP%20GemcitabineFDAlabel42005.pdf

10. Reid, J. M., Qu, W., Safgren, S. L., Ames, M. M., Krailo, M. D., Seibel, N. L.*, et al.* (2004), *Phase I trial and pharmacokinetics of gemcitabine in children with advanced solid tumors,* J CLIN ONCOL, 22 (12), 2445-2451.

11. Storniolo, A. M., Allerheiligen, S. and Pearce, H. L., editors. Preclinical, pharmacologic, and phase I studies of gemcitabine. Seminars in oncology; 1997.

12. Mackey, J. R., Mani, R. S., Selner, M., Mowles, D., Young, J. D., Belt, J. A.*, et al.* (1998), *Functional nucleoside transporters are required for gemcitabine influx and manifestation of toxicity in cancer cell lines,* Cancer research, 58 (19), 4349-4357.

13. Ueno, H., Kiyosawa, K. and Kaniwa, N. (2007), *Pharmacogenomics of gemcitabine: can genetic studies lead to tailor-made therapy?,* British journal of cancer, 97 (2), 145-151.

14. Hodge, L., Taub, M. and Tracy, T. (2011), *Effect of its deaminated metabolite, 2', 2'-difluorodeoxyuridine, on the transport and toxicity of gemcitabine in HeLa cells,* Biochemical pharmacology, 81 (7), 950-956.

15. Mori, R., Ishikawa, T., Ichikawa, Y., Taniguchi, K., Matsuyama, R., Ueda, M.*, et al.* (2007), *Human equilibrative nucleoside transporter 1 is associated with the chemosensitivity of gemcitabine in human pancreatic adenocarcinoma and biliary tract carcinoma cells,* Oncology reports, 17 (5), 1201-1205.

16. Kroep, J. R., van Moorsel, C. J., Veerman, G., Voorn, D. A., Schultz, R. M., Worzalla, J. F.*, et al.* (1998), *Role of deoxycytidine kinase (dCK), thymidine kinase 2 (TK2), and deoxycytidine deaminase (dCDA) in the antitumor activity of gemcitabine (dFdC),* Advances in experimental medicine and biology, 431 657-60.

17. Moysan, E., Bastiat, G. and Benoit, J. P. (2013), *Gemcitabine versus Modified Gemcitabine: a review of several promising chemical modifications,* Molecular pharmaceutics, 10 (2), 430-44.

18. Huang, P., Chubb, S., Hertel, L. W., Grindey, G. B. and Plunkett, W. (1991), *Action of 2', 2'-difluorodeoxycytidine on DNA synthesis,* Cancer research, 51 (22), 6110-6117.

19. Plunkett, W., Huang, P. and Gandhi, V. (1995), *Preclinical characteristics of gemcitabine,* Anti-cancer drugs, 6 7-13.

20. Heinemann, V., Xu, Y.-Z., Chubb, S., Sen, A., Hertel, L. W., Grindey, G. B.*, et al.* (1992), *Cellular elimination of 2', 2'-difluorodeoxycytidine 5'-triphosphate: a mechanism of self-potentiation,* Cancer research, 52 (3), 533-539.

21. Clarke, M. L., Mackey, J. R., Baldwin, S. A., Young, J. D. and Cass, C. E. The role of membrane transporters in cellular resistance to anticancer nucleoside drugs. Clinically Relevant Resistance in Cancer Chemotherapy: Springer; 2002. p. 27-47.

22. Rauchwerger, D. R., Firby, P. S., Hedley, D. W. and Moore, M. J. (2000), *Equilibrative-sensitive nucleoside transporter and its role in gemcitabine sensitivity,* Cancer research, 60 (21), 6075-6079.

23. Santini, D., Schiavon, G., Vincenzi, B., E Cass, C., Vasile, E., D Manazza, A.*, et al.* (2011), *Human equilibrative nucleoside transporter 1 (hENT1) levels predict response to gemcitabine in patients with biliary tract cancer (BTC),* Current cancer drug targets, 11 (1), 123-129.

24. Maréchal, R., Mackey, J. R., Lai, R., Demetter, P., Peeters, M., Polus, M.*, et al.* (2009), *Human equilibrative nucleoside transporter 1 and human concentrative nucleoside transporter 3 predict survival after adjuvant gemcitabine therapy in resected pancreatic adenocarcinoma,* Clinical cancer research, 15 (8), 2913-2919.

25. Sebastiani, V., Ricci, F., Rubio-Viquiera, B., Kulesza, P., Yeo, C. J., Hidalgo, M.*, et al.* (2006), *Immunohistochemical and genetic evaluation of deoxycytidine kinase in pancreatic cancer: relationship to molecular mechanisms of gemcitabine resistance and survival,* Clinical Cancer Research, 12 (8), 2492-2497.

26. Obata, T., Endo, Y., Tanaka, M., Uchida, H., Matsuda, A. and Sasaki, T. (2001), *Deletion mutants of human deoxycytidine kinase mRNA in cells resistant to antitumor cytosine nucleosides,* Cancer Science, 92 (7), 793-798.

27. Kroep, J. R., Loves, W. J., van der Wilt, C. L., Alvarez, E., Talianidis, I., Boven, E.*, et al.* (2002), *Pretreatment Deoxycytidine Kinase Levels Predict in Vivo Gemcitabine Sensitivity 1 Supported by Eli Lilly & Co, International and The Netherlands. 1,* Molecular cancer therapeutics, 1 (6), 371-376.

28. Fujita, H., Ohuchida, K., Mizumoto, K., Itaba, S., Ito, T., Nakata, K.*, et al.* (2010), *Gene expression levels as predictive markers of outcome in pancreatic cancer after gemcitabine-based adjuvant chemotherapy,* Neoplasia, 12 (10), 807-IN8.

29. Zhou, B.-S., Tsai, P., Ker, R., Tsai, J., Ho, R., Yu, J.*, et al.* (1998), *Overexpression of transfected human ribonucleotide reductase M2 subunit in human cancer cells enhances their invasive potential,* Clinical & experimental metastasis, 16 (1), 43-49.

30. Zhou, J., Oliveira, P., Li, X., Chen, Z. and Bepler, G. (2010), *Modulation of the ribonucleotide reductase-antimetabolite drug interaction in cancer cell lines,* Journal of nucleic acids, 2010

31. Duxbury, M. S., Ito, H., Zinner, M. J., Ashley, S. W. and Whang, E. E. (2004), *RNA interference targeting the M2 subunit of ribonucleotide reductase enhances pancreatic adenocarcinoma chemosensitivity to gemcitabine,* Oncogene, 23 (8), 1539-1548.

32. Bold, R. J., Chandra, J. and McConkey, D. J. (1999), *Gemcitabine-induced programmed cell death (apoptosis) of human pancreatic carcinoma is determined by Bcl-2 content,* Annals of surgical oncology, 6 (3), 279-285.

33. Shi, X., Liu, S., Kleeff, J., rg, o., Friess, H. and Büchler, M. W. (2002), *Acquired resistance of pancreatic cancer cells towards 5-Fluorouracil and gemcitabine is associated with altered expression of apoptosis-regulating genes,* Oncology, 62 (4), 354-362.

34. Huang, P. and Plunkett, W., editors. Induction of apoptosis by gemcitabine. Seminars in oncology; 1995.

35. Huang, P. and Plunkett, W. (1995), *Fludarabine-and gemcitabine-induced apoptosis: incorporation of analogs into DNA is a critical event,* Cancer chemotherapy and pharmacology, 36 (3), 181-188.

36. Amaral, J. D., Xavier, J. M., Steer, C. J. and Rodrigues, C. M. (2010), *The role of p53 in apoptosis,* Discov Med, 9 (45), 145-52.

37. Tolis, C., Peters, G., Ferreira, C., Pinedo, H. and Giaccone, G. (1999), *Cell cycle disturbances and apoptosis induced by topotecan and gemcitabine on human lung cancer cell lines,* European journal of cancer, 35 (5), 796-807.

38. Lima, C. M. R., Green, M. R., Rotche, R., Miller, W. H., Jeffrey, G. M., Cisar, L. A.*, et al.* (2004), *Irinotecan plus gemcitabine results in no survival advantage compared with gemcitabine monotherapy in patients with locally advanced or metastatic pancreatic cancer despite increased tumor response rate,* J CLIN ONCOL, 22 (18), 3776-3783.

39. Chakravarthy, A., Abrams, R. A., Yeo, C. J., Korman, L. T., Donehower, R. C., Hruban, R. H.*, et al.* (2000), *Intensified adjuvant combined modality therapy for resected periampullary adenocarcinoma: acceptable toxicity and suggestion of improved 1-year disease-free survival,* International Journal of Radiation Oncology* Biology* Physics, 48 (4), 1089-1096.

40. Han, H.-K. and Amidon, G. L. (2000), *Targeted prodrug design to optimize drug delivery,* AAPS PharmSci, 2 (1), 48-58.

41. Mero, A., Clementi, C., Veronese, F. M. and Pasut, G. Covalent conjugation of poly (ethylene glycol) to proteins and peptides: strategies and methods. Bioconjugation Protocols: Springer; 2011. p. 95-129.

42. Harris, J. M. and Chess, R. B. (2003), *Effect of pegylation on pharmaceuticals,* Nature Reviews Drug Discovery, 2 (3), 214-221.

43. Caliceti, P. and Veronese, F. M. (2003), *Pharmacokinetic and biodistribution properties of poly (ethylene glycol)–protein conjugates,* Advanced drug delivery reviews, 55 (10), 1261-1277.

44. Maeda, H., Wu, J., Sawa, T., Matsumura, Y. and Hori, K. (2000), *Tumor vascular permeability and the EPR effect in macromolecular therapeutics: a review,* Journal of controlled release, 65 (1), 271-284.

45. Szebeni, J. (2005), *Complement activation-related pseudoallergy: a new class of drug-induced acute immune toxicity,* Toxicology, 216 (2), 106-121.

46. Pasut, G. and Veronese, F. M. (2009), *PEG conjugates in clinical development or use as anticancer agents: an overview,* Advanced drug delivery reviews, 61 (13), 1177-1188.

47. Vandana, M. and Sahoo, S. K. (2010), *Long circulation and cytotoxicity of PEGylated gemcitabine and its potential for the treatment of pancreatic cancer,* Biomaterials, 31 (35), 9340-9356.

48. Bareford, L. M. and Swaan, P. W. (2007), *Endocytic mechanisms for targeted drug delivery,* Advanced drug delivery reviews, 59 (8), 748-758.

49. Chuang, K.-H., Wang, H.-E., Chen, F.-M., Tzou, S.-C., Cheng, C.-M., Chang, Y.-C.*, et al.* (2010), *Endocytosis of PEGylated agents enhances cancer imaging and anticancer efficacy,* Molecular cancer therapeutics, 9 (6), 1903-1912.

50. Iwakiri, S., Sonobe, M., Nagai, S., Hirata, T., Wada, H. and Miyahara, R. (2008), *Expression status of folate receptor α is significantly correlated with prognosis in non-small-cell lung cancers,* Annals of surgical oncology, 15 (3), 889-899.

51. Hartmann, L. C., Keeney, G. L., Lingle, W. L., Christianson, T. J., Varghese, B., Hillman, D.*, et al.* (2007), *Folate receptor overexpression is associated with poor outcome in breast cancer,* International journal of cancer, 121 (5), 938-942.

52. Basal, E., Eghbali-Fatourechi, G. Z., Kalli, K. R., Hartmann, L. C., Goodman, K. M., Goode, E. L.*, et al.* (2009), *Functional folate receptor alpha is elevated in the blood of ovarian cancer patients,* PLoS One, 4 (7), e6292.

53. Pasut, G., Canal, F., Dalla Via, L., Arpicco, S., Veronese, F. M. and Schiavon, O. (2008), *Antitumoral activity of PEG–gemcitabine prodrugs targeted by folic acid,* Journal of Controlled Release, 127 (3), 239-248.

54. Schiavon, O., Pasut, G., Moro, S., Orsolini, P., Guiotto, A. and Veronese, F. (2004), *PEG–Ara-C conjugates for controlled release,* European journal of medicinal chemistry, 39 (2), 123-133.

55. Bender, D. M., Bao, J., Dantzig, A. H., Diseroad, W. D., Law, K. L., Magnus, N. A.*, et al.* (2009), *Synthesis, crystallization, and biological evaluation of an orally active prodrug of gemcitabine,* Journal of medicinal chemistry, 52 (22), 6958-6961.

56. Koolen, S. L., Witteveen, P. O., Jansen, R. S., Langenberg, M. H., Kronemeijer, R. H., Nol, A.*, et al.* (2011), *Phase I study of Oral gemcitabine prodrug (LY2334737) alone and in combination with erlotinib in patients with advanced solid tumors,* Clinical cancer research : an official journal of the American Association for Cancer Research, 17 (18), 6071-82.

57. Newmark, H. L. (1997), *Squalene, olive oil, and cancer risk: a review and hypothesis,* Cancer Epidemiology Biomarkers & Prevention, 6 (12), 1101-1103.

58. Couvreur, P., Stella, B., Reddy, L. H., Hillaireau, H., Dubernet, C., Desmaële, D.*, et al.* (2006), *Squalenoyl nanomedicines as potential therapeutics,* Nano letters, 6 (11), 2544-2548.

59. Jordheim, L. P., Cros, E., Gouy, M.-H., Galmarini, C. M., Peyrottes, S., Mackey, J.*, et al.* (2004), *Characterization of a Gemcitabine-Resistant Murine Leukemic Cell Line Reversion of In vitro Resistance by a Mononucleotide Prodrug,* Clinical Cancer Research, 10 (16), 5614-5621.

60. Gourdeau, H., Clarke, M. L., Ouellet, F., Mowles, D., Selner, M., Richard, A.*, et al.* (2001), *Mechanisms of uptake and resistance to troxacitabine, a novel deoxycytidine nucleoside analogue, in human leukemic and solid tumor cell lines,* Cancer research, 61 (19), 7217-7224.

61. Réjiba, S., Reddy, L. H., Bigand, C., Parmentier, C., Couvreur, P. and Hajri, A. (2011), *Squalenoyl gemcitabine nanomedicine overcomes the low efficacy of gemcitabine therapy in pancreatic cancer,* Nanomedicine: Nanotechnology, Biology and Medicine, 7 (6), 841-849.

62. Bildstein, L., Dubernet, C., Marsaud, V., Chacun, H., Nicolas, V., Gueutin, C.*, et al.* (2010), *Transmembrane diffusion of gemcitabine by a nanoparticulate squalenoyl prodrug: an original drug delivery pathway,* Journal of Controlled Release, 147 (2), 163-170.

63. Reddy, L. H., Dubernet, C., Mouelhi, S. L., Marque, P. E., Desmaele, D. and Couvreur, P. (2007), *A new nanomedicine of gemcitabine displays enhanced anticancer activity in sensitive and resistant leukemia types,* Journal of Controlled Release, 124 (1), 20-27.

64. Immordino, M. L., Brusa, P., Rocco, F., Arpicco, S., Ceruti, M. and Cattel, L. (2004), *Preparation, characterization, cytotoxicity and pharmacokinetics of liposomes containing lipophilic gemcitabine prodrugs,* Journal of Controlled Release, 100 (3), 331-346.

65. Brusa, P., Immordino, M. L., Rocco, F. and Cattel, L. (2007), *Antitumor activity and pharmacokinetics of liposomes containing lipophilic gemcitabine prodrugs,* Anticancer research, 27 (1A), 195-199.

66. Dasari, M., Lee, S., Sy, J., Kim, D., Lee, S., Brown, M.*, et al.* (2010), *Hoechst-IR: an imaging agent that detects necrotic tissue in vivo by binding extracellular DNA,* Organic letters, 12 (15), 3300-3303.

67. Dasari, M., Acharya, A. P., Kim, D., Lee, S., Lee, S., Rhea, J.*, et al.* (2013), *H-Gemcitabine: A New Gemcitabine Prodrug for Treating Cancer,* Bioconjugate chemistry, 24 (1), 4-8.

68. Bergman, A. M., Adema, A. D., Balzarini, J., Bruheim, S., Fichtner, I., Noordhuis, P.*, et al.* (2011), *Antiproliferative activity, mechanism of action and oral antitumor activity of CP-4126, a fatty acid derivative of gemcitabine, in in vitro and in vivo tumor models,* Investigational new drugs, 29 (3), 456-466.

69. Adema, A., Bijnsdorp, I., Sandvold, M., Verheul, H. and Peters, G. (2009), *Innovations and opportunities to improve conventional (deoxy) nucleoside and fluoropyrimidine analogs in cancer,* Curr Med Chem, 16 (35), 4632-4643.

70. Bergman, A., Kuiper, C., Voorn, D., Comijn, E., Myhren, F., Sandvold, M.*, et al.* (2004), *Antiproliferative activity and mechanism of action of fatty acid derivatives of arabinofuranosylcytosine in leukemia and solid tumor cell lines,* Biochemical pharmacology, 67 (3), 503-511.

71. Galmarini, C. M., Myhren, F. and Sandvold, M. L. (2009), *CP-4055 and CP-4126 are active in ara-C and gemcitabine-resistant lymphoma cell lines,* British journal of haematology, 144 (2), 273-275.

72. Adema, A. D., Smid, K., Losekoot, N., Honeywell, R. J., Verheul, H. M., Myhren, F.*, et al.* (2012), *Metabolism and accumulation of the lipophilic deoxynucleoside analogs elacytarabine and CP-4126,* Investigational new drugs, 30 (5), 1908-1916.

73. Sandvold, M. L., Galmarini, C., Myhren, F. and Peters, G. (2010), *The activity of the lipophilic nucleoside derivatives elacytarabine and CP-4126 in a panel of tumor cell lines resistant to nucleoside analogues,* Nucleosides, Nucleotides and Nucleic Acids, 29 (4-6), 386-393.

74. Gagnadoux, F., Le Pape, A., Urban, T., Montharu, J., Vecellio, L., Dubus, J.-C.*, et al.* (2005), *Safety of pulmonary administration of gemcitabine in rats,* Journal of aerosol medicine, 18 (2), 198-206.

75. Ali, S. M., Khan, A. R., Ahmad, M. U., Chen, P., Sheikh, S. and Ahmad, I. (2005), *Synthesis and biological evaluation of gemcitabine–lipid conjugate (NEO6002),* Bioorganic & medicinal chemistry letters, 15 (10), 2571-2574.

76. Sakamoto, T., Inoue, T., Otomo, Y., Yokomori, N., Ohno, M., Arai, H.*, et al.* (2012), *Deficiency of cardiolipin synthase causes abnormal mitochondrial function and morphology in germ cells of Caenorhabditis elegans,* Journal of Biological Chemistry, 287 (7), 4590-4601.

77. Chien, P.-Y., Khan, A. R., Miller, B., Sheikh, S., Ali, S. M., Ahmad, M. U., *et al.* (2005), *A novel gemcitabine-cardiolipin conjugate induced cytotoxicity in cancer cells through an equilibrative nucleoside transporter-independent pathway,* Cancer research, 65 (9 Supplement), 1197-1197.

78. Chen, P., Chien, P.-Y., Khan, A. R., Sheikh, S., Ali, S. M., Ahmad, M. U., *et al.* (2006), *In-vitro and in-vivo anti-cancer activity of a novel gemcitabine–cardiolipin conjugate,* Anti-cancer drugs, 17 (1), 53-61.

79. Galmarini, C. M., Warren, G., Senanayake, M. T. and Vinogradov, S. V. (2010), *Efficient overcoming of drug resistance to anticancer nucleoside analogs by nanodelivery of active phosphorylated drugs,* International journal of pharmaceutics, 395 (1), 281-289.

80. Tobias, S. C. and Borch, R. F. (2001), *Synthesis and biological studies of novel nucleoside phosphoramidate prodrugs,* Journal of medicinal chemistry, 44 (25), 4475-4480.

81. Patent: Patent application, WO/2009/053654, ***Gemcitabine phosphoester prodrugs as anticancer agents****, Gemcitabine phosphoester prodrugs as anticancer agents*, Perigaud, C. P., S.; Dumontet, C. , 2009

82. Wu, W., Sigmond, J., Peters, G. J. and Borch, R. F. (2007), *Synthesis and biological activity of a gemcitabine phosphoramidate prodrug,* Journal of medicinal chemistry, 50 (15), 3743-3746.

83. Tsume, Y., Incecayir, T., Song, X., Hilfinger, J. M. and Amidon, G. L. (2014), *The development of orally administrable gemcitabine prodrugs with d-enantiomer amino acids: Enhanced membrane permeability and enzymatic stability,* European Journal of Pharmaceutics and Biopharmaceutics, 86 (3), 514-523.

84. Copolovici, D. M., Langel, K., Eriste, E. and Langel, U. l. (2014), *Cell-penetrating peptides: design, synthesis, and applications,* ACS nano, 8 (3), 1972-1994.

85. Sewald, N. and Jakubke, H.-D. Biologically Active Peptides. Peptides: Chemistry and Biology: Wiley-VCH Verlag GmbH & Co. KGaA; 2003. p. 61-134.

86. Heitz, F., Morris, M. C. and Divita, G. (2009), *Twenty years of cell-penetrating peptides: from molecular mechanisms to therapeutics,* British journal of pharmacology, 157 (2), 195-206.

87. Mitchell, D. J., Steinman, L., Kim, D., Fathman, C. and Rothbard, J. (2000), *Polyarginine enters cells more efficiently than other polycationic homopolymers,* The Journal of Peptide Research, 56 (5), 318-325.

88. Tang, H., Yin, L., Kim, K. H. and Cheng, J. (2013), *Helical poly (arginine) mimics with superior cell-penetrating and molecular transporting properties,* Chemical Science, 4 (10), 3839-3844.

89. Myrberg, H., Zhang, L., Mäe, M. and Langel, Ü. (2007), *Design of a tumor-homing cell-penetrating peptide,* Bioconjugate chemistry, 19 (1), 70-75.

90. Howl, J., Matou-Nasri, S., West, D. C., Farquhar, M., Slaninová, J., Östenson, C.-G.*, et al.* (2012), *Bioportide: an emergent concept of bioactive cell-penetrating peptides,* Cell Mol Life Sci, 69 (17), 2951-2966.

91. Svensen, N., Walton, J. G. and Bradley, M. (2012), *Peptides for cell-selective drug delivery,* Trends in pharmacological sciences, 33 (4), 186-192.

92. Mäe, M. and Langel, Ü. (2006), *Cell-penetrating peptides as vectors for peptide, protein and oligonucleotide delivery,* Current opinion in pharmacology, 6 (5), 509-514.

93. Fonseca, S. B., Pereira, M. P. and Kelley, S. O. (2009), *Recent advances in the use of cell-penetrating peptides for medical and biological applications,* Advanced drug delivery reviews, 61 (11), 953-964.

94. Deshayes, S., Plénat, T., Aldrian-Herrada, G., Divita, G., Le Grimellec, C. and Heitz, F. (2004), *Primary amphipathic cell-penetrating peptides: structural requirements and interactions with model membranes,* Biochemistry, 43 (24), 7698-7706.

95. Madani, F., Lindberg, S., Langel, Ü., Futaki, S. and Gräslund, A. (2011), *Mechanisms of cellular uptake of cell-penetrating peptides,* Journal of Biophysics, 2011

96. Mueller, J., Kretzschmar, I., Volkmer, R. and Boisguerin, P. (2008), *Comparison of cellular uptake using 22 CPPs in 4 different cell lines,* Bioconjugate chemistry, 19 (12), 2363-2374.

97. Nakase, I., Hirose, H., Tanaka, G., Tadokoro, A., Kobayashi, S., Takeuchi, T.*, et al.* (2009), *Cell-surface accumulation of flock house virus-derived peptide leads to efficient internalization via macropinocytosis,* Molecular Therapy, 17 (11), 1868-1876.

98. Stewart, K. M., Horton, K. L. and Kelley, S. O. (2008), *Cell-penetrating peptides as delivery vehicles for biology and medicine,* Organic & biomolecular chemistry, 6 (13), 2242-2255.

99. Aroui, S., Brahim, S., De Waard, M., Bréard, J. and Kenani, A. (2009), *Efficient induction of apoptosis by doxorubicin coupled to cell-penetrating peptides compared to unconjugated doxorubicin in the human breast cancer cell line MDA-MB 231,* Cancer letters, 285 (1), 28-38.

100. Derossi, D., Joliot, A. H., Chassaing, G. and Prochiantz, A. (1994), *The third helix of the Antennapedia homeodomain translocates through biological membranes,* Journal of Biological Chemistry, 269 (14), 10444-10450.

101. Jain, M., Chauhan, S. C., Singh, A. P., Venkatraman, G., Colcher, D. and Batra, S. K. (2005), *Penetratin improves tumor retention of single-chain antibodies: a novel step toward optimization of radioimmunotherapy of solid tumors,* Cancer research, 65 (17), 7840-7846.

102. Regberg, J., Srimanee, A. and Langel, Ü. (2012), *Applications of cell-penetrating peptides for tumor targeting and future cancer therapies,* Pharmaceuticals, 5 (9), 991-1007.

103. Elmquist, A., Lindgren, M., Bartfai, T. and Langel, Ü. (2001), *VE-Cadherin-Derived Cell-Penetrating Peptide, pVEC, with Carrier Functions,* Experimental Cell Research, 269 (2), 237-244.

104. Web Page by BACHEM: *Solid Phase Peptide Synthesis*. Accessed November 11th, 2015; available from: https://www.bachem.com/fileadmin/user_upload/pdf/Catalogs_Brochures/Solid_Phase_Peptide_Synthesis.pdf

105. Blondelle, S. E.; **"Understanding Biology Using Peptides: Proceedings of the Nineteenth American Peptide Symposium"**, Springer Science & Business Media, **2007**.

106. Postma, T. M., Giraud, M. and Albericio, F. (2012), *Trimethoxyphenylthio as a highly labile replacement for tert-butylthio cysteine protection in Fmoc solid phase synthesis,* Organic letters, 14 (21), 5468-5471.

107. Monks, A., Scudiero, D., Skehan, P., Shoemaker, R., Paull, K., Vistica, D.*, et al.* (1991), *Feasibility of a high-flux anticancer drug screen using a diverse panel of cultured human tumor cell lines,* Journal of the National Cancer Institute, 83 (11), 757-766.

108. Skehan, P., Storeng, R., Scudiero, D., Monks, A., McMahon, J., Vistica, D.*, et al.* (1990), *New colorimetric cytotoxicity assay for anticancer-drug screening,* Journal of the National Cancer Institute, 82 (13), 1107-1112.

6. SUPPLEMENTARY INFORMATION

6.1. Stability studies – periodic HPLC analysis over 6 days

6.1.1. Gemcitabine–Linker–Penetratin Conjugate

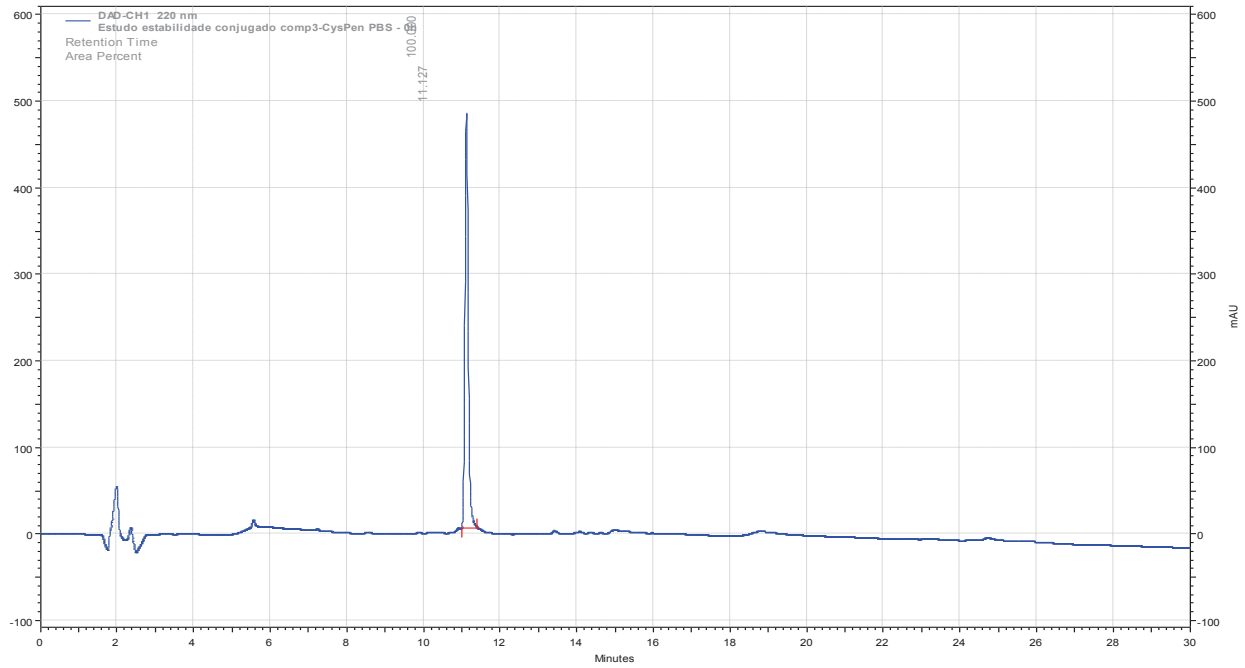

Figure 56: Stability study of the Gemcitabine–Linker–Penetratin conjugate: HPLC analysis performed in the beginning of the study (0 h). Chromatogram acquired with a HPLC-DAD system, with a C18 column, using ACN in water with 0.05% TFA as eluent, in gradient mode (0 – 100%), for 30 minutes, at a flow of 1 mL/min and detection at λ = 220 nm.

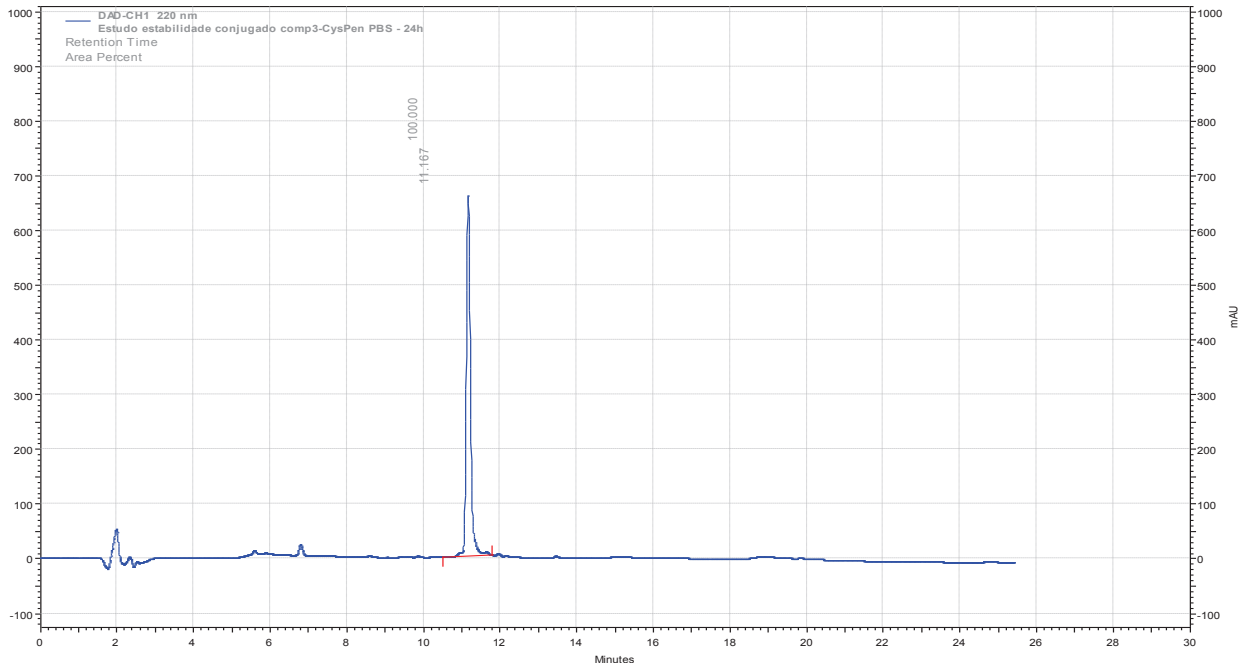

Figure 57: Stability study of the Gemcitabine–Linker–Penetratin conjugate: HPLC analysis performed after 24 h. Chromatogram acquired with a HPLC-DAD system, with a C18 column, using ACN in water with 0.05% TFA as eluent, in gradient mode (0 – 100%), for 30 minutes, at a flow of 1 mL/min and detection at λ = 220 nm.

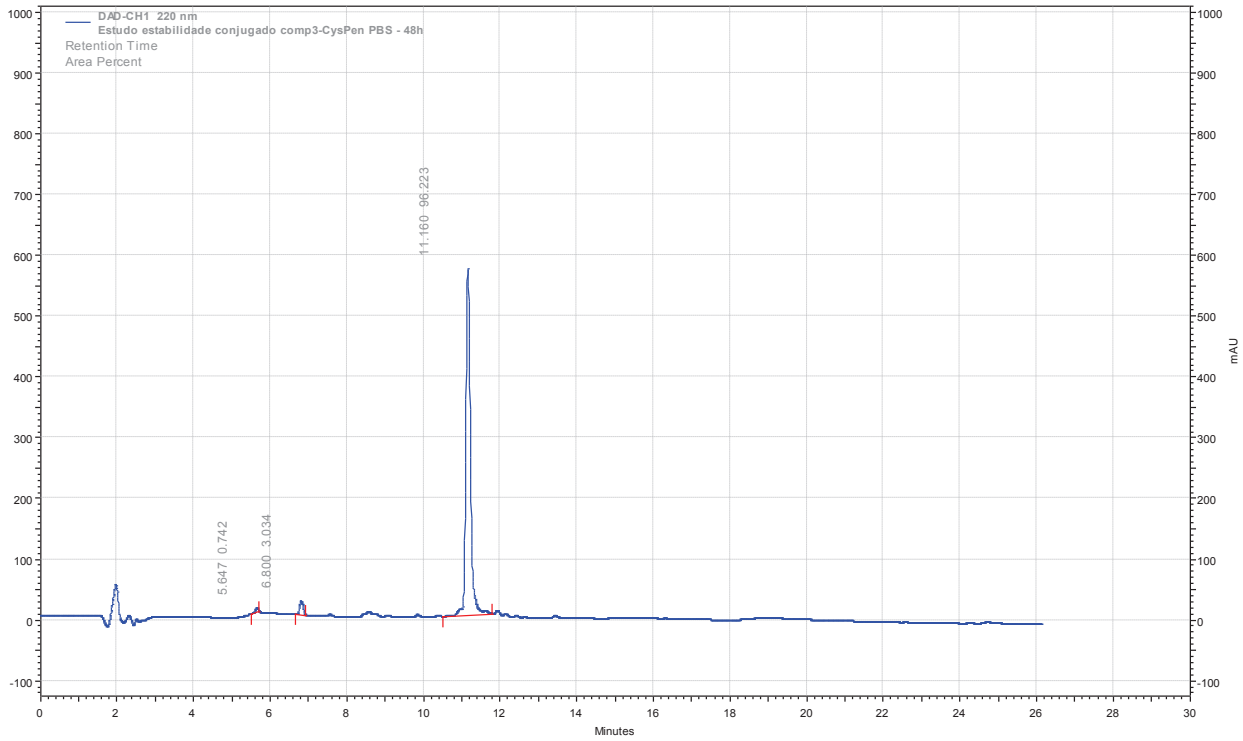

Figure 58: Stability study of the Gemcitabine–Linker–Penetratin conjugate: HPLC analysis performed after 48 h. Chromatogram acquired with a HPLC-DAD system, with a C18 column, using ACN in water with 0.05% TFA as eluent, in gradient mode (0 – 100%), for 30 minutes, at a flow of 1 mL/min and detection at λ = 220 nm.

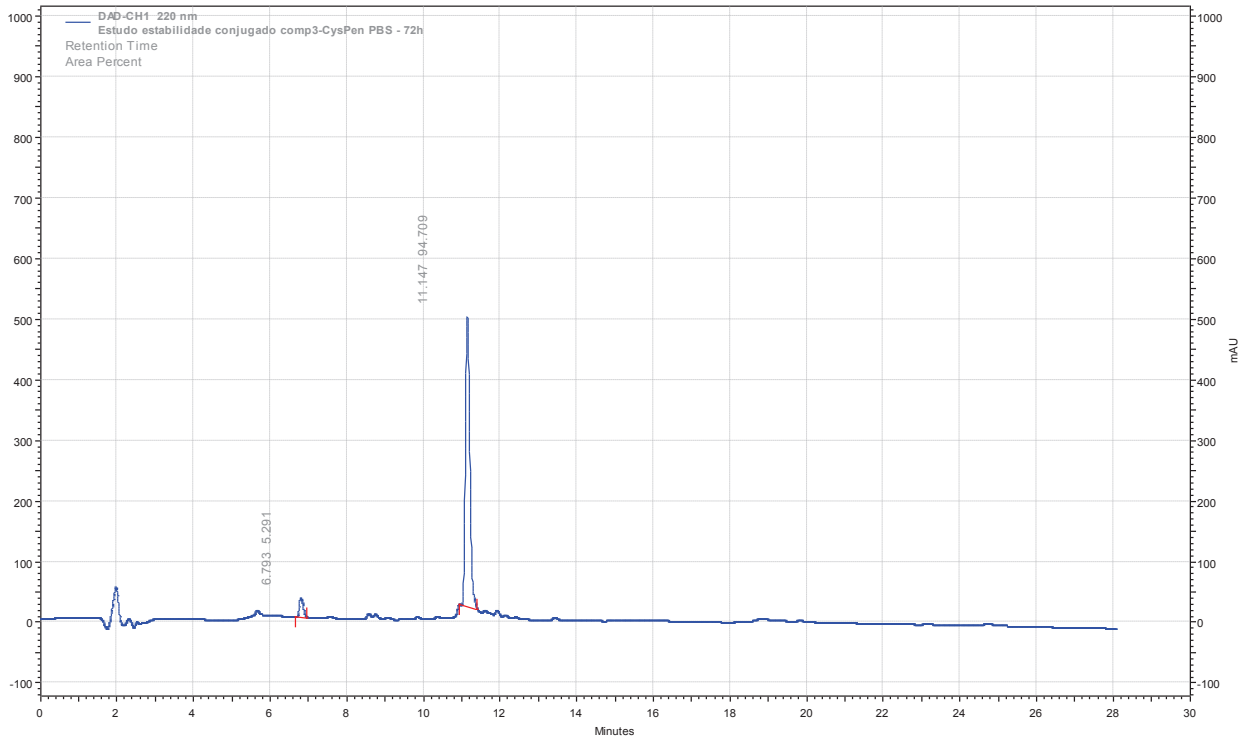

Figure 59: Stability study of the Gemcitabine–Linker–Penetratin conjugate: HPLC analysis performed after 72 h. Chromatogram acquired with a HPLC-DAD system, with a C18 column, using ACN in water with 0.05% TFA as eluent, in gradient mode (0 – 100%), for 30 minutes, at a flow of 1 mL/min and detection at λ = 220 nm.

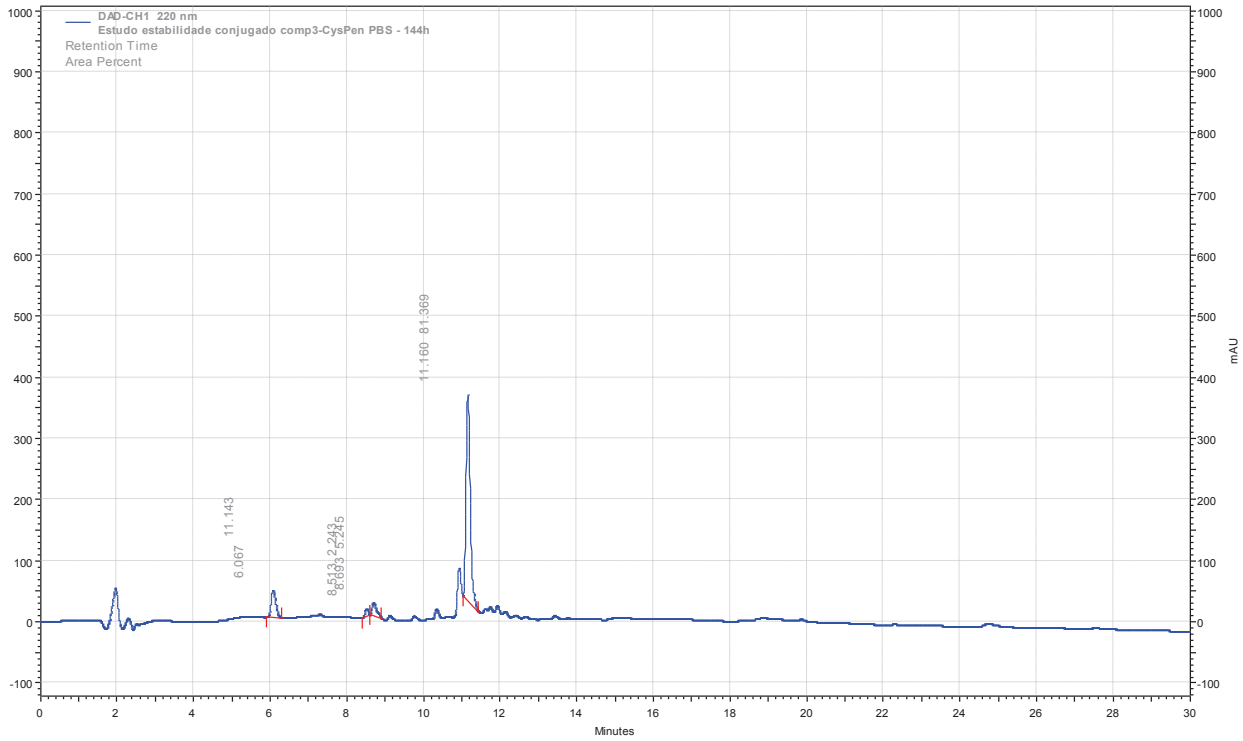

Figure 60: Stability study of the Gemcitabine–Linker–Penetratin conjugate: HPLC analysis performed after 144 h. Chromatogram acquired with a HPLC-DAD system, with a C18 column, using ACN in water with 0.05% TFA as eluent, in gradient mode (0 – 100%), for 30 minutes, at a flow of 1 mL/min and detection at λ = 220 nm.

6.1.2. Gemcitabine–Linker–pVEC Conjugate

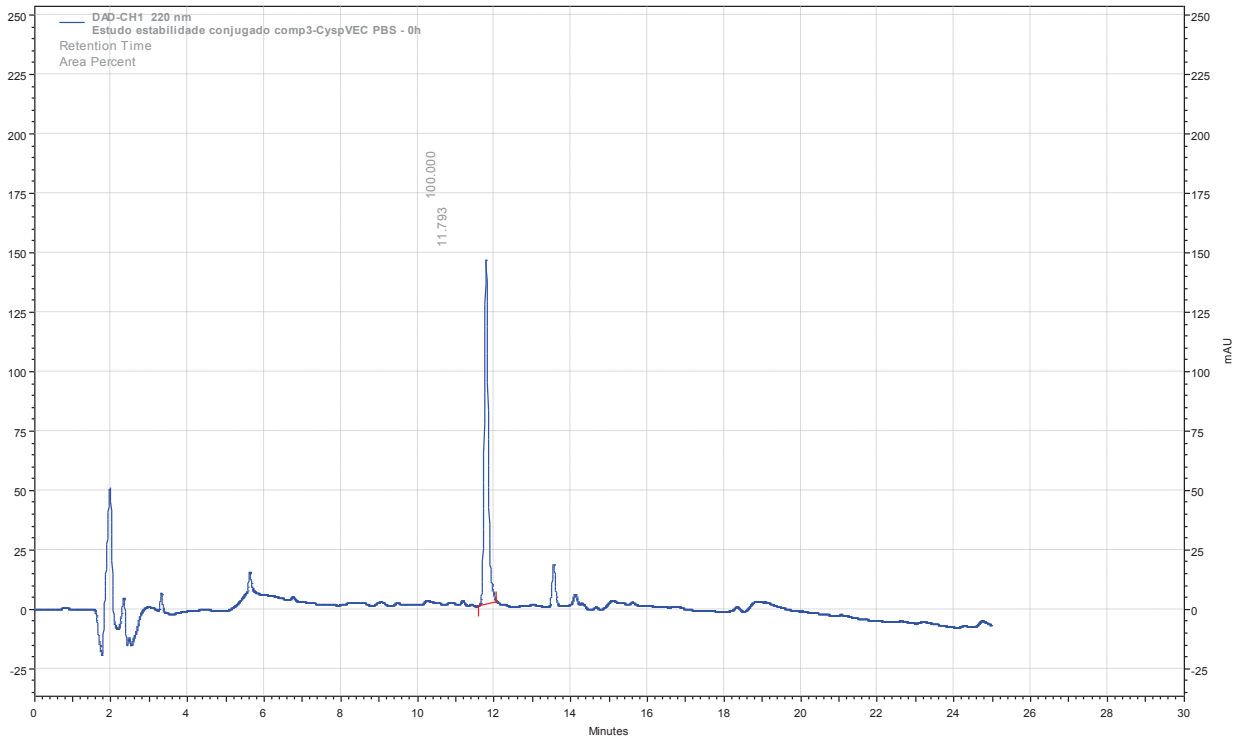

Figure 61: Stability study of the Gemcitabine–Linker–pVEC conjugate: HPLC analysis performed in the beginning of the study (0 h). Chromatogram acquired with a HPLC-DAD system, with a C18 column, using ACN in water with 0.05% TFA as eluent, in gradient mode (0 – 100%), for 30 minutes, at a flow of 1 mL/min and detection at λ = 220 nm.

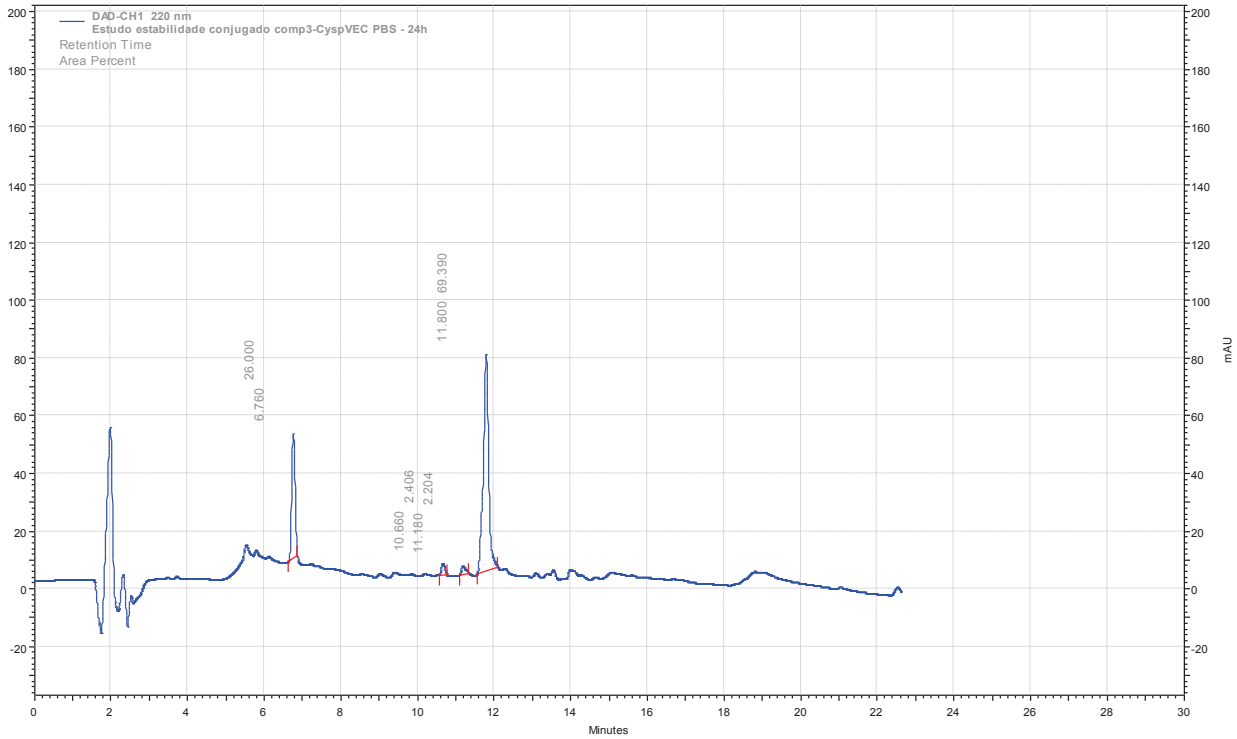

Figure 62: Stability study of the Gemcitabine–Linker–pVEC conjugate: HPLC analysis performed after 24 h. Chromatogram acquired with a HPLC-DAD system, with a C18 column, using ACN in water with 0.05% TFA as eluent, in gradient mode (0 – 100%), for 30 minutes, at a flow of 1 mL/min and detection at λ = 220 nm.

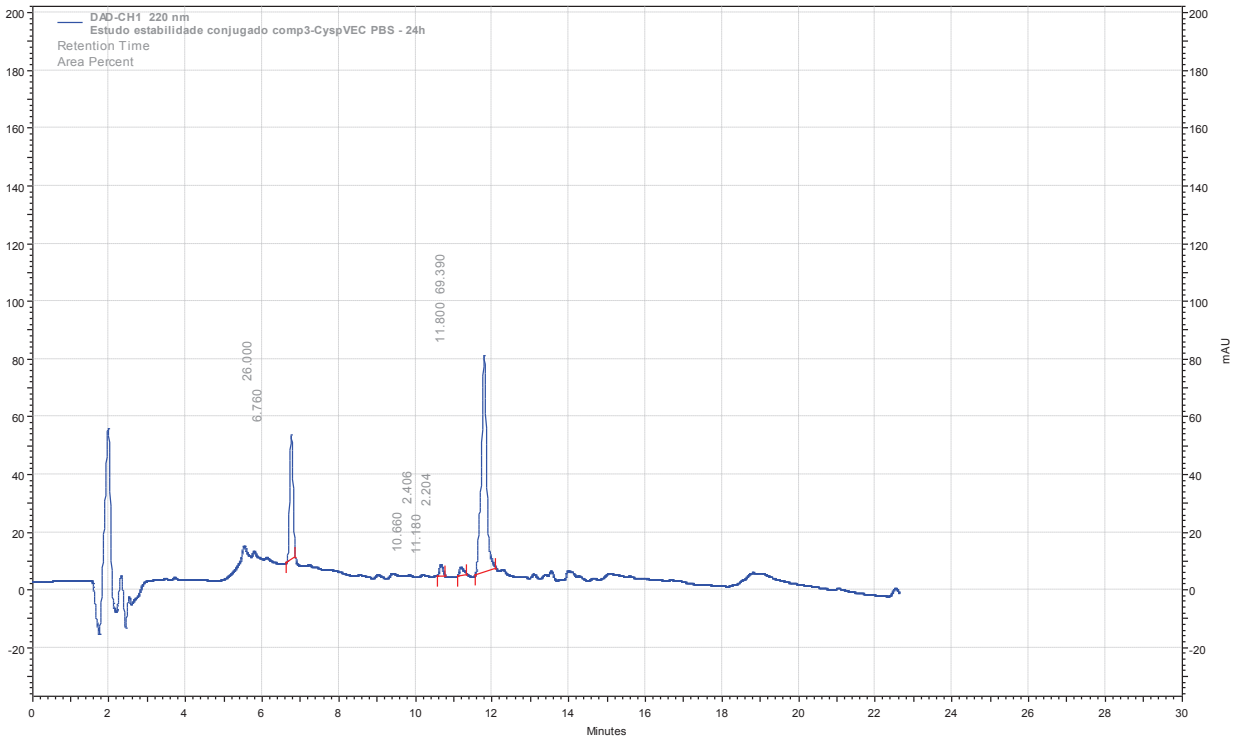

Figure 63: Stability study of the Gemcitabine–Linker–pVEC conjugate: HPLC analysis performed after 48 h. Chromatogram acquired with a HPLC-DAD system, with a C18 column, using ACN in water with 0.05% TFA as eluent, in gradient mode (0 – 100%), for 30 minutes, at a flow of 1 mL/min and detection at λ = 220 nm.

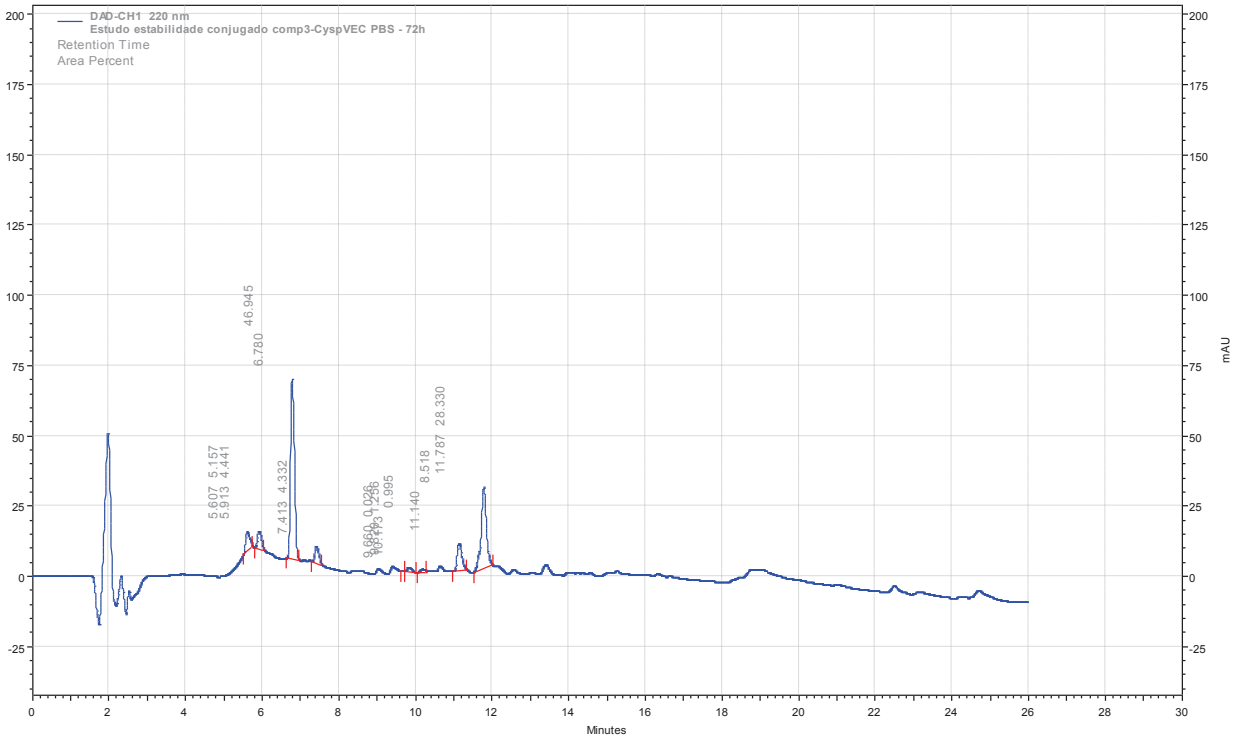

Figure 64: Stability study of the Gemcitabine–Linker–pVEC conjugate: HPLC analysis performed after 72 h. Chromatogram acquired with a HPLC-DAD system, with a C18 column, using ACN in water with 0.05% TFA as eluent, in gradient mode (0 – 100%), for 30 minutes, at a flow of 1 mL/min and detection at λ = 220 nm.

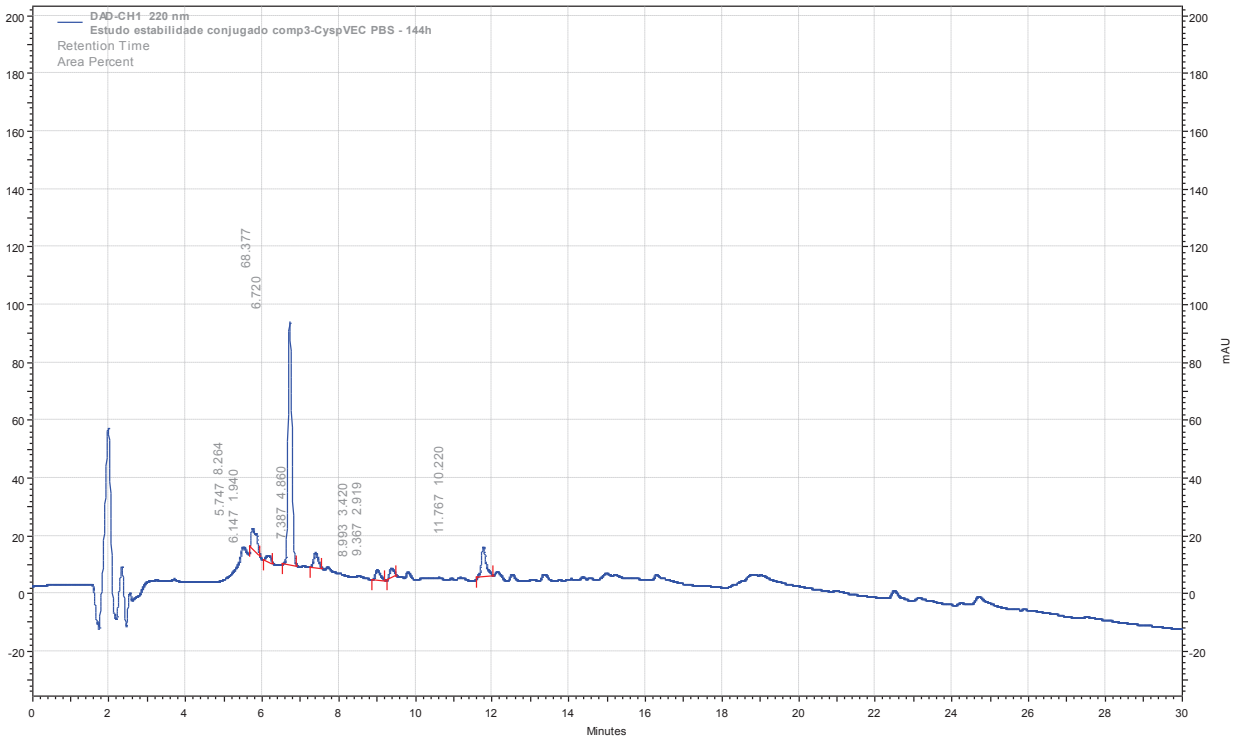

Figure 65: Stability study of the Gemcitabine–Linker–pVEC conjugate: HPLC analysis performed after 144 h. Chromatogram acquired with a HPLC-DAD system, with a C18 column, using ACN in water with 0.05% TFA as eluent, in gradient mode (0 – 100%), for 30 minutes, at a flow of 1 mL/min and detection at λ = 220 nm.

6.2. Stability of the Gemcitabine–Linker–Penetratin conjugate – periodic HPLC analysis over 22 days

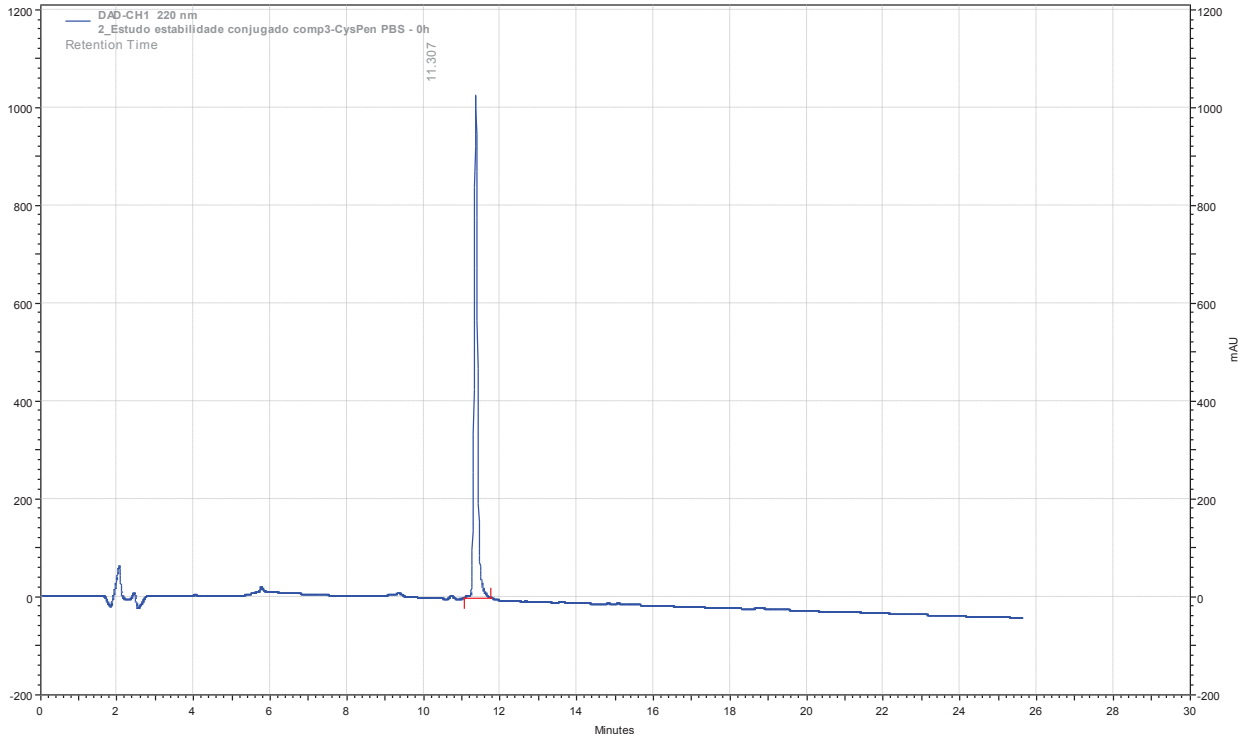

Figure 66: Stability study of the Gemcitabine–Linker–Penetratin conjugate: HPLC analysis performed in the beginning of the study (0 h). Chromatogram acquired with a HPLC-DAD system, with a C18 column, using ACN in water with 0.05% TFA as eluent, in gradient mode (0 – 100%), for 30 minutes, at a flow of 1 mL/min and detection at λ = 220 nm.

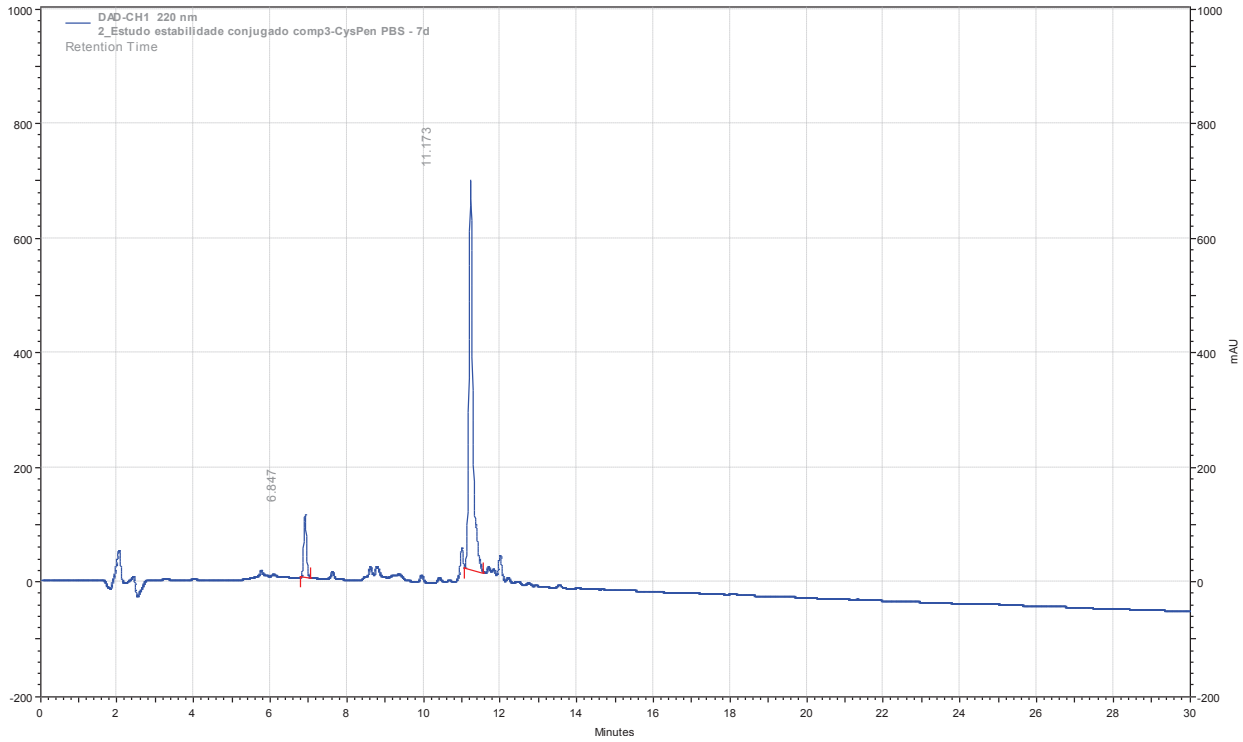

Figure 67: Stability study of the Gemcitabine–Linker–Penetratin conjugate: HPLC analysis performed after 7 days. Chromatogram acquired with a HPLC-DAD system, with a C18 column, using ACN in water with 0.05% TFA as eluent, in gradient mode (0 – 100%), for 30 minutes, at a flow of 1 mL/min and detection at λ = 220 nm.

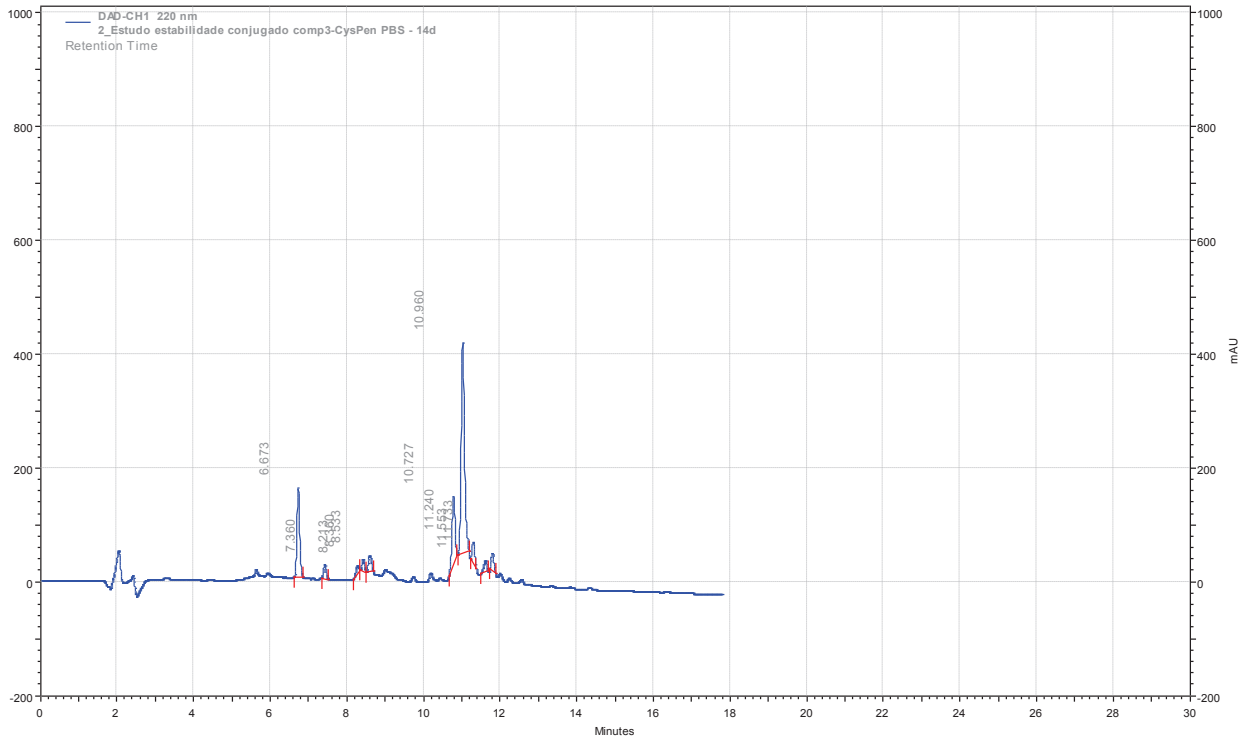

Figure 68: Stability study of the Gemcitabine–Linker–Penetratin conjugate: HPLC analysis performed after 14 days. Chromatogram acquired with a HPLC-DAD system, with a C18 column, using ACN in water with 0.05% TFA as eluent, in gradient mode (0 – 100%), for 30 minutes, at a flow of 1 mL/min and detection at λ = 220 nm.

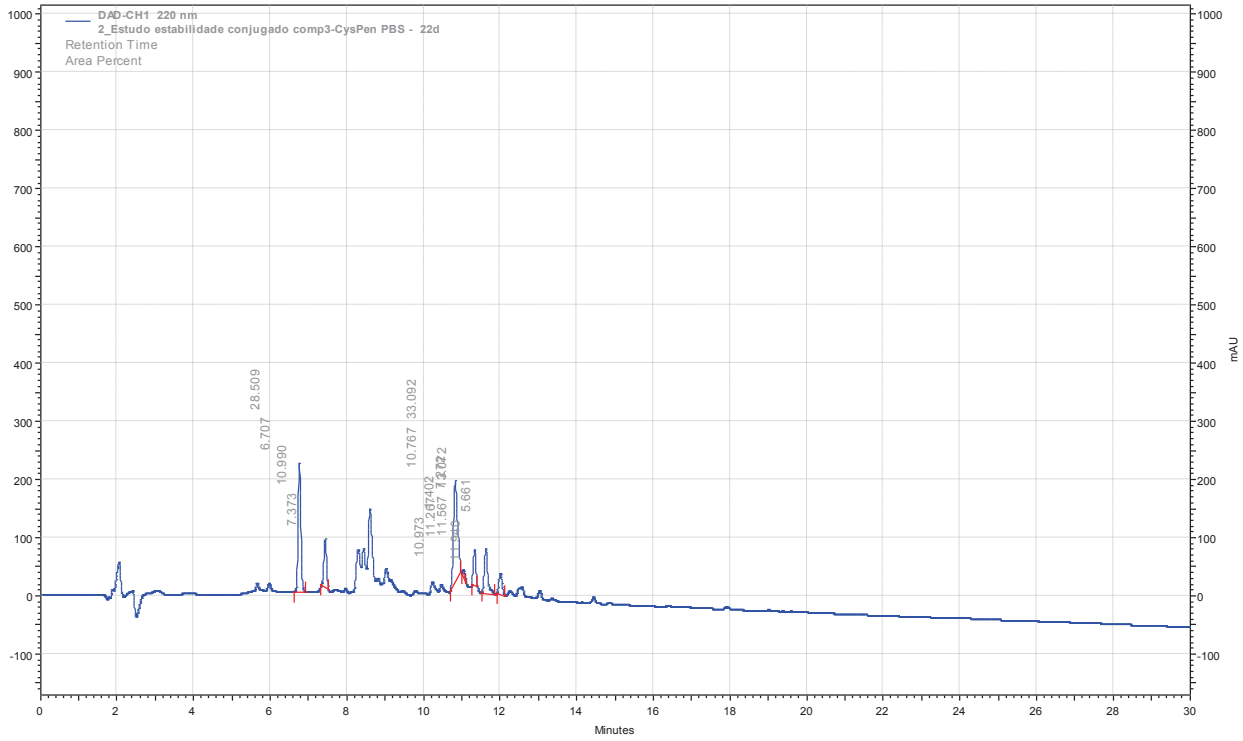

Figure 69: Stability study of the Gemcitabine–Linker–Penetratin conjugate: HPLC analysis performed after 22 days. Chromatogram acquired with a HPLC-DAD system, with a C18 column, using ACN in water with 0.05% TFA as eluent, in gradient mode (0 – 100%), for 30 minutes, at a flow of 1 mL/min and detection at λ = 220 nm.

6.3. LC-MS chromatograms of the CPPs and the conjugates

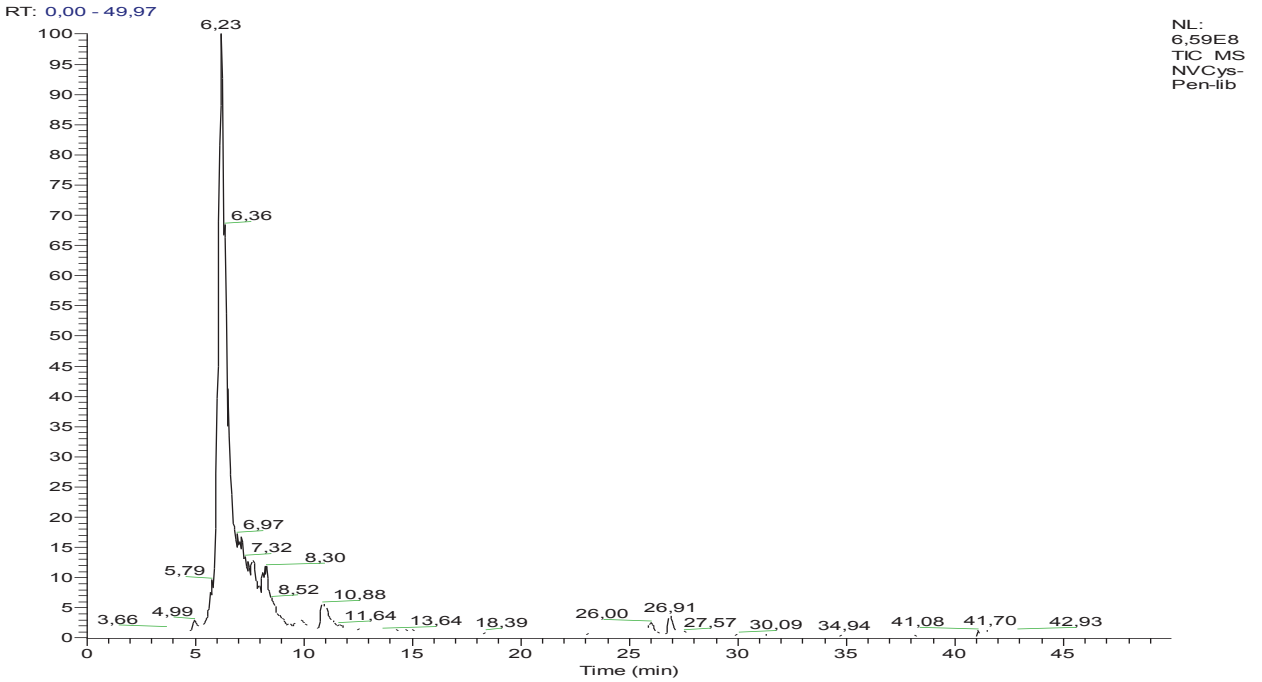

Figure 70: LC-MS chromatogram of the Cys-Penetratin peptide, synthesized in the CEM Liberty1 MW assisted peptide synthesizer.

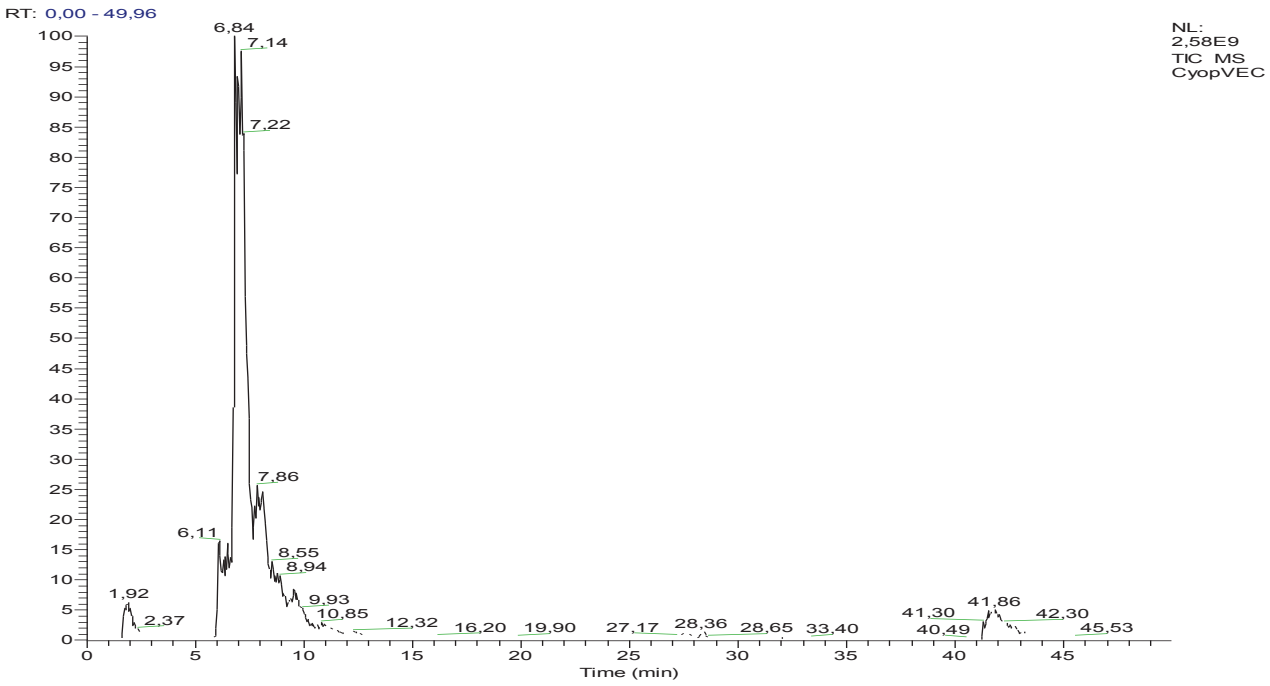

Figure 71: LC-MS chromatogram of the Cys-pVEC peptide, synthesized in the CEM Liberty1 MW assisted peptide synthesizer.

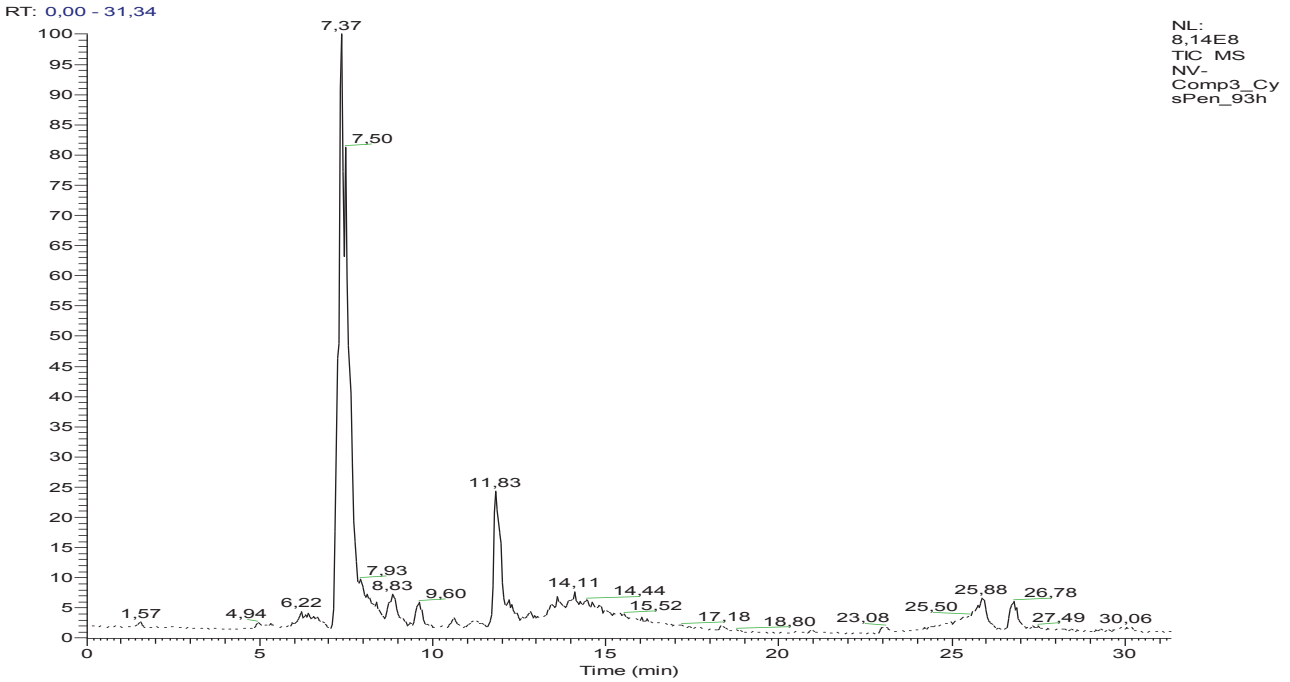

Figure 72: LC-MS chromatogram of the Gemcitabine–Linker–Penetratin conjugate.

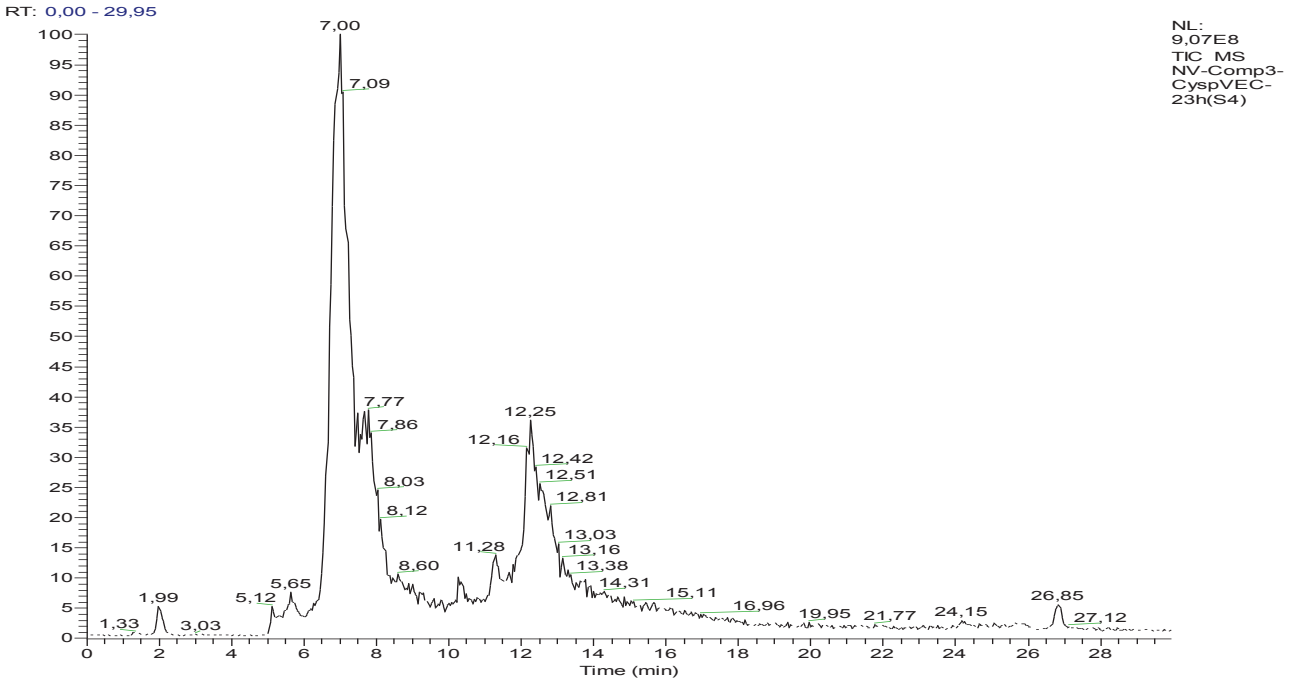

Figure 73: LC-MS chromatogram of the Gemcitabine–Linker–pVEC conjugate.